学 位 論 文

Theoretical Study on the Origin of

π-Facial Diastereoselectivity of Hydride Reduction

ヒドリド還元における面選択性の理論的考察

平成8年12月博士（理学）申請

東京大学大学院理学系研究科

化学専攻

千 住 孝 俊

①

学 位 論 文

Theoretical Study on the Origin of

π-Facial Diastereoselectivity of Hydride Reduction

ヒドリド還元における面選択性の理論的考察

平成8年12月博士（理学）申請

東京大学大学院理学系研究科

化学専攻

千 住 孝 俊

Theoretical Study on

the Origin of π-Facial Diastereselectivity

of

Hydride Reduction

by

Takatoshi Senju

Submitted to the Department of Chemistry,

Graduate School of Science

in partial fulfillment of the requirements for the degree of

Doctor of Science

at

THE UNIVERSITY OF TOKYO

December 1996

To My Parents

Acknowledgements

Acknowledgments

The author is sincerely grateful to Professor Shuji Tomoda for his close guidance of this work. His valuable suggestions and heartfelt encouragements always helped the author during the course of this work. His close reading of the manuscript is highly appreciated as well.

The author wishes to express his gratitude to Associate Professor Keiichiro Ogawa for his valuable comments on this work, without whom the author could never have acquired such high level skills and techniques of computer operations.

The author wishes to thank Dr. Michio Iwaoka for his helpful advices and his Fortran source code.

The author wishes to thank laboratory members for helpful suggestions.

Finally, the author wishes to express his uttermost gratitude to his parents for their lasting support and encouragement.

Takatoshi Senju

December 1996

Contents

List of Tables

iv

List of Figures

Abbreviations and Symbols

AAS	Atomic accessible space
AO	Atomic orbital
au	Atomic unit
EFOE	Exterior Frontier Orbital Extension
eu	Entropy unit
HF	Hartree-Fock
HOMO	Highest occupied molecular orbital
LAH	Lithium aluminum hydride
LCAO	Linear combination of atomic orbitals
LUMO	Lowest unoccupied molecular orbital
MO	Molecular orbital
MP2	Møller-Plesset second order perturbation theory
THF	Tetrahydrofuran
TS	Transition state
ZPVE	Zero-point vibrational energy
δ	Distortion index
$\Delta H^{\ddagger}$	Activation enthalpy
$\Delta S^{\ddagger}$	Activation entropy
S	Overlap integral
Ψ	Molecular orbital
χ	Atomic orbital
ψ	Molecular orbital

Chapter 1

Introduction

Hydride reduction of carbonyl compounds is one of the most fundamental and basic reactions in organic synthesis and it has been utilized in a number of organic syntheses as a convenient and efficient method for converting a carbonyl functionality to an alcoholic hydroxyl group. A variety of reducing agents have been developed to date, and experimental results using such reagents can be found in a number of literatures.[1]

One extremely important aspect of this reaction is that when the two faces of the carbonyl group have different environments due to the proximate geometrical environments, diastereomeric isomers are to be produced. The ratio of one isomer over the other depends on both the kind of the reducing reagents employed and reaction conditions. Spurred by the high needs in asymmetric syntheses of complex natural products, much efforts have been made to develop highly stereoselective reducing agents.

Although a very large number of successful results of stereoselective reductions

have been reported, the fundamental reason for the observed stereoselectivity has not yet been solved. This is partly because of limited information as to the mechanism and the nature of the transition state of the reduction process. Nonetheless, several empirical and theoretical rationalizations have been reported in the literature.[2-5] These rationalizations can be mainly divided into two categories, namely between transition state models and ground state models.

The former models mainly consider the difference of the stabilization energy of activated complex of substrates and reagents at the transition state as the main factor for the resulting product ratios. On the other hand, the latter models generally attribute the ground state properties of the substrate to the observed stereochemical outcomes.

By virtue of the recent rapid progress in computer facilities, it has become available to compare both propositions by sophisticated theoretical calculations which could never be performed some years ago at all. Nonetheless, there seems to be no general consensus about the validity of each model up to now. Therefore, more extensive study must be done to clarify the essential reason of the diastereofacial stereoselectivity of reduction reactions.

In the subsequent sections, previous typical empirical and theoretical models reported to date will be briefly introduced and discussed in terms of their scope and limitations.

1.1   1,2-Asymmetric Induction in Acyclic Systems

In 1952, Cram and Abd Elhafez reported an empirical rationalization, which is now widely known as "the Cram model".[6] They examined six types of nucleophilic addition reactions on thirty five acyclic compounds. The investigated reactions were the Grignard reaction, lithium aluminum hydride reduction, metal sodium reduction in ethanol, aluminum isopropoxide reduction, sodium amalgam reduction of carbonyl compounds, and the reduction of oximes to amines with sodium amalgam. Close inspection led them to the famous general principle, *i.e.*, "In non-catalytic reactions of the type shown, that diastereomer will predominate which would be formed by the approach of the entering group from the least hindered side of the double bond when the rotational conformation of the C–C bond is such that the double bond is flanked by the two least bulky groups attached to the adjacent asymmetric center" (Figure 1-1(a)).[6]

Although their model was widely accepted as a useful rationalization for a prediction of the predominant product in such reactions, it suffered from the obscurity of determining the order of bulkiness of substituents (S, M, L) attached on an adjacent asymmetric center.

Cram's model was extended to compounds having polar substituents such as chlorine by Cornforth,[7] and this variant is called "the Cornforth model". In this model, it is assumed that polar groups play the role of the largest substituent (L) in the Cram model. The reason for the inclination of the polar group positioning *anti* with respect to the carbonyl group was thought to originate from the dipole-dipole repulsion between the polar substituent and the highly polarized metal-oxygen bond.

(a) The Cram (Cornforth) model
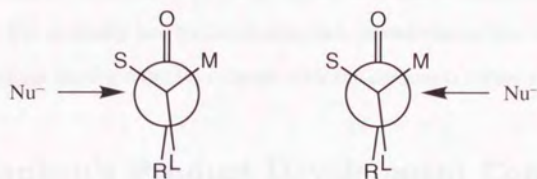
(b) The Karabatsos model

(c) The Felkin model

Major   Minor
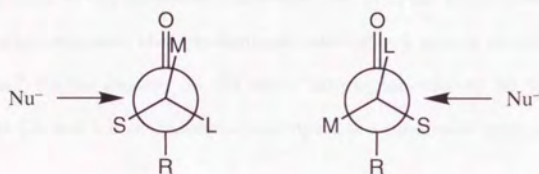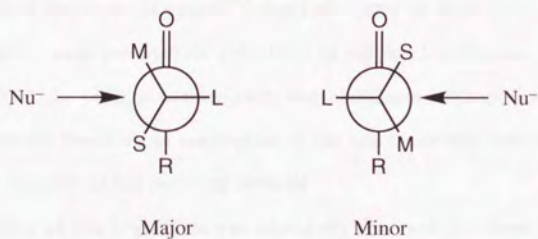
Figure 1-1. Transition state conformations of the representative models for 1,2-asymmetric induction. (a) The Cram (Cornforth) model (top), (b) the Karabatsos model (middle), and (c) the Felkin model (bottom)). S, M, L signifies the effective bulkiness of the substituents (S = small, M = middle, L = large).

Karabatsos also presented similar empirical model for 1,2-asymmetric induction in 1967.[8] He suggested that the preferential approach of a nucleophile to the carbonyl occurs from the sterically less hindered side, but, in contrast to the Cram model, with the medium sized group (M) eclipsed with the carbonyl.(Figure 1-1(b)).

1.2   Dauben's Product Development Control Hypothesis

Generalization of the stereoselectivity observed in cyclic ketones was first made by Barton, who suggested that predominant axial attack occurs on unhindered cyclohexanones.[9] Richer focused on the steric interaction exerted by the two axial hydrogens at C2 and C6 of cyclohexanone upon the equatorial approach of nucleophile.[10]

An empirical rule for the stereoselectivity of nucleophilic additions to relatively unhindered rigid cyclic ketones was then formulated by Dauben in 1956.[11] He proposed "product development control" hypothesis based on Barton's suggestion. He and co-workers examined hydride reductions of alkylcyclohexanones with lithium aluminum hydride, sodium borohydride, and aluminum isopropoxide, and interpreted the results based on an assumption of the late transition state and the thermodynamic stability of the resulting alcohols.

The validity of this hypothesis was intensively disputed by others. Later it was suggested that the product development control is not the determinative factor of the π-facial preference by Brown *et al.* who performed kinetic analysis of sodium borohydride reduction of acetaldehyde and found that the activation enthalpy of the

reduction is very small ($\Delta H^\ddagger = 7.6$ kcal mol^{-1}) contrary to the assumption of the late transition state assumption of the product development control hypothesis.[12] Consequently, it was established that the transition state of hydride reduction appears at an early stage of the reaction, and the product ratios should be dictated kinetically, not thermodynamically.

1.3 The Felkin-Anh Model

Cram's model and Karabatsos' model (section 1.1) seemed to be widely applicable to a variety of open-chain molecules. In the case of cyclic ketones, however, the effect of the variation of the size of the substituents on adjacent carbons has been found to be unaccountable with these explanations. In this context, Felkin, in 1968, proposed a novel transition state hypothesis for nucleophilic addition reactions which is applicable to both acyclic and cyclic ketones based on the assumption of reactant-like transition state.[13,14] In the case of cyclic ketones, he pointed out the presence of larger torsional strain in the equatorial transition state of nucleophilic additions to cyclohexanone than in the axial transition state, and explained the observed stereoselectivity in terms of the difference of this steric strain.[14] In the case of acyclic systems, he assumed that the largest group on an adjacent carbon (L) occupies the antiperiplanar position with respect to the incoming nucleophile in order to minimize the torsional strain with nearby allylic bonds at the transition state (Figure 1-1(c)).

Eight years later, Anh and Eisenstein carried out *ab initio* calculations using minimal basis set (STO-3G) to compare relative energies of the transition state corre-

sponding to Cram's, Karabatsos', and Felkin's model.[15-17] He chose 2-chloropropanal and 2-methylbutanal as model compounds for hydride reduction and located a bear hydride at 1.5 Å distance on the normal plane with respect to the carbonyl π plane, with other bond lengths and bond angles being fixed at the standard geometries. He then changed the position of the substituents on the asymmetric carbon to evaluate the difference of the total energies of each conformation. The results of these calculations obviously supported the Felkin model as the most plausible one, since the most stable and the second most stable transition state conformation on the energy surface corresponded to the two transition structures predicted by Felkin. The most stable one corresponded to the conformation which leads to the major product, and the second most stable one corresponded to the conformation which leads to the minor product. Both of them are staggered conformation, *i.e.*, the largest group (L) occupies the antiperiplanar position with respect to the forming $H^- \cdots C$ bond. Other conformations corresponding to both Cram's and the Karabatsos' model are energetically higher than the conformations proposed by Felkin and, furthermore, they are not at energy minima on the potential energy surface.

An important contribution made by Anh to Felkin's version of the Cram model is the incorporation of the "non-perpendicular attack" notion. This notion had been proposed by Bürgi *et al.*, who had reported a series of papers dealing with the reaction paths at the trigonal carbon centers.[18-22] Crystallographic studies on several ketones, supplemented by *ab initio* model calculations,[23] revealed that nucleophiles approach to the carbonyl at an average angle of 107° with respect to the C=O double bond. At this approaching angle, steric interaction between a nucleophile and substituents on an adjacent carbon is minimized when the S group flanks near

Major   Minor
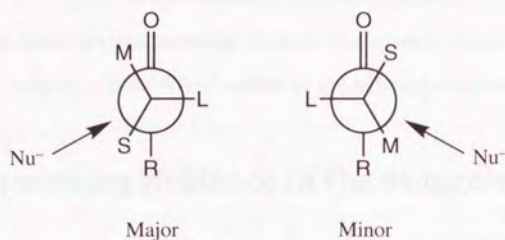
Figure 1-2. Anh's interpretation of the Felkin model for acyclic stereo differentiation.

S   Small group
M   Medium group
L   Large (polar) group
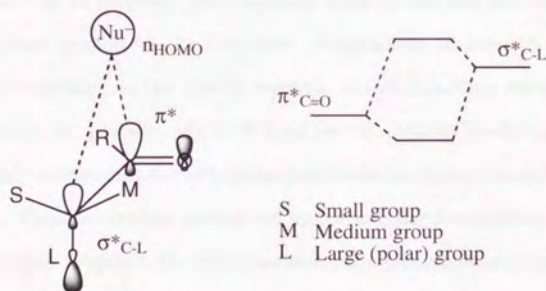
Figure 1-3. Secondary orbital interaction scheme of the Felkin type transition state of nucleophilic addition to acyclic ketones proposed by Anh.

the R group (Figure 1-2).

Another very important suggestion is that the energy difference of each transition state conformation arises from the secondary orbital interaction between the highest occupied molecular orbital (HOMO) of the nucleophile and the σ^* orbital of the antiperiplanar C–L (L = Cl or Me) bond next to the carbonyl group of the substrate

(Figure 1-3). This implies that the transition state is supposed to be electron-rich, and it should gain extra stabilization by electron delocalization from the σ orbital of the forming bond ($\sigma_{Nu\cdots C}$) into the σ^* orbital of the adjacent acceptor bond (σ^*_{C-L}).

1.4   Supporting Evidence of the Staggered Model

Anh's results were later reconfirmed by the more sophisticated *ab initio* calculations performed by Houk *et al.*[24, 25] They investigated the transition structures of nucleophilic (hydride), electrophilic (proton and BH_3), and radical (hydrogen atom) addition reactions to propene. The transition state geometries were optimized using the gradient method for the first time. Approaching trajectories of incoming species vary depending on the type of reaction, but all transition states have staggered conformation, *i.e.* with one C–H bond on the adjacent methyl group orients antiperiplanar with respect to the forming bond between the carbon and the attacking species. These structures correspond to the staggered transition state model proposed by Anh (Figure 1-2). The transition state structures of nucleophilic and radical addition reaction calculated by Houk have an additional unique feature. The incoming species approaches the central carbon atom of propene at an angle of 123° for a hydride and 102° for a hydrogen radical, both away from the terminal carbon atom of the double bond. This nonperpendicular approaching angles are in agreement with the aforementioned Bürgi-Dunitz trajectory (mean value is 107° for aminoketones). They interpreted these reaction paths in terms of favorable interaction between the frontier orbitals.

The preference of the staggered conformation of the adjacent group was first in-

terpreted in terms of unfavorable secondary orbital interaction between the frontier orbitals of reagents and substrates. Namely, methyl group rotates such that the antibonding interaction of the HOMO of the hydride with the LUMO of the methyl group of propene, and conversely that of the HOMO of the methyl group with the LUMO of the hydride are minimized.[24] Successively they claimed that the closed shell repulsion between the partially formed bond and the adjacent σ-bond is responsible for the staggered structure.[25] In any event, they assumed electronic effects (hyperconjugative effects) are of less importance for the preference of the staggered structure than the steric demand at the transition state.

1.5   The Cieplak Model

Cieplak presented a completely novel interpretation to explain the stereochemical outcomes observed in nucleophilic addition reactions to cyclic ketones in 1981.[26] His proposal has been a subject of a number of intense debates (most recent review on this subject is ref 27). In contrast to the previous suggestions, he stated "the very definition of the incipient bond suggests that this bond is intrinsically electron deficient". From this point of view, he placed more importance on hyperconjugative interaction between the electron rich σ_{C-L} (L = H or C) bond and the partially formed bond rather than the hyperconjugation between the electron deficient σ^*_{C-L} bond and the electron rich incipient nucleophile-carbon bond (Figure 1-4). The mechanism of electron delocalization is reversed with respect to that of the Felkin-Anh model. He mostly argued his hypothesis with the stabilization energy at the transition state, which is expressed as,
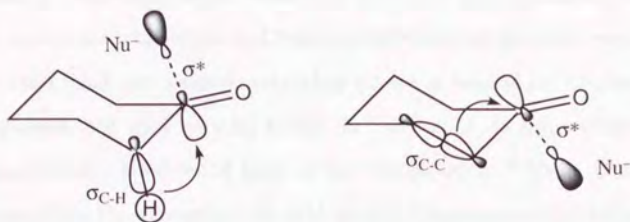
Figure 1-4. Hyperconjugative interaction described by Cieplak.

$$SE(\sigma_i, \sigma^*_\ddagger) \approx \frac{S^2\sigma_i\sigma^*_\ddagger}{\Delta\varepsilon(\sigma_i, \sigma^*_\ddagger)} \tag{1.1}$$

where $SE(\sigma_i, \sigma^*_\ddagger)$ represents the stabilization energy, in which σ_i is the filled σ orbital of the adjacent allylic bonds and $\sigma^*_\ddagger$ is the vacant orbital of the forming bond, $S^2\sigma_i\sigma^*_\ddagger$ is the overlap integral of σ_i and $\sigma^*_\ddagger$, and $\Delta\varepsilon(\sigma_i, \sigma^*_\ddagger)$ is the energy separation between σ_i and $\sigma^*_\ddagger$.

The differences of reaction rates at the axial and the equatorial face of cyclohexane-based systems were rationalized with the variation of $SE(\sigma_i, \sigma^*_\ddagger)$. To explain the origin of the difference of $SE(\sigma_i, \sigma^*_\ddagger)$, he introduced the assumption of the order of electron donation ability of σ_{C-C} and σ_{C-H} orbital. He proposed that the C–H bond has larger donating ability than the C–C bond based on several spectroscopic evidences which seem to support his notion (e.g. the Baker-Nathan effect). This assumption has brought about tremendous amounts of debates among organic as well as theoretical chemists. For instance, Houk and co-workers refuted this assumption based on the experimental and theoretical investigation of inonization

potentials of methylpiperidines.[28] Heathcock discovered that the antiperiplanarity in Anh sense is more important in 1,2-asymmetric induction in acyclic compounds. On the other hand, some experimental chemists are in favor of the Cieplak model and explained their work with his model. le Noble *et al.* interpreted his results on adamantanone derivatives in terms of the Cieplak model.[29] Mehta *et al.* similarly rationalized the stereoselectivity of bicyclo[2.2.1]heptanones with this model.[30] Halterman also supported this model based on his findings about diarylcyclopentanones and diarylcyclopentadienes.[31,32] Senda carried out investigations of 2- and 3-methoxycyclohexanones and supported this model.[33,34]

Although such a number of successful applications to cyclic ketones have been reported, there is one crucial problem in this model. Stereochemical outcome exhibited by acyclic carbonyl compounds can rarely be rationalized by his model.

1.6 Effects of Polar Groups

As briefly noted earlier (section 1.4, page 9), Houk conducted a series of transition state calculations and concluded that the torsional strain proposed by Felkin and the antiperiplanarity and the nonperpendicular attack suggested by Anh are generally valid in nucleophilic as well as electrophilic reactions.

To account for the selectivity of nucleophilic as well as electrophilic additions to acyclic systems and some rigid cyclic ketones having polar substituent, he invoked the electrostatic interaction argument, *i.e.*, attractive or repulsive electrostatic interaction between the reagent and the polar groups in the substrate controls the selectivity.[35-39] Adcock's work on adamantanones[40] and Wipf's report on dienone

derivatives[41] seem to support this argument.

1.7   Orbital Distortion Model

1.7.1   Klein's Model

Effect of the spatial extension of molecular orbital on stereochemical preference was first pointed out by Klein in 1973.[42] He and co-workers first interpreted the results of reduction of alkylsubstituted cyclohexanones with lithium tri-t-butoxy-aluminum hydride in terms of the Felkin torsional model.[43] Later he changed his interpretation so as to explain the results of hydroboration of methylenecyclohexanes.[44] Three years after that, he again changed his interpretation and proposed a new concept, which for the first time took into account the possibility of different extension of the π and π^* orbitals might influence the stereochemical course of nucleophilic as well as electrophilic reactions. He asserted that hyperconjugative interaction between the π orbital at the double bond and symmetrical σ^* orbitals of β-C–C bonds (C2–C3, C5–C6) results in accumulation of more electron densities on the equatorial side of the double bond in the case of methylenecyclohexanes, whereas hyperconjugation involving π^* orbital at the carbonyl and symmetrical σ orbitals at the β-C–C bonds makes the π^* orbital at the carbonyl more extend to the axial side in the case of cyclohexanones. In his model, electrophilic additions to methylenecyclohexanes are expected to be facilitated from the equatorial side, whereas nucleophilic additions to cyclohexanones would preferentially occur from the axial side.

The problem is that his interpretation is solely based on qualitative arguments

(a) (b)

(c) (d)
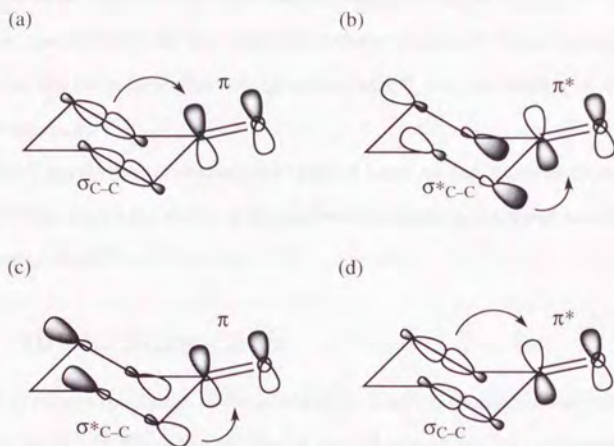
Figure 1-5. Hyperconjugative interaction between (a) σ_{C-C} and π, (b) σ^*_{C-C} and π^*, (c) σ^*_{C-C} and π, and (d) σ_{C-C} and π^* proposed by Klein.

and no theoretical basis was presented. Indeed, according to the recent *ab initio* theoretical study by Frenking *et al.*,[45] the extension of the π orbital at the *exo*-methylene bond of methylenecyclohexane has been revealed to be largely distorted toward the axial side, not to the equatorial side.

1.7.2   Other Empirical Orbital Distortion Models

Another empirical model which centered on orbital distortion was presented by Liotta.[46,47] He pointed out the interaction between the π orbital and adjacent σ_{C-H} bond causes the antisymmetrical orbital extension with respect to the nodal plane of the double bond in terms of basically qualitative arguments. Later, he estimated

the degree of orbital distortion qualitatively using the sign of the second-order perturbation coefficients.[48] He also reported a theoretical study which focused on the analysis of the trajectory of attacking nucleophile,,[49] but the validity of this treatment is uncertain.

Hudec suggested the distortion of π^* orbital based on the "twist angle approach" theory.[50] This model has rarely been used since it leads to incorrect conclusions in a number of cases.[29]

1.7.3   Orbital Mixing Rule

A theoretical explanation of the mechanism of orbital distortion was put forward by Fukui *et al.*[51,52] They had derived a general mathematical expression for the mechanism of deformation of molecular orbital caused by the mixing of other atomic orbitals using perturbation theory.[53,54] They focused on the sign of the coefficient of the second order term in the perturbed molecular orbital wave function. This coefficient was used as an indicator of a phase relationship of intramolecular orbital mixing.

They successfully explained several π-face selections using this technique, such as *exo*-selectivity of norbornene, Diels-Alder reactions of 5-substituted cyclopentadienes, *etc.*, although some raised critical debates about the validity of this model.[28,55]

1.7.4   Frenking's Interpretation

Asymmetric orbital extension was reconsidered as a fundamental source of the stereoselection at the beginning of the 90's. Frenking *et al.* carried out *ab ini-*

tio molecular orbital calculation of cyclohexanone and 3-fluorocyclohexanone at the Hartree-Fock 3-21G level.[45] They also located transition state structures of lithium hydride (LiH) addition to them at the same level of theory and evaluated relative energies using the Möller-Plesset second order perturbation theory[56] and 6-31G* basis set. They found that the LUMO of cyclohexanone largely deviates from symmetry with respect to the π-nodal plane: the LUMO at the carbonyl carbon largely extends toward the axial direction. They also showed that the same feature of orbital distortion is found in methylenecyclohexane in contrast to Klein's proposition (see section 1.7.1, page 13). They stated that the Cieplak model is "paradoxical", since it violates the frontier molecular orbital theory, and that the observed axial preference in addition reactions to 3-substituted cyclohexanones "can be explained without difficulties by the frontier-orbital model."

The mechanism of orbital distortion was discussed based on the fact that the π^* orbital interacts better with the σ_{C-H} orbitals rather than the σ_{C-C} orbitals according to the Natural Bond Orbital (NBO) analyses.[57]

1.7.5 Dannenberg's PPFMO Model

Most recent approach attributing the reason of the diastereofacial stereoselectivity to asymmetric orbital extension was made by Dannenberg *et al.*[58-60] They have proposed a new *quantitative* model, which they call "Polarized π-Frontier Molecular Orbital (PPFMO) Model". In general, p-orbitals of unsaturated portion of a molecule are unsymmetrical due to the proximate geometrical environment. Predictions by means of the frontier molecular orbital (FMO) theory are not suitable in such situations. Consequently, they extended the concept of the FMO theory to

the cases where π orbitals are rigorously asymmetric. Their procedure requires construction of a p-orbital from three independent orbitals, namely atomic p-function and additional two s-type gaussian functions having opposite signs, each of them placed at an appropriate distance from the nodal plane of the π system (χ_+, χ_-). Then the entire molecular orbital is optimized until it fulfills the requirement of the convergence criterion generally imposed on self-consistent field (SCF) calculation. The difference of the resulting coefficients on the two supplemental s-type gaussian functions (c_+, c_-) will then become a predictive indicator of π-orbital polarization (p),

$$p = c_+\chi_+ + c_-\chi_-$$

Their method seems to have several advantages. It demands little time, as the required geometry optimizations can be performed with semi-empirical AM1 method.[61] Moreover, molecular orbital calculation can be done using inexpensive minimal basis set (STO-3G). Nonetheless, the reported results of their calculation are surprisingly in good agreement with experimental results of simple metal hydride reductions of a number of carbonyl compounds[59] and deuteration and sufenylation of substituted alkenes.[60]

However, there seem to be some inherent problems in this model. Firstly, the use of the AM1 method for geometry optimizations is questionable. Since the shape of the molecular orbital may be substantially affected by molecular structure, this level of optimization could lead to incorrect orbital extension in some cases where their difference between the two faces is small. Secondly, MO coefficients were determined

with STO-3G, which might cause erroneous assignments of the direction of orbital extension due to the low precision of the basis set.

1.7.6   Charge Density Study of Cyclohexanone

Recently, orbital distortion model was subjected to a severe scrutiny by Shi and Boyd in 1993.[62] They carried out charge density study using the Atoms in Molecules (AIM) theory developed by Bader.[63, 64] They also reported transition state calculations of additions of LiH to cyclohexanone and 4-chlorocyclohexanone.

Within the AIM scheme of charge distribution study, they investigated the Laplacian of the charge density $(\nabla^2 \rho)$ in the valence shell of cyclohexanone, and concluded that the unsymmetrical charge concentration between the two faces of the carbonyl group has no significance for the selectivity. They also suggested that the face selection is simply the result of the differing electrostatic field around the carbonyl function based on the transition state calculations.

1.8   Summary and Objectives of This Work

Each rationalization introduced so far has both their adherents and critics. At present, two transition state models, *i.e.*, the Felkin-Anh model and the Cieplak model, seem to have a general acceptance. The Felkin-Anh model has widely been used basically in explaining asymmetric induction of acyclic compounds. The Cieplak model has been supported by numerous experimental results of conformationally rigid cyclic ketones. When polar groups are present in a substrate, the electrostatic interaction has been invoked to explain otherwise inexplicable high se-

lectivity. Nonetheless, the ground state model, which basically relies on the frontier orbital theory as its base, has still sometimes been invoked to explain the selectivity by both theoretical and experimental chemists.

In the next chapter (Chapter 2), the significance of the orbital effects upon the π-facial diastereoselectivity of cyclohexanone derivatives will be scrutinized with introducing a new theoretical parameter, the EFOE density value, as an indicator of the magnitude of the LUMO extension at the very frontier of a molecule, where the reaction initially takes place. It will be shown that orbital effect is indeed of substantial significance on the stereoselection of cyclohexanones in contrast to the recent several criticisms. It will be also shown that neither the steric strain nor the hyperconjugative stabilization is important for the stereoselectivity of cyclohexanone systems.

In Chapter 3, the same method will be employed to investigate a wide variety of cyclic ketones. Those compounds whose selectivities have been interpreted with the transition state models and the electrostatic arguments will be mainly considered. Unlike six-membered ketones, other factors other than the orbital effect may be important for those systems. The relative importance of each factor will be compared to uncover the origin of π-facial selectivity of those compounds.

Chapter 2

EFOE Model

Several earlier models have been introduced in the previous chapter. Although each of them has succeeded in explaining π-facial stereoselectivity to some extent, there are still on-going debates as to which model best describes the essential factor for the stereoselectivity.

From this viewpoint, we have devised a new quantitative, quantum chemical method in order to evaluate the magnitude of the frontier orbital effects on nucleophilic addition reactions to carbonyl compounds. The theoretical basis of this new method will be introduced in the first part of this chapter, and then, its versatility will be examined first with cyclohexanone and then with alkyl-substituted cyclohexanones as representative model compounds of simple metal hydride reduction in the latter part of this chapter.

2.1   Transition State of Hydride Reduction of Cyclohexanone

Experimental results of metal hydride reduction of 4-*tert*-butylcyclohexanone in the solution phase have been known to have the following features: (i) hydride preferentially attacks from the more hindered axial side. For example, lithium aluminum hydride (LiAlH$_4$) reduction of 4-*tert*-butylcyclohexanone was reported to have approximately 90% axial selectivity.[65,66] And (ii) the activation enthalpy of this reaction is very low. The former indicates steric factor alone would not be the controlling factor for the stereoselectivity and implies electronic factor should be taken into account. The latter feature is generally seen in metal hydride reduction. For instance, reduction of acetone with sodium borohydride is very exothermic ($\Delta H^\circ = -128.2$ kcal mol^{-1}),[67] and the activation enthalpy is only $\Delta H^\ddagger = 7.6$ kcal mol^{-1}.[68] The kinetic analysis of sodium borohydride reduction of 4-*tert*-butylcyclohexanone in 2-propanol has been reported and the observed activation enthalpy is 5.7 ± 0.2 kcal mol^{-1}, and the activation entropy ($\Delta S^\ddagger$) is -44.7 ± 0.3 eu. The substantial negative activation entropy indicates this reaction has a somewhat compact transition state.[69] Even in the case of somewhat bulkier reducing reagent, such as LiAl(OBu^t)$_3$H, the activation enthalpy $\Delta H^\ddagger$ ranges from 5.8 to 8.2 kcal mol^{-1} and the activation entropy $\Delta S^\ddagger$ varies from -33 to -42 eu.[70] In the gas phase, non-existence of activation barrier for the axial attack of hydride has been suggested.[71] In fact, almost exclusive axial selectivity of cyclohexanone (99:1) was observed in a recent experiment using alkoxysiliconate hydrides as a hydride source.[72] This strongly indicates that the stereoselectivity observed in sterically undemanding metal hydride

reduction of cyclohexanone is solely governed by the intrinsic nature of the substrate, since neither solvent effects nor counter-cation effects are relevant to the gas phase selectivity.

According to the Hammond postulate,[73] the small activation enthalpies indicate the transition state of the reduction process generally appears at an early stage along the reaction coordinate, and the structure of the substrate at the transition state is expected to be very similar to that at the ground state. The earliness of the transition state in these reactions has been confirmed with theoretical calculations. Frenking *et al.* calculated the axial and the equatorial transition states of lithium hydride addition to cyclohexanone as a model of lithium aluminum hydride reduction at the Hartree-Fock level using 3-21G basis set and evaluated the relative energies including electron correlation effects with the Møller-Plesset perturbation theory up to second order (MP2)[56] using 6-31G* basis set with the frozen geometries obtained using 3-21G basis set (*i.e.*, MP2/6-31G*//HF/3-21G).[45] Houk *et al.* also calculated the same model.[35] The geometries were optimized at the HF/3-21G level and the energies were computed with HF/6-31G*//HF/3-21G level of theory. Calculated energy difference between the equatorial and axial transition states at these levels were 1.0 kcal mol^{-1}(HF/3-21G),[35] 1.8 kcal mol^{-1}(HF/6-31G*//HF/3-21G),[35] and 1.4 kcal mol^{-1}(MP2/6-31G*//HF/3-21G)[45] respectively. These transition state energy differences are approximately in good agreement with the experimental product ratio of axial (equatorial attack) and equatorial (axial attack) alcohols (10 : 90) observed in the reduction of 4-*tert*-butylcyclohexanone.[65, 66]

Figures 2-1 and 2-2 show the axial and the equatorial transition state structures of LiH addition to cyclohexanone at various levels of theory including the results

reported by Frenking and Houk performed at the HF/3-21G level, and selected geometrical parameters are listed in Table 2-1 and Table 2-2. Computational details are described in Appendix A on page 129.

At the HF/3-21G level, the distance between the hydride and the carbonyl carbon (H$\cdots$C) is 2.057 Å in the axial transition state and 2.027 Å in the equatorial transition state, indicating possible earliness of the transition state. The axial transition state is slightly earlier with respect to the equatorial transition state as indicated by the longer H$\cdots$C distance (0.030 Å) of the former.

The structures obtained with higher theoretical levels are all quite similar. Basis set dependence of optimized structures seems to be small, but bond lengths in cyclohexanone moiety become generally shorter at the HF/6-31G* and HF/6-311++G** levels than the HF/3-21G level. However, when the electron correlation effect is taken into account, slight elongation of these bonds is observed. Furthermore, the length of the partially forming bond (H$\cdots$C) becomes longer than that obtained at the Hartree-Fock levels. H$\cdots$C distance obtained with the MP2 level is 2.286 Å in the axial transition state and 2.250 Å in the equatorial transition state, both much longer than the corresponding bond lengths of 1.971 Å in the axial TS and 1.965 Å in the equatorial TS at the HF/6-31G* level. This feature becomes more relevant when the three parameter-hybrid exchange functional of Becke[74, 75] and the gradient-corrected correlation functional of Lee, Yan, and Parr[76] implemented on Gaussian 94 suite of program[77] were used for the density functional method (abbreviated as B3LYP method[78]). In this case, the H$\cdots$C bond lengths become much longer than those obtained at the MP2 level. The electron correlation effect on the length of the H$\cdots$C bond in transition structures of LiH addition has never been
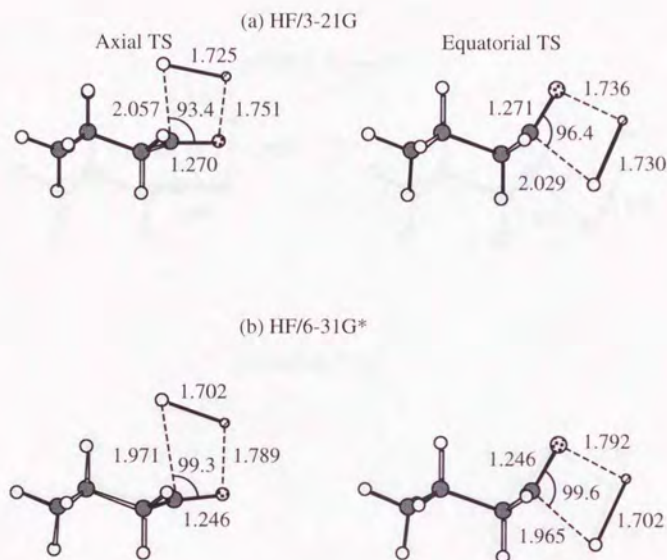
Figure 2-1. Axial (left) and equatorial (right) transition state structures of LiH addition to cyclohexanone. (a) HF/3-21G, (b) HF/6-31G* level. Bond lengths are given in Å.

described in the literature. This substantial elongation of the H···C bond suggests that the transition state of hydride reduction of cyclohexanone possibly appears at a very early stage of the reaction.

The energy differences (ΔE) of the axial and equatorial transition states are collected in Table 2-3. Dependence on the levels of calculations employed seems to be marginal. The energy difference at the MP2/6-31G*//MP2/6-31G* level is 1.24 kcal mol^{-1}, 0.61 kcal mol^{-1} smaller than that obtained at the HF/6-31G*//HF/6-

(c) HF/6-311++G**

(d) MP2/6-31G*
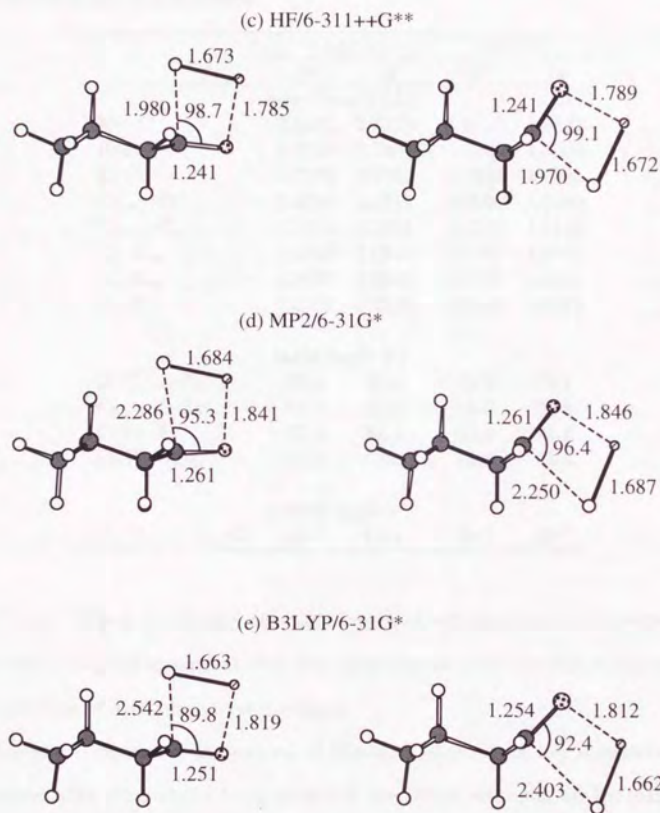
(e) B3LYP/6-31G*

Figure 2-2. Axial (left) and equatorial (right) transition state structures of LiH addition to cyclohexanone (continued). (c) HF/6-311++G**, (d) MP2/6-31G*, (e) B3LYP/6-31G* level. Bond lengths are given in Å.

Table 2-1. Selected Geometrical Parameters of the Transition State Structures of LiH Addition to Cyclohexanone

	3-21G		6-31G*	
	ax	*eq*	*ax*	*eq*
	bond length (Å)			
H$\cdots$C	2.0571	2.0278	1.9713	1.9647
H–Li	1.7245	1.7301	1.7020	1.7022
Li–O	1.7506	1.7359	1.7885	1.7923
$C_{C=O}$–O	1.2704	1.2711	1.2460	1.2460
$C_{C=O}$–C_α	1.5124	1.5101	1.5137	1.5128
C_α–H_{ax}	1.0808	1.0796	1.0921	1.0825
C_α–H_{eq}	1.0908	1.0805	1.0825	1.0825
C_α–C_β	1.5361	1.5544	1.5292	1.5419
	bond angle (°)			
H–$C_{C=O}$–O	93.4	96.4	99.3	99.6
$C_{C=O}$–O–Li	97.7	96.9	94.2	93.9
O–Li–H	92.8	92.2	91.3	91.2
Li–H–$C_{C=O}$	74.2	74.5	75.3	75.4
	torsion angle (°)			
C_α–$C_{C=O}$–C_α–C_β	43.2	62.6	39.9	60.7

31G* level. When the density functional method was employed, it becomes 1.70 kcal mol^{-1}, in good agreement with the experimental axial and equatorial ratio of the reduction of 4-*tert*-butylcyclohexanone.

Energies computed with removal of lithium hydride from the transition state structures with other atoms being fixed will give rough estimates for the strain energy of the ring at the transition state (Table 2-4). Frenking suggested based on their results at the MP2/6-31G*//HF/3-21G level that cyclohexanone ring in the equatorial transition state is less strained compared to that in the axial transition state.[45] However, with the larger basis set, the axial transition state becomes less

Table 2-2. Selected Geometrical Parameters of the Transition State Structures of LiH Addition to Cyclohexanone

	6-311++G**		MP2/6-31G*		B3LYP/6-31G*	
	ax	eq	ax	eq	ax	eq
bond length (Å)						
H$\cdots$C	1.9801	1.9701	2.2863	2.2495	2.5418	2.4031
H–Li	1.6731	1.6715	1.6842	1.6870	1.6629	1.6624
Li–O	1.7850	1.7891	1.8412	1.8460	1.8186	1.8121
$C_{C=O}$–O	1.2414	1.2414	1.2607	1.2618	1.2512	1.2540
$C_{C=O}$–C_α	1.5130	1.5125	1.5092	1.5066	1.5147	1.5143
C_α–H_{ax}	1.0931	1.0830	1.1027	1.0938	1.1042	1.0946
C_α–H_{eq}	1.0825	1.0828	1.0938	1.0933	1.0940	1.0937
C_α–C_β	1.5286	1.5411	1.5291	1.5421	1.5384	1.5513
bond angle (°)						
H–$C_{C=O}$–O	98.7	99.1	95.3	96.4	89.8	92.4
$C_{C=O}$–O–Li	93.9	93.6	94.7	94.0	97.8	96.1
O–Li–H	92.1	91.9	100.5	99.5	108.6	105.0
Li–H–$C_{C=O}$	75.2	75.4	69.5	70.1	63.8	66.4
torsion angle (°)						
C_α–$C_{C=O}$–C_α–C_β	39.4	60.8	41.1	60.3	41.4	57.3

Table 2-3. Calculated Absolute Energy, ZPVE[b], and Relative Energy of the Axial and Equatorial Transition States

	axial TS		equatorial TS		ΔE^a
	au	ZPVE[b]	au	ZPVE[b]	
HF/3-21G	−314.155 21	106.32	−314.153 72	106.35	0.93
HF/6-31G*	−315.910 70	106.44	−315.907 76	106.54	1.85
HF/6-311G++G**	−315.991 74	105.19	−315.989 06	105.34	1.68
MP2/6-31G*	−316.881 65	101.25	−316.879 67	101.28	1.24
B3LYP/6-31G*	−318.008 96	99.05	−318.006 26	99.21	1.70

[a] $\Delta E = E_{eq} - E_{ax}$ in kcal mol^{-1}. Scale factors for ZPVE correction are: 0.9207 (HF/3-21G), 0.9135 (HF/6-31G*), 0.9670 (MP2(fc)/6-31G*), 0.9806 (B3LYP/6-31G*).[79] [b] Zero-point vibrational energy in kcal mol^{-1}.

Table 2-4. Relative Energies of the Axial and Equatorial Transition States

	3-21G	6-31G*	$E_{eq} - E_{ax}$ (kcal mol^{-1}) 6-311++G**	MP2/6-31G*	B3LYP/6-31G*
TS	0.94	1.85	1.68	1.28	1.70
−H	−0.72	−0.05	−0.06	−1.27	0.17
−Li	3.05	3.86	1.86	4.39	4.41
−LiH	−0.04	0.64	0.53	−0.08	0.85

strained. The energy difference ($E_{eq} - E_{ax}$) becomes as large as 0.85 kcal mol^{-1} at the B3LYP/6-31G* level. However, it reduces to −0.08 kcal mol^{-1} at the MP2/6-31G* level. Owing to the numerical errors of the energy calculations, it seems difficult to determine in which transition state the cyclohexanone ring is more strained from these results. However, one could at least say that the strain energies in the cyclohexanone ring in the two transition states are almost identical. It is therefore assumed that the ring strain alone would not be the decisive factor for the stereoselectivity.

The importance of the hyperconjugative interaction between the forming H$\cdots$C bond and the adjacent allylic bonds is a central part of both the Felkin-Anh model and the Cieplak model. To know how much extent this interaction plays a role, we quantitatively evaluated the second-order perturbation energy of the orbital interaction between the $\sigma_{H\cdots C}$ and σ^*_{C-L} (L = H or C) orbitals, which corresponds to the hyperconjugation in the Felkin-Anh model, and that between the $\sigma^*_{H\cdots C}$ and σ_{C-L} orbitals, which corresponds to the hyperconjugation in the Cieplak model. These orbital interaction energy can be calculated with the Natural Bond Orbital method of Weinhold et al.,[57,80] and it is expressed as

$$E_2 = q_i \frac{F(i,j)^2}{\Delta E_{ij}} \tag{2.1}$$

where i and k correspond to the occupied and the vacant natural bond orbitals under consideration, $F(i,j)$ is the (i,j) element of the Fock matrix obtained by single point *ab initio* calculation, and q_i is the occupancy (electron population) of the ith orbital. The geometry obtained at the HF/6-31G* level was used for these calculations and the single point calculations were also performed at the HF/6-31G* level of theory to obtain E_2. Table 2-5 summarizes the results.

Surprisingly, the hyperconjugation in Felkin-Anh sense (the second column) is virtually null in both transition states. This can be due to the very early transition state, where the delocalization of electrons from the hydride to the bonding region of the $H \cdots C$ bond is substantially small. Since the electron population of $\sigma_{H \cdots C}$, which corresponds to q_i in equation (2.1), directly affects the magnitude of E_2, it should become almost nothing.

On the other hand, the hyperconjugation in Cieplak sense (the third column) is greater than that in Anh sense in both transition states. Since the σ orbital of the adjacent bonds has nearly two electrons, this interaction inevitably becomes larger than that of the Felkin-Anh type. These results indicate that the transition states of LiH addition are significantly electron deficient, and in such cases, the stabilization in Cieplak sense generally predominates over the stabilization in Anh sense. However, the stabilization energy in the equatorial transition state (1.26 kcal mol^{-1}) is slightly larger than that in the axial transition state (1.11 kcal mol^{-1}). It follows that the hyperconjugative interaction proposed in the Felkin-Anh and the

Cieplak models may be of no importance for the stereoselectivity of cyclohexanone.

Table 2-5. Quantitative Evaluation of the Hyperconjugative Interaction at the Transition States of LiH Addition to Cyclohexanone in terms of the Orbital Interaction Energy E_2 Derived by the NBO Method

	E_2 (kcal mol^{-1})	
	Felkin-Anh	Cieplak
	$\sigma_{H\cdots C} \rightarrow \sigma^*_{C-L}$	$\sigma_{C-L} \rightarrow \sigma^*_{H\cdots C}$
ax TS	0.00	1.11
eq TS	0.05	1.26

2.2 The Shape of the LUMO of Cyclohexanone

From the earliness of the transition state in metal hydride reduction of cyclohexanone described in the last section, and the fact that no large difference was observed in the torsional strain energies between the axial and equatorial transition states, and the failure of the hyperconjugative stabilization hypothesis described above, it is expected that the frontier molecular orbital interaction between reducing reagent and substrate ketones at an early stage of the reaction plays a role in the reaction process of hydride reduction.

In order to examine whether the frontier orbital effect is important or not in metal hydride reductions, *ab initio* molecular orbital calculation was performed and the feature of the lowest unoccupied molecular orbital (LUMO) of cyclohexanone was thoroughly investigated.

The geometry optimization of cyclohexanone was performed at several theoretical levels: the Hatree-Fock level using STO-3G, 3-21G, and 6- 31G* basis sets, and the

MP2/6-31G* level. Molecular orbital coefficients were calculated at the Hartree-Fock level using STO-3G, 3-21G, 4-31G, 6-31G*, and 6-31G** basis sets with the preoptimized frozen geometries. Contour diagrams of the LUMO of cyclohexanone at these theoretical levels are depicted in Figures 2-3, 2-4, and 2-5.

The shape of the LUMO of cyclohexanone calculated using STO-3G differs significantly in shape from other more sophisticated levels (Figure 2-3(a)). There seems to be no difference in the magnitude of the extension of the lobe at the carbonyl carbon at the axial and the equatorial sides at the HF/STO-3G level. On the other hand, when double zeta split valence basis set, which would usually produce more accurate results in *ab initio* calculations than minimal basis sets (e.g. STO-3G), was used in single point calculations, the LUMO of cyclohexanone significantly becomes distorted toward the axial face of cyclohexanone (Figure 2-3(a,b), Figure 2-4(c,d), and Figure 2-5(e)). This significant antisymmetry of the LUMO should contribute to the experimentally observed high axial face selectivity of the reduction of cyclohexanones.

Inspection of the molecular orbital coefficients of the LUMO at the carbonyl carbon of cyclohexanone has revealed following important points (Table 2-6). When the calculation is performed with STO-3G, the mixing of the 2s orbital at the carbonyl carbon is virtually null. The small negative value (-0.015) indicates the π^* orbital is slightly distorted to the equatorial side. This direction of the orbital distortion is the opposite to the observed stereoselectivity. On the other hand, the 2s coefficients at the carbonyl carbon calculated with 3-21G or larger basis sets are all positive and become greater as the accuracy of the basis sets is improved. This suggests that not only the correct direction of the orbital distortion but its magnitude depends heavily

(a) HF/STO-3G

the axial side

the equatorial side
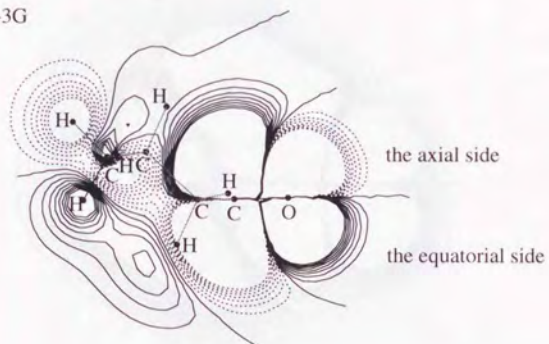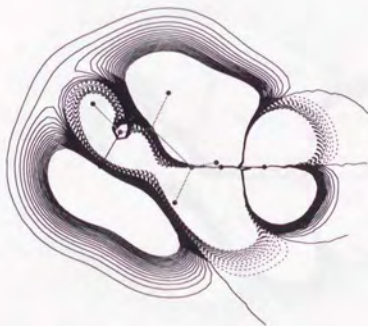
(b) HF/3-21G

Figure 2-3. Contour diagram of the LUMO of cyclohexanone at the various theoretical levels of theory: (a) HF/STO-3G, (b) HF/3-21G//HF/3-21G.

(c) HF/4-31G
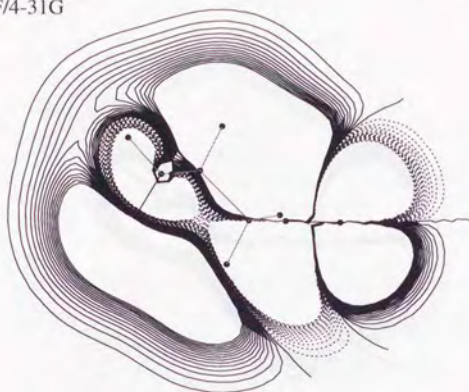
(d) HF/6-31G*
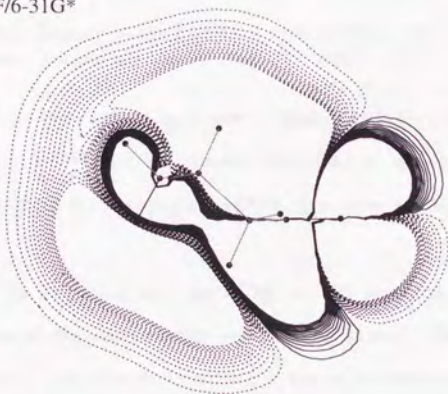
Figure 2-4. Contour diagram of the LUMO of cyclohexanone at the various theoretical levels of theory (continued): (c) HF/4-31G//HF/3-21G, (d) HF/6-31G*//HF/6-31G*.
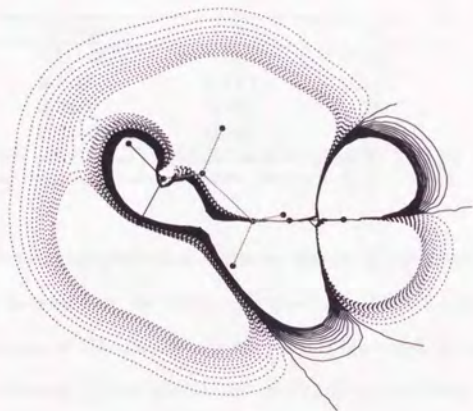
(e) HF/6-31G**

Figure 2-5. Contour diagram of the LUMO of cyclohexanone at the various theoretical levels of theory (continued): (e) HF/6-31G**//HF/6-31G*.

upon the choice of the basis set. It is, therefore, understandable without difficulty that Anh[16,17] and others[28,81] did not consider the effect of the orbital distortion as the fundamental factor for the stereoselectivity, since they employed less precise basis sets.

The mixing of the 2s orbital into the LUMO at the carbonyl carbon can be understood in terms of the second order perturbation theory. The cause of the mixing of the 2s orbital was formerly attributed to the hyperconjugative interaction of β-C–C bonds by Klein,[42] Frenking, on the other hand, ascribed it to the C–H bonds, which have larger interaction with the π^* orbital indicated by the Natural Bond Orbital analysis.[45]

Table 2-6. The 2s and 2p Orbital Coefficients[a] of the LUMO of the Carbonyl Carbon of Cyclohexanone Calculated at Several Levels of Theory

basis set	2s	2p
STO-3G	−0.015	0.795
3-21G	0.143	0.530
4-31G[b]	0.165	0.524
6-31G*	0.256	0.487

[a] Only outer orbital coefficients are listed except for STO-3G.
[b] Using the geometry obtained at the HF/3-21G level.

We show here by using the perturbation theory that the LUMO distortion toward the axial direction is caused by the three methylene unit (C3–C4–C5) rather than by the axial hydrogens at C2 and C6. As shown in Figure 2-6, the second-order perturbational coefficients (c''_{ji}) for the LUMO of cyclohexanone using the equation derived by Imamura[82] at the extended Hückel level[83, 84] suggest that the 2s orbital mixing into the LUMO at the carbonyl carbon through the three methylene unit (C3–C4–C5) is greater than that through the two axial hydrogens at C2 and C6: namely, the second order mixing coefficients (c''_{ji}) of the three occupied orthogonal MO's of C=O containing 2s orbital of the carbonyl carbon (−13.78, −19.19 and −34.25 eV) into the LUMO (−9.82 eV) through the three methylene unit (C3–C4–C5) are 0.173, 0.093 and 0.014, respectively, while the corresponding mixing coefficients through the two axial hydrogens at C2 and C6 are 0.104, 0.056 and 0.009, respectively.

Defining a new parameter which is capable of characterizing the magnitude of orbital distortion would be appropriate here for the sake of convenience. Let us call this parameter a distortion index, δ. The definition of δ is,
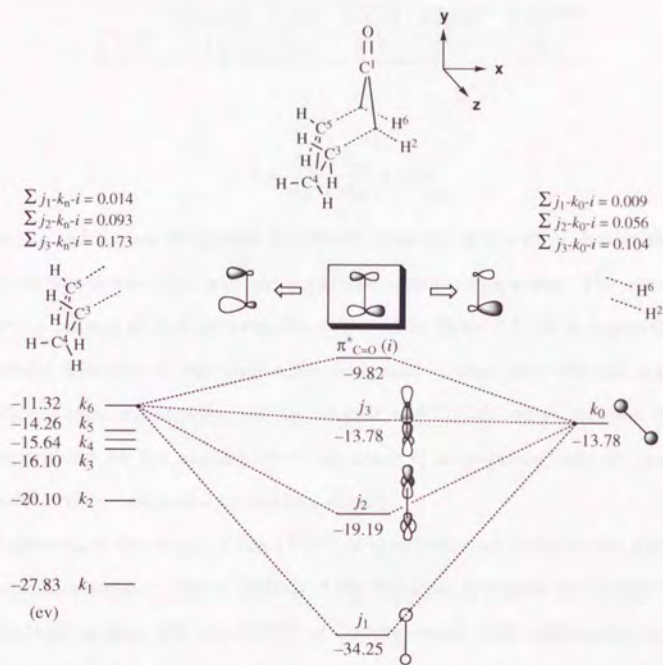
Figure 2-6. Mechanism of π^* orbital distortion. Secondary perturbation coefficients of the mixing of MO j (σ_{C-O}) into MO i ($\pi^*_{C=O}$) through MO k (C^3H_2-C^4H_2-C^5H_2 or H^2-H^6) were obtained at the extended Hückel level. Total mixing coefficients for MO j, which contains 2s AO contribution at the carbonyl carbon, are denoted as $\sum j_m$-k_n-i (m = 1, 2, 3; n = 0, 1, 2, 3, 4, 5, 6). Major interactions $\sum j_m$-k_n-i (m = 1, 2, 3; n = 0 or 6), all of which are out-of-phase mixing, are indicated by dotted lines.

Table 2-7. The Calculated Distortion Index for the LUMO of the Carbonyl Carbon of Cyclohexanone

	STO-3G	3-21G	4-31G	6-31G*	6-31G**
δ (%)	−2.2	31.4	35.5	55.1	53.6

$$\delta = \frac{d_{ax} - d_{eq}}{d_{ax} + d_{eq}} \times 100 \tag{2.2}$$

where d_{ax} and d_{eq} are integrated probability densities of the π^* orbital at the carbonyl carbon in the axial and the equatorial region respectively. The calculated distortion indices at various levels are collected in Table 2-7. It is apparent that the orbital distortion is very large when using split valence basis sets, but marginal and directs even the opposite side in the case of STO-3G, which provides further strong evidence for the importance of the choice of appropriate basis set upon the estimation of the integrated probability density.

Inspection of the shape of the LUMO of cyclohexanone revealed one more important characteristic. The 1s orbitals of the two axial hydrogens at C2 and C6 are substantially mixing into the LUMO of cyclohexanone with antibonding fashion. This antibonding contribution of the 1s orbitals at the axial hydrogens formerly attributed to the cause of the secondary orbital interaction in the equatorial attack by Kurita *et al.*[85] Due to the mixing of these orbitals into the LUMO, there arises a node in the equatorial region proximate to the carbonyl group. This node could become a harsh obstacle which impedes electron delocalization from the nucleophile into the electron deficient LUMO and retards the rate of reaction from the equatorial side. On the other hand, there is no such node in the axial area, indicating

Table 2-8. Data for Plots of the Location of the Node along the Linear Approach of Nucleophile against the Approaching Angle θ of Hydride. The Location is Expressed by the x-Coordinate of the Node in Å Unit.

$\theta(°)$	HF/6-31G*	MP2/6-31G*
90	3.00	3.31
95	2.72	2.96
100	2.50	2.69
105	2.33	2.48
110	2.20	2.31
115	2.10	2.18
120	2.02	2.08
125	1.96	2.00

the charge transfer from the incoming nucleophile into the LUMO would proceed smoothly without intervention.

The location of the node, where the value of the LUMO wave function becomes exactly null, was quantitatively estimated by calculating the values of the wave function at points along the linear paths passing through the carbonyl carbon and lying on a plane perpendicular to the carbonyl plane (Figure 2-7). When the nucleophile approaches from rectangular direction with respect to the π plane ($\theta = 90°$), the node appears at about 3.0 Å distance from the carbonyl carbon irrespective of the level of calculation. As the approaching angle (θ) is increased, the location (x-coordinate) of the node becomes monotonously closer to the carbonyl carbon. When θ equals 120°, it falls down to 1.8 Å, which is still outside the van der Waals (VDW) surface of carbon atom (The VDW radius for carbon is 1.70 Å[86]). This strongly indicates that the stereoselectivity would be determined outside the molecular surface.
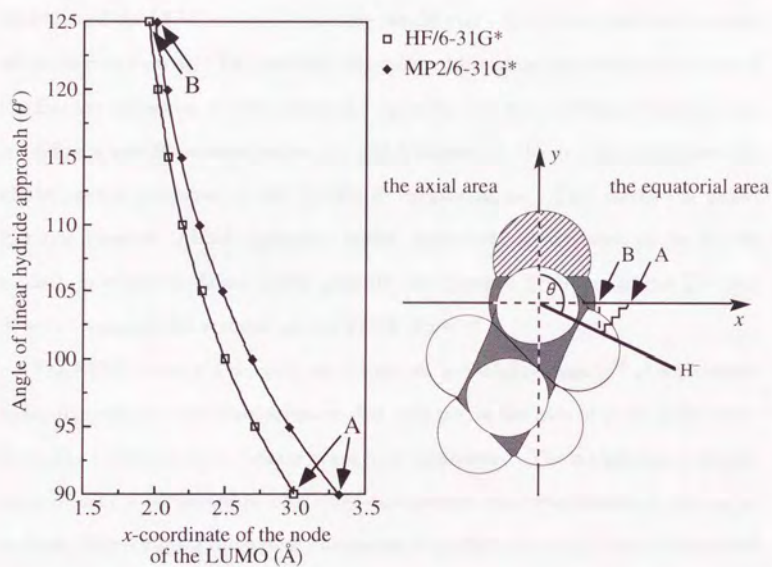
Figure 2-7. The location (x-coordinate) of the node in the equatorial region of cyclohexanone.

2.3   Description of the EFOE Model

From the earliness of the transition state and the existence of the node in the equatorial region of the molecule described in the previous section, it is indicated that the frontier molecular orbital interaction between the HOMO of the attacking hydride and the LUMO of cyclohexanone should play a significant role for the origin of the stereoselectivity. To quantitatively assess the magnitude of the importance of the frontier molecular orbital interaction upon the selection of the preferential face, we define a new theoretical parameter which focuses on the ground state character of the spatial extension of the LUMO of cyclohexanone. This method is called Exterior Frontier Orbital Extension model (henceforth abbreviated as the EFOE model), in which we define a new quantity, the Exterior Frontier Orbital Electron density (hereafter abbreviated as the EFOE density).

The EFOE density is basically an integrated probability density[87] of a canonical molecular orbital under consideration. For instance, in the case of nucleophilic reactions, the LUMO of the substrate is generally considered. The integration of probability density is performed in each three-dimensional space partitioned by the nodal π-plane. Approximate numerical integration is performed on all three-dimensional lattice points where the following two conditions are fulfilled:

i) These points should exist outside repulsive molecular surface (the exterior region) defined by an assembly of spherical atoms approximated by the van der Waals radii.[86] For the sake of computation time, those points located within 5 au (2.65 Å) from the approximated molecular surface, beyond which the value of a wave function is virtually null, are scanned incrementally along

the three Cartesian coordinate axes by the program.

ii) The probability density calculated at each point is assigned to a specific atom, if the absolute total value of the wave functions belonging to this atom makes the maximum contribution to the value of the whole wave function at that point.

The second condition is of crucial importance, for selection of such points should give an assembly of spatial points where the orbital overlap between reagents and substrate carbonyl effectively occurs. Namely, in the case of nucleophilic reactions of cyclohexanone, it means we choose such points where the two-electron stabilizing interaction arising from the overlap of the HOMO of the nucleophile and the LUMO of the substrate is substantial. An additional merit of considering only the outside area of molecule is that steric effects upon the approach of a nucleophile at an early stage of the reaction would be intrinsically incorporated into the integrated values to some extent.

To be more specific, suppose the entire LUMO wave function of the substrate ketone is expressed as $\Psi_L(r)$, and it can be linearly expanded with a summation of constituent basis functions within the LCAO approximation formalism, *i.e.*,

$$\Psi_L(r) = \sum_{i=1}^{N} C_i \psi_i(r) \tag{2.3}$$

where N is the number of atoms, C_i is a coefficient of the ith atom, and ψ_i is a set of atomic orbitals (basis functions) of the ith atom. ψ_i is further decomposed in the conventional treatment of *ab initio* molecular orbital theory to a set of primitive Gaussian type functions (GTO) as,[88]

$$\psi_i(r) = \sum_{j=1}^{M} c_{ji}\chi_{ji}(r), \tag{2.4}$$

where $j(= 1, \cdots, M)$ is a number of primitive GTOs associated with the ith atom.

The absolute value of $C_i\psi_i(x, y, z)$ is evaluated at each lattice point (x, y, z) in Cartesian coordinate space, and if it has the greatest contribution to the value of $\Psi_L(x, y, z)$ at that point than those of other atoms, $i.e.$,

$$|C_i\psi_i(x, y, z)| > |C_k\psi_k(x, y, z)|, \qquad (k \neq i). \tag{2.5}$$

then, $|\Psi_L(x, y, z)|^2 dr^3$ is assigned to the ith atom. dr^3 is the infinitely small volume at that point (x, y, z). Note here that we integrate $|\Psi_L(x, y, z)|^2 dr^3$. Previous orbital distortion models were mainly concerned only with the π^* orbital at the carbonyl carbon, whereas our method takes the entire LUMO wave function (Ψ_L) into account. Such an approach has never been done in previous studies on π-facial diastereoselection.

The integration of $|\Psi_L(x, y, z)|^2$ within the exterior region of a molecule gives the EFOE density.[89] Practically, the definite integral is approximated by a numerical integration as,

$$(EFOE) = \int_{\Omega} |\Psi_L(x, y, z)|^2 dr^3 \approx \Delta v \sum_{l,m,n} |\Psi_L(l, m, n)|^2, \tag{2.6}$$

where l, m, and n are a whole number corresponding to x, y, z coordinate respectively, and Δv is a finite minute volume which is a product of the three small increments along the three coordinate axes, $i.e.$,

$$\Delta v = \Delta l \Delta m \Delta n. \tag{2.7}$$

Here, for simplicity, we assume $\Delta x = \Delta y = \Delta z = \Delta r$, hence Δv can be written as Δr^3.

Since the required time of computation simply varies inversely with the cube of the increment (Δr^3) and the accuracy of the resulting integrated value is dependent proportionally to Δr^3, the smaller the increment, the longer it would take to accomplish the integration and the accuracy of the integration improved. Therefore, appropriate increment size must be chosen to speed up the calculation without affecting the reasonable accuracy of the resulting values. Therefore, we chose 0.2 Å for the unit length of the increment, as it was confirmed that the increment of this size is appropriate in terms of computation time as well as of the accuracy. If the lattice unit smaller than 0.2 Å was used, the resulting numerical errors occur in the third decimal place of the integrated values.

As mentioned above, steric effect is intrinsically incorporated into the EFOE density itself to some degree. However, this is not sufficient presumably due to the oversimplified approximation of the spherical atomic surface and the neglect of the size and shape of the reagent. Therefore, we will supplement steric discussions in terms of another steric parameter, atomic accessible space (abbreviated as AAS), which shows the magnitude of steric congestion around the carbonyl functionality. The AAS is defined as the spatial volume which is located in the closest proximity to the surface of the carbonyl carbon. The volume was computed within the same region where the EFOE density is integrated, and $\Delta v (= \Delta r^3)$ is collected if the

distance between the point and the surface of the carbonyl carbon is nearest than that of the remaining atoms.

It should be mentioned here that the EFOE density calculation has a close relationship with the Exterior Electron model proposed by Ohno *et al.*[90,91] The exterior electron density (EED) was introduced for a theoretical interpretation of experimental branching ratios observed in He* (2^3S) Penning ionization electron spectroscopy(PIES).[92] In the Exterior Electron model, electron density of a certain canonical molecular orbital outside repulsive molecular surface is considered. The electron density calculated with this method has been found to have a good correlation to the experimental band intensity for the corresponding molecular orbital in PIES spectra. Basis set dependence of calculated electron density along with the verification of the precision of wave function tails for several commonly used basis sets were also thoroughly studied by them.[91,93-97] The exterior electron model was successfully applied to a number of experimental results,[98-103] although it was also shown that the simple spherical atom model using van der Waals radii was inadequate in some cases.[90,92] They further investigated to gain insight for a better description of anisotropic molecular surface by intensive theoretical calculations in this regard, but the results reported were limited to some very simple molecules due to the laborious large scale computation.[104]

The exterior electron model mainly centers on a better description of the shape of a canonical molecular orbital. In contrast to this, our method intends to describe a specific reactivity of a certain spatial region of a canonical molecular orbital of a molecule in question. With selecting those spatial points where overlap between the frontier orbitals is large, one can readily extract the relative reactivity of a specific

exterior region of the molecule if the reaction under consideration is controlled by the FMO interaction. This point will be examined thoroughly with cyclohexanone and alkyl-substituted cyclohexanones as representative model compounds in the next section.

2.3.1 The EFOE Density of the LUMO of Cyclohexanone

A series of EFOE density calculations of the LUMO of cyclohexanone were carried out at various theoretical levels to investigate the effect of the theoretical level used upon the integrated density values. The calculated EFOE densities at various levels along with atomic accessible space values for each optimized geometry, distortion indices of the LUMO at the carbonyl carbon, and the energy level of the LUMO in hartrees are collected in Table 2-9. The geometry of cyclohexanone was optimized at the Hartree-Fock as well as the MP2 level, and molecular orbital coefficients for the density calculation were obtained from single point calculations performed at the Hartree-Fock levels using several basis sets specified in the table.

The values of atomic accessible space of the axial and the equatorial side around the carbonyl carbon indicate that substantially larger steric hindrance would be expected in the axial attack of nucleophile. The column of the distortion indices clearly shows the basis set dependence of this value as previously noted in Table 2-7 on page 37.

The calculated EFOE densities have the following noticeable tendencies. (i) When the calculation is performed using STO-3G basis set with whatever geometries listed in the table, there is only a slight difference in the axial and the equatorial density values. (ii) However, the axial and the equatorial differences calculated using

Table 2-9. EFOE Density, Atomic Accessible Space, Distortion Index, and the Energy Level of the LUMO of Cyclohexanone at Various Theoretical Levels

Basis	EFOE density (%)		AAS[a] (au³)		Distortion	LUMO
	ax	eq	ax	eq	index δ (%)	level (au)
STO-3G structure						
STO-3G	0.149	0.138	17.0	56.0	3.1	0.29910
3-21G structure						
STO-3G	0.138	0.130	14.9	55.8	−1.9	0.30059
3-21G	1.275	0.573	14.9	55.8	28.8	0.16332
4-31G	1.348	0.387	14.9	55.8	31.9	0.15059
6-31G*	1.679	0.388	14.9	55.8	49.3	0.15625
6-31G* structure						
STO-3G	0.153	0.114	19.4	47.2	−2.2	0.30832
3-21G	1.416	0.458	19.4	47.2	31.4	0.16855
4-31G	1.543	0.266	19.4	47.2	35.5	0.15542
6-31G*	1.940	0.249	19.4	47.2	55.1	0.16065
MP2/6-31G* structure						
6-31G*	1.647	0.394	14.6	55.2	46.0	0.15140

[a] Atomic accessible space.

double zeta basis sets become larger than that obtained with STO-3G. As the precision of the basis set increases, the density of the axial side monotonously increases, whereas that of the equatorial side monotonically decreases. At the extreme, when the HF/6-31G*//HF-6-31G* level is employed, the difference between the axial and the equatorial density reaches to 1.691%. This significant large difference in the calculated EFOE densities indicates that some correlation may exist between facial selectivity of reduction of cyclohexanone and the EFOE density values.

It should be noted that when the geometry obtained at the MP2 level is used, the integrated EFOE density at the axial side slightly decreases and that of the

equatorial side slightly increases compared to those values at the HF/6-31G* level. These values become roughly the same as those obtained at the HF/3-21G//HF/3-21G level. This change in magnitude of the EFOE densities can be attributed to the precision of the optimized molecular geometry. The geometrical parameters of cyclohexanone obtained at the MP2 level are similar to those at the HF/3-21G level (Table 2-10). It is known that the bond lengths calculated at the Hartree-Fock level are likely to become shorter than experimentally determined equilibrium bond lengths due to both the neglect of electron correlation effects and the anharmonicity effects. Furthermore, bond lengths obtained with 6-31G* is generally shorter than those obtained with 3-21G basis set for large molecules.[105] These too short bond lengths can be corrected by the Møller-Plesset perturbation theory which takes into account electron correlation effect in a moderate degree. Bond lengths obtained at the MP2 level are much closer to the experimental values even when 6-31G* basis set is used. However, it was *experimentally* proved that the 3-21G or lower basis sets are generally inadequate for electron density calculation.[91,93-95,97] To better reproduce the experimentally observed PIES band intensity of a spatially expanding orbital, such as the lone-pair orbital on nitrogen, it was shown that 4-31G or larger basis must be used. In the assessment of the LUMO extension of the carbonyl compounds, we deal with spatially more extended π-type vacant orbital than bonding orbitals whose electrons are generally concentrated within the bonding region between nuclei. Therefore, it is relevant that basis sets larger than 4-31G must be used for a proper description of the distribution of electron density for virtual orbitals. From the above consideration, it is assumed that the true values would lie somewhere in between those obtained at the 3-21G and 6-31G* levels. Though it would be desirable to

Table 2-10. Selected Geometrical Parameters of Cyclohexanone
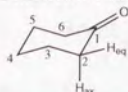
	3-21G	6-31G*	6-311++G**	MP2/6-31G*
		bond length (Å)		
C=O	1.2120	1.1929	1.1893	1.2287
C^1–C^2	1.5150	1.5171	1.5160	1.5154
C^2–H_{ax}	1.0869	1.0895	1.0900	1.0993
C^2–H_{eq}	1.0814	1.0827	1.0828	1.0937
C^2–C^3	1.5472	1.5366	1.5359	1.5363
		torsion angle (°)		
C^2–C^1–C^6–C^5	54.5	49.0	49.5	52.0

perform all the geometry optimizations at the more accurate MP2/6-31G* level, this level of theory is very costly and time-consuming. Therefore, the EFOE densities presented henceforth will be those values obtained at both HF/3-21G//HF/3-21G and HF/6-31G*//HF/6-31G* levels.

2.3.2 Alkyl-Substituted Cyclohexanones

To examine whether the EFOE model is generally applicable to a wide variety of six-membered ketones, we next investigated several alkyl-substituted cyclohex-anones (Figure 2-8). Calculated data at the HF/3-21G level are listed in Table 2-11 and those at the HF/6-31G* level are shown in Table 2-12.

In the case of 4-*tert*-butylcyclohexanone (**2**), whose stereoselectivity data have been amply reported, the EFOE densities at the axial side at both 3-21G and 6-31G*
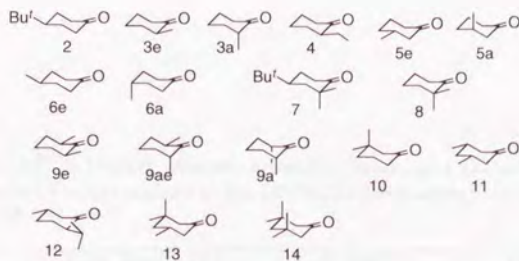
Figure 2-8. Various alkyl-substituted cyclohexanones investigated.

levels are larger than those at the equatorial side. This is in very good agreement
with the experimental results. 2-Methylcyclohexanones (**3a**, **3e**) are mobile in solu-
tion and they can easily transform each other. Both conformation may be involved
in the reaction. Wigfield reported that equatorial alcohol is solely derived from
the axial attack on the more stable conformer with equatorial methyl group (**3e**),
whereas 51% of axial alcohol is produced from axial attack on **3a** and the remaining
portion is derived from equatorial attack on **3e**.[106] The values of AAS of the equa-
torial side of **3a** are substantially smaller (3-21G: 17.0, 6-31G*: 14.9) compared to
those of **3e** (3-21G: 51.9, 6-31G*: 47.8), indicating large steric effect exist in the
equatorial attack of hydride on **3a**, which may cause predominant axial attack on
3e.

Selectivities of other cyclohexanones are generally in qualitative agreement with
the observed selectivity (Table 2-11 and 2-12).

Table 2-11. EFOE Density, Atomic Accessible Space, and Distortion Index of Alkyl-substituted Cyclohexanones at the HF/3-21G Level along with Experimental Product Ratio[a]

Compd	EFOE density (%)		AAS[a] (au³)		δ^b	Exp.[c]
	ax	eq	ax	eq	(%)	ax:eq
2	1.199	0.565	14.7	55.2	28.1	86:14
3a	1.265	0.579	14.6	17.0	19.9	
3e	1.189	0.579	11.0	51.9	28.3	70:30
4	1.194	0.576	12.0	51.3	28.6	65:35
5a	0.845	0.558	4.2	57.1	25.6	
5e	1.261	0.592	14.5	55.5	28.2	86:14
6a	1.296	0.552	14.1	55.1	28.1	
6e	1.237	0.563	14.7	54.9	29.0	86:14
7	1.192	0.551	13.7	17.4	18.4	92:8
8	1.249	0.578	13.7	17.3	19.0	
9e	1.124	0.590	10.2	46.0	28.2	62:38
9a	1.247	0.433	41.5	3.2	−6.5	
9ae	1.198	0.609	14.0	14.9	18.6	
10	0.805	0.555	5.0	56.7	25.9	48:52
11	1.237	0.605	14.3	55.2	27.6	
12	1.008	0.582	8.9	30.1	28.4	69:31
12′[d]	1.108	0.566	11.2	46.5	28.4	
13	0.789	0.576	5.0	56.7	25.3	48:52
14	0.391	0.665	1.5	64.5	20.4	45:55[e]

[a] Atomic accessible space. [b] Distortion index (positive in the axial side). [c] NaBH$_4$ in 2-PrOH. [d] The second most stable isomer. [e] LiAlH$_4$.

Table 2-12. EFOE Density, Atomic Accessible Space, and Distortion Index of Alkyl-substituted Cyclohexanones at the HF/6-31G* Level along with Experimental Product Ratio[a]

Compd	EFOE density (%)		AAS[a] (au^3)		δ^b	Exp.[c]
	ax	eq	ax	eq	(%)	ax:eq
2	1.799	0.249	19.6	46.7	52.8	86:14
3a	1.868	0.369	22.1	14.9	37.5	
3e	1.793	0.274	15.0	47.8	53.4	70:30
4	1.744	0.306	14.6	47.7	51.1	65:35
5a	1.447	0.211	7.9	48.4	52.5	
5e	1.884	0.304	18.4	47.8	47.9	86:14
6a	2.005	0.219	19.5	45.7	56.4	
6e	1.882	0.245	19.7	46.5	54.0	86:14
7	1.815	0.319	16.9	14.8	37.2	92:8
8	1.925	0.348	16.7	15.0	38.8	
9	1.665	0.298	12.5	44.9	52.4	62:38
9a	1.527	0.661	38.0	3.6	−7.1	
9ae	1.772	0.392	17.0	14.3	36.4	
10	1.292	0.232	6.9	48.4	49.6	48:52
11	1.824	0.349	17.5	48.3	47.2	
12	1.264	0.478	9.1	29.3	38.4	69:31
12$^{\prime d}$	1.731	0.282	13.0	42.1	50.0	
13	1.221	0.282	6.5	49.1	46.2	48:52
14	0.788	0.313	2.8	43.1	45.9	45:55^d

[a] Atomic accessible space. [b] Distortion index (positive in the axial side). [c] NaBH$_4$ in 2-PrOH. [d] The second most stable isomer. [e] LiAlH$_4$.

2.4   Correlation of the EFOE Density with

Kinetic Parameters

To be physically meaningful, the EFOE density values should have some corre-
lation with certain experimental values relating to the respective rate of reaction
at the axial and the equatorial face. In this regard, relationship of experimental
activation parameters and calculated values were examined.

Based on the FMO theory, it is expected that within a series of compounds of
similar structure, the activation enthalpy for the axial and the equatorial additions
to cyclohexanone ($\Delta H_{ax}^{\ddagger}$ and $\Delta H_{eq}^{\ddagger}$ respectively) should be roughly proportional to
the square of the overlap integral (S) between the HOMO of a nucleophile and the
LUMO of a substrate ketone. Therefore, it can be assumed that the square of the
EFOE density value at one side of the carbonyl plane should have some correlation
with the corresponding activation enthalpy. The larger the square of the overlap
integral between the frontier orbitals, the lower the activation enthalpy. This sug-
gests that the EFOE density should have some correlation with the experimentally
determined activation enthalpy differences ($\Delta\Delta H^{\ddagger} = \Delta H_{eq}^{\ddagger} - \Delta H_{ax}^{\ddagger}$). It is therefore
expected that $\Delta\Delta H^{\ddagger}$ should be roughly proportional to the difference in the square
of the EFOE density values ($\lambda = EFOE(ax)^2 - EFOE(eq)^2$) between the two faces
of the carbonyl plane.

To be more specific, this assumption can be qualitatively explicable within the
framework of the extended Hückel theory. The two-electron stabilization energy ΔE
for the interaction of the frontier orbitals can be expressed as

$$\Delta E = \frac{(\beta - S\varepsilon_H)^2}{\varepsilon_L - \varepsilon_H} \tag{2.8}$$

where ε_H and ε_L are the energy level of the HOMO of a hydride and the LUMO of a ketone respectively, and β and S are the resonance integral and the overlap integral of these frontier orbitals respectively. Substituting β in equation (2.8) with the Wolfsberg-Helmholz equation

$$\beta \approx \frac{K}{2}S(\varepsilon_L + \varepsilon_H) \tag{2.9}$$

where K is a constant, one obtains a relationship between ΔE and S as

$$\Delta E \propto \frac{1}{\varepsilon_L - \varepsilon_H}\{\frac{K}{2}S(\varepsilon_L + \varepsilon_H) - S\varepsilon_H\}^2 \tag{2.10}$$

$$= S^2 \frac{1}{\varepsilon_L - \varepsilon_H}\{\frac{K}{2}(\varepsilon_L + \varepsilon_H) - \varepsilon_H\}^2 \tag{2.11}$$

Since it can be assumed there would be no large difference in ε_L in structurally similar compounds (see Table 2-11 and 2-12), ε_L can be considered as almost a constant. ε_H is the energy level of the HOMO of a hydride, which can also be considered as a constant. Since K is also a constant, one can assume that the following relation between ΔE and S holds:

$$\Delta E \propto S^2 \tag{2.12}$$

From equation (2.8), the difference in the stabilization energy between the axial and the equatorial attack can be written as follows

$$\Delta\Delta E = \Delta E_{ax} - \Delta E_{eq} \tag{2.13}$$

$$\propto S_{ax}^2 - S_{eq}^2 \tag{2.14}$$

$$\propto \Delta\Delta H^\ddagger \tag{2.15}$$

where S_{ax} and S_{eq} correspond to the overlap integral of the axial and the equatorial transition state respectively and

$$\Delta\Delta H^\ddagger = \Delta H_{eq}^\ddagger - \Delta H_{ax}^\ddagger \tag{2.16}$$

Since the EFOE density assigned to an atom represents the probability of finding that portion of electrons in the exterior region of that atom, it may be assumed that there is some relationship between the EFOE density and the overlap integral. Since both the EFOE density and the overlap integral have the same dimension, they should roughly be related as

$$S \propto EFOE \tag{2.17}$$

Using this relationship, equation (2.15) now becomes

$$\Delta\Delta E \propto S_{ax}^2 - S_{eq}^2 \tag{2.18}$$

$$\propto EFOE(ax)^2 - EFOE(eq)^2 \tag{2.19}$$

Therefore, we obtain proportional relationship between $\Delta\Delta H^{\ddagger}$ and the square of the EFOE density values, *i.e.*,

$$\Delta\Delta H^{\ddagger} \propto EFOE(ax)^2 - EFOE(eq)^2 \qquad (= \lambda) \qquad (2.20)$$

The above condition (equation (2.17)) is indeed oversimplified. However, since the attacking nucleophile is completely ignored in the EFOE density calculation and furthermore this density describes a property of a molecule at the ground state, not that at the transition state, it seems difficult to obtain exact relationships of p_{ax}, p_{eq}, q_{ax}, and q_{eq} only through purely mathematical considerations. Although a precise relationship would be desirable, if some proportionality like equation (2.20) was indeed observed between experimental and calculated values, it could be thought as a strong evidence that supports a significance of orbital effects in π-facial stereoselective reactions. Besides, it would be possible to gain insight into a relationship between $EFOE$ and S from such proportionality of a plot of these values.

Therefore, relationship between available $\Delta\Delta H^{\ddagger}$ and calculated values was investigated. Appropriate data for such an objective were found in Wigfield's paper, in which $\Delta\Delta H^{\ddagger}$ determined from kinetic analyses of sodium borohydride reductions in 2-propanol for various alkyl-substituted cyclohexanones were reported.[69] Numerical data of $\Delta\Delta H^{\ddagger}$ and calculated λ for ten alkyl-substituted cyclohexanones including three sterically crowded ketones are presented in Table 2-13, and plots of these values are shown in Figure 2-9.

One may recognize good linear correlations in both levels ($r^2 = 0.96$ (HF/3-21G) and 0.94 (HF/6-31G*)). These linear correlations between the EFOE values (λ)
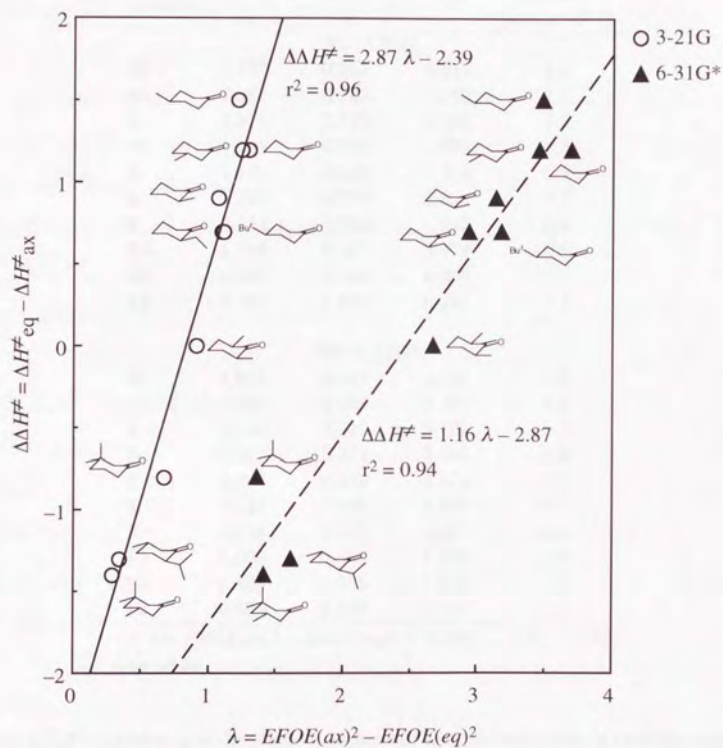
Figure 2-9. Linear relationship between the difference in the square of the EFOE density for the two faces (λ) and experimentally determined activation enthalpy (solid line: HF/3-21G, dashed line: HF/6-31G*).

Table 2-13. λ and Activation Enthalpy of Alkyl-substituted Cyclohexanones

| Compd | EFOE density (%) | | λ^a | $\Delta\Delta H^{\ddagger b}$ |
	ax	eq		(kcal mol^{-1})
	HF/3-21G			
6e	1.237	0.563	1.213	1.5
5e	1.261	0.592	1.239	1.2
1	1.275	0.573	1.298	1.2
3e	1.189	0.579	1.078	0.9
2	1.199	0.565	1.119	0.7
4	1.194	0.576	1.094	0.7
9	1.124	0.590	0.915	0.0
12	1.008	0.582	0.678	−0.8
10	0.805	0.555	0.339	−1.3
13	0.789	0.576	0.291	−1.4
	HF/6-31G*			
6e	1.882	0.245	3.481	1.5
5e	1.884	0.304	3.457	1.2
1	1.940	0.249	3.701	1.2
3e	1.793	0.274	3.141	0.9
2	1.799	0.249	3.174	0.7
4	1.744	0.306	2.947	0.7
9	1.124	0.590	2.682	0.0
12	1.008	0.582	1.369	−0.8
10	0.805	0.555	1.616	−1.3
13	0.789	0.576	1.412	−1.4

^{a} $\lambda = EFOE(ax)^2 - EFOE(eq)^2$. ^{b} $\Delta\Delta H^{\ddagger} = \Delta H_{eq}^{\ddagger} - \Delta H_{ax}^{\ddagger}$ from ref 69.

and $\Delta\Delta H^{\ddagger}$ indicate that the stereochemistry of hydride reduction in cyclohexanone based systems may be dictated in large part by the spatial extension of the LUMO at two faces of the carbonyl plane of a substrate ketone.

These plots provide an important finding related to the physical meaning of the EFOE density. As can be seen in these plots, sterically hindered ketones, such as

3,3,5-trimethylcyclohexanone (**13**), show only marginal deviation from the least-square regression line. The experimental ratio of the axial and the equatorial attack of **13** in NaBH$_4$ reduction is 48:52, and the activation enthalpy difference ($\Delta\Delta H^{\ddagger}$) is -1.4 kcal mol^{-1}, indicating the proportion of the axial attack is decreased due to the steric hindrance of the axial methyl group at C3. This reversal of face selectivity is not reproduced by the EFOE density values at both 3-21G and 6-31G* levels. The $EFOE(ax)$ values are larger than the $EFOE(eq)$ values at both levels. This discrepancy between qualitative predictions based on the EFOE density values and the experimental selectivity can also be seen in 3,3-dimethylcyclohexanone (**10**). This strongly indicates that the qualitative prediction using the EFOE density values is not valid in some cases where other than genuine orbital effects, such as steric effects, play significant roles in the determination of the preferential reaction course. In other words, when the qualitative prediction based on the EFOE density fails, some other factors are expected to be of importance. That is, the EFOE density value really is a useful parameter that serves to unravel the relative importance of the frontier orbital effects in nucleophilic reactions using sterically undemanding nucleophiles.

One more important point should be addressed. From Figure 2-9, one can obtain a rough insight into how much the initial state interaction directly relates to the activation enthalpy difference. From the slope of the least-square regression lines, it can be estimated about 35% ($= 1/2.87 \times 100$) to 86% ($= 1/1.16 \times 100$) of the ground state stabilization survives in the activation enthalpy differences. As noted previously (section 2.3.1), the true density values are expected to lie in between the values obtained at the HF/3-21G and the HF/6-31G* levels. Therefore, in a very

rough estimate, one can say that the average of 60% of $\Delta\Delta H^{\ddagger}$ is derived from the initial interaction of the reagent and the substrate.

2.5 Summary

The stereoselectivity observed in simple metal hydride reductions of cyclohexanone and its alkyl derivatives has been revealed to be controlled by the frontier orbital effects to large extent. The EFOE model is introduced to inspect the significance of such orbital effects in hydride reductions of these compounds. There is a good linear correlation between the calculated EFOE density values and the experimentally determined activation enthalpy of these compounds. This strongly suggests that the energy stabilization derived from the initial frontier orbital interaction correlates to the activation barriers of the reaction. Other factors seen at the transition state, such as torsional effects or hyperconjugative interactions, seem to be of less importance for the stereoselectivity.

The physical meaning of the EFOE density values lies in its relation to the overlap integral of the HOMO of a nucleophile and the LUMO of a substrate ketone at the initial state. Exact relationship of these values could not be determined owing to the neglect of reactants in the EFOE model. However, the linear correlation observed in Figure 2-9 suggests asymmetric orbital extension of the LUMO at the carbonyl in the ground state is significant in π-facial stereoselection in contrast to the recent criticisms of others.

In such cases where steric effects override orbital effects, qualitative predictions in terms of the EFOE model may fail. However, the proportionality between the

EFOE density values and the activation enthalpies still remains in these situations. Therefore, one cannot attribute the origin of the π-facial stereoselectivity of cyclo-hexanones solely to orbital effects in general. Steric effects ought to be considered as well in equal weight in such cases.

Chapter 3

π-Facial Stereoselectivity of Various Cyclic Ketones

The significance of the orbital effects on the π-facial stereoselectivity of hydride reduction of cyclohexanone and its alkyl derivatives has been clarified in the last chapter. In this chapter, various cyclic ketones will be investigated and the importance of the orbital effects upon the stereoselectivity of these compounds will be examined.

3.1   Substituted *trans*-Decalones

Owing to the geometrical similarity with cyclohexanone, the stereoselectivity of substituted *trans*-decalone derivatives has attracted interests. Houk *et al.* investigated the stereoselectivity of a series of *trans*-decalones substituted by electron-withdrawing groups at C4 both experimentally and computationally.[35] His results of sodium borohydride reductions are listed in Table 3-1.

All the substrates have axial preference. A particularly noteworthy feature is that the percentage of the axial attack (A) differs depending on the choice of 4-substituent as well as on its direction. When the 4-substituent points to the axial direction, the percentage of the axial attack increases 12–24 % relative to the equatorial substitution.

Table 3-1. Experimental Results of Sodium Borohydride Reduction of 4-Substituted *trans*-Decalones[a]
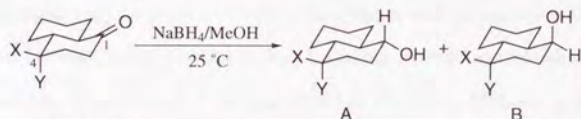
Compd	X	Y	A:B
15	H	H	60:40
16e	OH	H	61:39
16a	H	OH	85:15
17e	OAc	H	71:29
17a	H	OAc	83:17
19e	Cl	H	71:29
19a	H	Cl	88:12
18e	Br	H	66:34
20a	H	F	87:13

[a] ref. 35
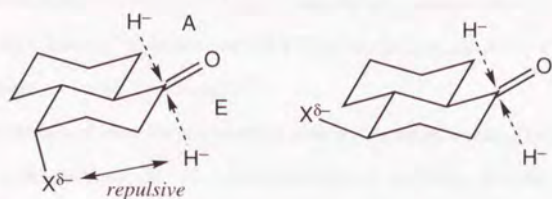
Figure 3-1. Repulsive electrostatic interaction proposed by Houk.[35]

Houk interpreted these results through a series of model calculations using 4-substituted cyclohexanones. He evaluated relative activation energies of transition states of LiH addition to 4-substituted cyclohexanones through single point energy calculations using the fully optimized transition structures of the same reaction to cyclohexanone. 4-Substituted cyclohexanones were not optimized. Substituents were simply attached at C4 with standard geometries. He insisted that both the torsional strain generally found in cyclohexanone systems and the repulsive electrostatic interaction between the 4-substituent and incoming hydride are responsible for the stereoselectivity (Figure 3-1). Namely, when the electron-withdrawing substituent points to the axial direction, severe electrostatic repulsion emerges between the partially negatively charged substituent and hydride which impedes the approach of the hydride from the equatorial direction, causing decrease of the equatorial selectivity. On the other hand, there would be no such impedance when the substituent points to the equatorial direction.

The Cieplak model fails to account for the change in selectivity, since the direction of the 4-substituent would not be expected to exert noticeable differences in the

electron donating ability of β-C–C bonds. Dannenberg claimed that the results are explicable with their π^*-polarization (PPFMO) method again using 4-substituted cyclohexanones as model compounds.[59]

We also examined these stereochemical preferences using 4-substituted cyclohexanones as model compounds. The results are shown in Tables 3-2 and 3-3. In the calculation of **23** (X = Br) at the HF/6-31G* level, the Huzinaga (43321/4321/311*) basis was used for a bromine atom.[88] In the case of 4-amino- (**25**) and 4-hydroxy-cyclohexanones (**24**), two conformations of the substituents, $i.e.$, the lone pairs inside and outside the ring, are also considered as were treated by Houk and Dannenberg.[35,59] In both cases, the outside conformation is energetically more stable than the inside conformation at the ground state.

Obviously, it is unable to explain the selectivity with distortion indices alone. Since steric environments around the carbonyl group estimated by the AAS values are almost the same in all compounds, an explanation based on steric effects is difficult to be made.

Comparison of the EFOE values are somewhat problematic in these cases. For example, in the case of **24** (X = OH), the EFOE densities of the axial area is larger than those of the equatorial area, in agreement with the increase of the axial selectivity when the hydroxyl group points to the axial direction. However, the EFOE densities of the equatorial side are also affected by the direction of substituent as well as its conformation.

The difference of stereoselectivity with respect to the direction of the substituents seem to correlate with the difference of the square of the EFOE values of both faces ($\lambda = EFOE(ax)^2 - EFOE(eq)^2$). For instance, λ of **24a**(in) (3-21G: 1.542, 6-31G*:

Table 3-2. EFOE Density, Atomic Accessible Space, Distortion Index, and the LUMO Level of 4-Substituted Cyclohexanones at the HF/3-21G Level

	X
21	F
22	Cl
23	Br
24	OH
25	NH$_2$
26	SiH$_3$

Compd	X	EFOE density (%)		AAS^a (au^3)		δ^b	E_{LUMO}
		ax	eq	ax	eq	(%)	(au)
21e	F	1.276	0.546	16.7	51.7	32.4	0.15017
21a	F	1.368	0.684	15.5	52.8	31.3	0.16019
22e	Cl	1.096	0.582	16.1	52.7	37.4	0.14399
22a	Cl	0.620	0.487	15.5	54.3	40.8	0.14513
23e	Br	0.804	0.530	15.9	53.5	42.7	0.14838
23e	Br^e	0.232	0.056	15.9	53.5	−30.6	0.15312
23a	Br	0.348	0.297	15.6	53.7	42.2	0.14223
23a	Br^e	0.968	0.345	15.6	53.7	20.0	0.16993
24e(out)^c	OH	1.259	0.591	15.2	54.3	31.7	0.15438
24e(in)^d	OH	1.224	0.557	16.3	52.5	31.0	0.15712
24a(out)^c	OH	1.296	0.523	14.7	55.6	26.6	0.15224
24a(in)^d	OH	1.395	0.636	16.1	54.7	30.3	0.16774
25e(out)^c	NH$_2$	1.248	0.581	14.9	55.0	30.2	0.16103
25e(in)^d	NH$_2$	1.215	0.538	16.3	52.8	29.6	0.16229
25a(out)^c	NH$_2$	1.295	0.541	14.4	55.3	27.3	0.16114
25a(in)^d	NH$_2$	1.374	0.613	15.1	54.4	31.1	0.17230
26e	SiH$_3$	0.959	0.399	14.4	55.5	19.3	0.15589
26a	SiH$_3$	0.785	0.345	14.1	54.5	30.0	0.15053

^{a} Atomic accessible space. ^{b} Distortion index. ^{c} Lone pair outside the ring. ^{d} Lone pair inside the ring. ^{e} LUMO+1.

4.238) is larger than that of **24a**(out) (3-21G:1.407, 6-31G*:3.811) (Table 3-2 and 3-3). Conversely, λ of **24e**(in) (3-21G: 1.188, 6-31G*: 3.415) is smaller than that of **24e**(out) (3-21G:1.273, 6-31G*:3.589). These trends are in very good agreement with the calculated energy differences (ΔE) of the transition state structures of

Table 3-3. EFOE Density, Atomic Accessible Space, Distortion Index, and the LUMO Level of 4-Substituted Cyclohexanones at the HF/6-31G* Level

Compd	X	EFOE density (%)		AAS^a (au^3)		δ^b	E_{LUMO}
		ax	*eq*	*ax*	*eq*	(%)	(au)
21e	F	1.947	0.246	21.3	44.5	56.4	0.14951
21a	F	2.151	0.359	20.1	47.3	55.7	0.15788
22e	Cl	1.943	0.229	21.1	44.9	55.5	0.14646
22a	Cl	1.824	0.333	20.4	45.5	58.3	0.15134
23e	Br^e	0.001	0.008	20.8	45.2	−10.5	0.13436
23e	Br	1.861	0.255	20.8	45.2	57.1	0.14550
23a	Br^e	0.150	0.099	20.2	45.5	68.5	0.13166
23a	Br	1.894	0.224	20.2	45.5	53.5	0.15848
24e(out)^c	OH	1.916	0.289	19.7	46.7	56.3	0.15344
24e(in)^d	OH	1.862	0.230	21.3	44.5	55.4	0.15454
24a(out)^c	OH	1.961	0.184	18.7	47.7	54.3	0.15078
24a(in)^d	OH	2.077	0.275	20.0	46.6	55.6	0.16259
25e(out)^c	NH_2	1.882	0.265	19.6	46.9	55.2	0.15728
25e(in)^d	NH_2	1.823	0.217	21.5	44.2	54.4	0.15797
25a(out)^c	NH_2	1.970	0.190	19.1	46.6	54.9	0.15705
25a(in)^d	NH_2	2.026	0.248	20.6	45.4	51.9	0.16613
26e	SiH_3	0.744	0.085	19.3	47.2	40.7	0.14709
26a	SiH_3	0.864	0.090	19.2	45.8	56.2	0.14492

^{a} Atomic accessible space. ^{b} Distortion index. ^{c} Lone pair outside the ring. ^{d} Lone pair inside the ring. ^{e} LUMO+1.

LiH attack on 4-substituted cyclohexanones reported by Houk.[35] Dannenberg also pointed out their polarization values have similar trends.[59]

To further verify such a correlation, ΔE calculated by Houk as well as the natural logarithm of the experimental selectivity $\ln(ax/eq)$ were plotted against λ (Table 3-4).

At first glance, one cannot see relevant correlation in the two plots (Figures 3-2(a) and 3-3(a)). However, when the point corresponding to 4-*ax*-chlorocyclohexanone

(**22a**) are omitted from the plots, some kind of correlation can be seen between ΔE, $\ln(ax/eq)$ and λ (Figures 3-2(b) and 3-3(b)). In a plot of $\ln(ax/eq)$ against λ calculated at the HF/6-31G* level, the least-square linear regression correlation is surprisingly good. The correlation coefficient r equals as large as 0.96 ($r^2 = 0.92$). These relationship can be considered as another strong evidence that the orbital extension has significance for the stereoselectivity of six-membered ketones.

(a)

(b)
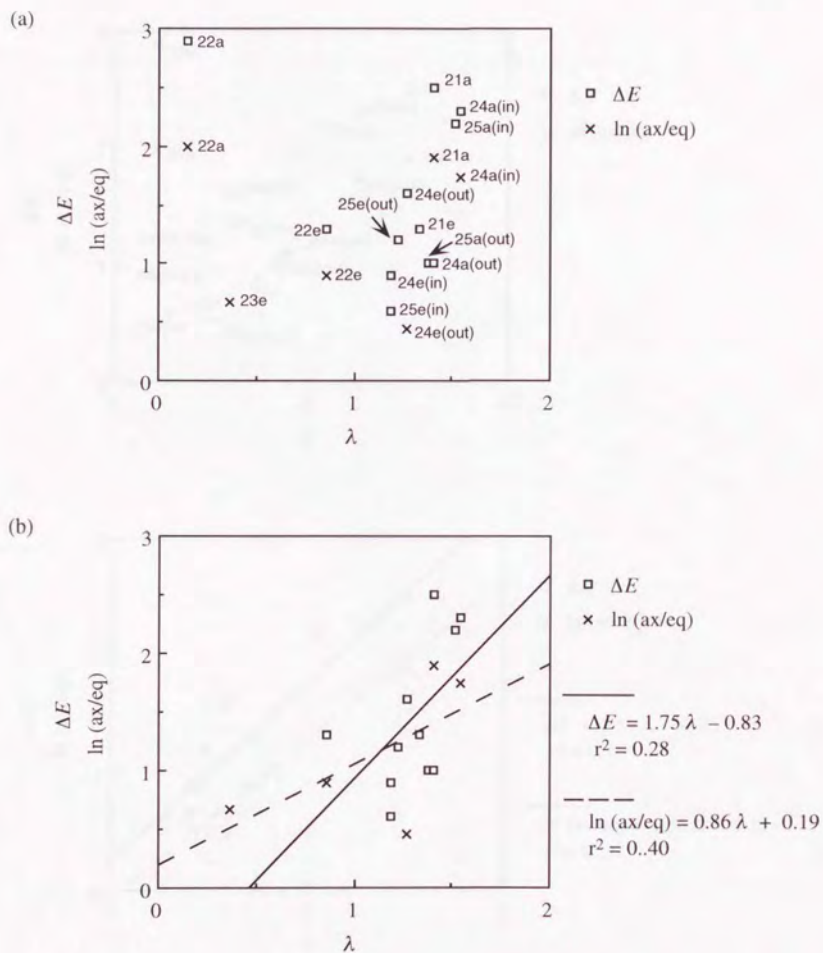
Figure 3-2. Plot of $\ln(ax/eq)$ and ΔE against λ for 4-substituted cyclohexanones at the HF/3-21G level. (a) with or (b) without ax-Cl (**22a**)

(a)

(b)

$$\Delta E = 1.51\,\lambda - 4.25$$
$$r^2 = 0.76$$

$$\ln(ax/eq) = 1.36\,\lambda - 4.15$$
$$r^2 = 0..92$$
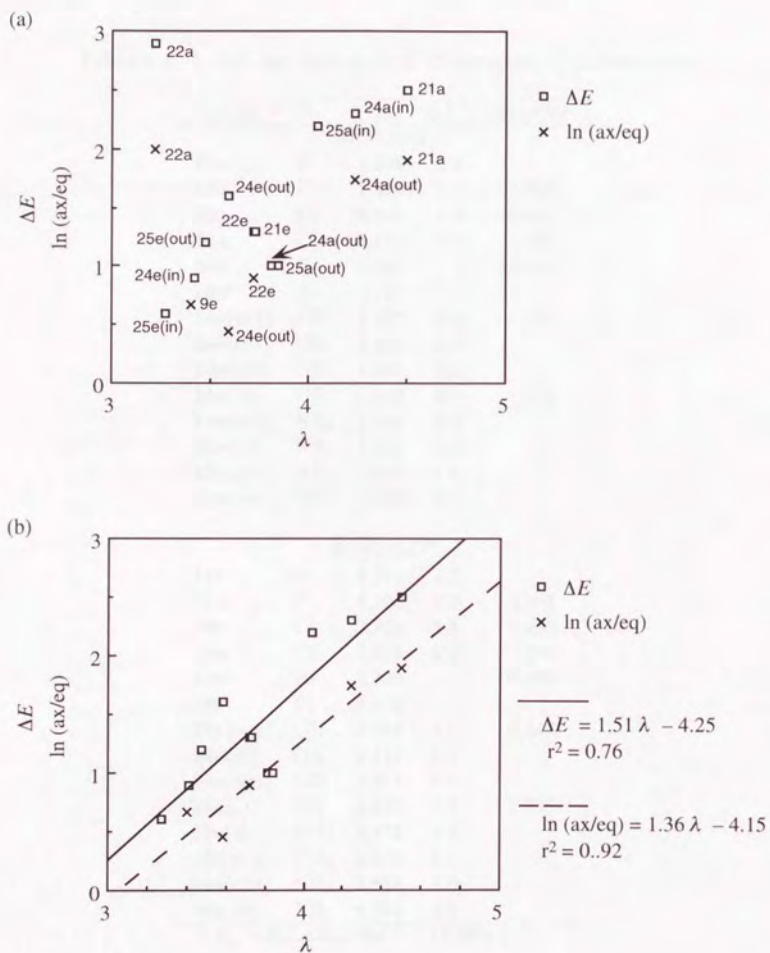
Figure 3-3. Plot of $\ln(ax/eq)$ and ΔE against λ for 4-substituted cyclohexanones at the HF/6-31G* Level. (a) with or (b) without ax-Cl (**22a**).

Table 3-4. λ, ΔE, and $\ln(ax/eq)$ of 4-Substituted Cyclohexanones

Compd	X	λ	ΔE^a	$\ln(ax/eq)$
		HF/3-21G*		
21e	F	1.329	1.3	
21a	F	1.405	2.5	1.901
22e	Cl	0.862	1.3	0.895
22a	Cl	0.148	2.9	1.992
23e	Br	0.366		0.663
23a^b	Br	0.819		
24e(out)	OH	1.273	1.6	0.447
24e(in)	OH	1.188	0.9	
24a(out)	OH	1.407	1.0	
24a(in)	OH	1.542	2.3	1.735
25e(out)	NH$_2$	1.220	1.2	
25e(in)	NH$_2$	1.186	0.6	
25a(out)	NH$_2$	1.383	1.0	
25a(in)	NH$_2$	1.513	2.2	
		HF/6-31G*		
21e	F	3.731	1.3	
21a	F	4.498	2.5	1.901
22e	Cl	3.721	1.3	0.895
22a	Cl	3.215	2.9	1.992
23e^b	Br	3.399		0.663
23a^b	Br	3.536		
24e(out)	OH	3.589	1.6	0.447
24e(in)	OH	3.415	0.9	
24a(out)	OH	3.811	1.0	
24a(in)	OH	4.238	2.3	1.735
25e(out)	NH$_2$	3.472	1.2	
25e(in)	NH$_2$	3.276	0.6	
25a(out)	NH$_2$	3.843	1.0	
25a(in)	NH$_2$	4.044	2.2	

^{a} $E_{eq} - E_{ax}$ in kcal mol^{-1}. ^{b} LUMO+1.

Next we examined computationally more demanding decalone derivatives themselves, hoping that similar close relationship would be observed. This actually turned out to be the case. Like 4-substituted cyclohexanones, a good linear correlation is found in a plot of $\ln(ax/eq)$ against λ (Figure 3-5(b)).

Table 3-5. EFOE Density, Atomic Accessible Space, Distortion Index, and the LUMO Level of 4-Substituted *trans*-Decalones at the HF/3-21G Level
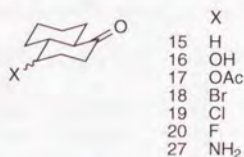
Compd	X	EFOE density (%)		AAS[a] (au³)		δ^b	E_{LUMO}
		ax	*eq*	*ax*	*eq*	(%)	(au)
15	H	1.162	0.610	12.0	51.2	27.2	0.16570
20e	F	1.161	0.565	13.6	49.3	31.0	0.15384
20a	F	1.264	0.709	13.1	51.1	30.0	0.16296
19e	Cl	0.943	0.587	12.8	50.1	37.1	0.14808
19a	Cl	0.503	0.519	12.6	50.3	38.6	0.14963
18e	Br	1.033	0.608	12.5	50.5	32.9	0.15353
18a	Br	1.033	0.608	12.4	50.5	36.2	0.15202
16e(out)[c]	OH	1.157	0.611	12.4	50.7	30.3	0.15773
16e(in)[d]	OH	1.114	0.565	13.1	49.7	29.6	0.16046
16a(out)[c]	OH	1.164	0.540	12.0	51.0	24.9	0.15551
16a(in)[d]	OH	1.278	0.674	12.7	51.1	29.1	0.17041
27e(out)[c]	NH₂	1.132	0.608	12.0	51.4	28.9	0.16393
27e(in)[d]	NH₂	1.122	0.561	12.9	49.5	28.3	0.16529
27a(out)[c]	NH₂	1.199	0.582	11.9	51.5	25.7	0.16451
27a(in)[d]	NH₂	1.283	0.657	12.7	50.6	30.0	0.17481

[a] Atomic accessible space. [b] Distortion index. [c] Lone pair outside the ring. [d] Lone pair inside the ring.

Table 3-6. EFOE Density, Atomic Accessible Space, Distortion Index, and the LUMO Level of 4-Substituted *trans*-Decalones at the HF/6-31G* Level

Compd	X	EFOE density (%)		AAS^a (au^3)		δ^b	E_{LUMO}
		ax	eq	ax	eq	(%)	(au)
15	H	1.708	0.343	14.5	47.3	48.2	0.16482
20e	F	1.726	0.327	13.1	45.8	50.7	0.15490
20a	F	1.955	0.458	15.0	47.6	49.9	0.16246
19e	Cl	1.692	0.326	15.0	46.6	49.5	0.15201
19a	Cl	1.711	0.440	15.7	45.8	52.6	0.15725
18e	Br	1.686	0.340	14.8	47.0	48.9	0.15087
18a	Br	1.991	0.300	15.7	45.5	51.5	0.16084
16e(out)^c	OH	1.730	0.379	14.6	47.4	50.6	0.15836
16e(in)^d	OH	1.618	0.307	15.4	46.2	49.7	0.15914
16a(out)^c	OH	1.671	0.241	14.2	47.6	47.2	0.15513
16a(in)^d	OH	1.911	0.353	15.3	46.8	49.9	0.16685
27e(out)^c	NH$_2$	1.645	0.351	14.2	47.8	49.1	0.16156
27e(in)^d	NH$_2$	1.622	0.306	15.5	45.8	48.7	0.16318
27a(out)^c	NH$_2$	1.761	0.252	14.8	46.7	48.9	0.16121
27a(in)^d	NH$_2$	1.956	0.232	15.5	46.1	51.9	0.17143

^{a} Atomic accessible space. ^{b} Distortion index. ^{c} Lone pair outside the ring. ^{d} Lone pair inside the ring.

(a)

(b)

$\Delta E = 1.56\,\lambda - 0.11$
$r^2 = 0.20$

$\ln(ax/eq) = 1.58\,\lambda - 0.28$
$r^2 = 0..42$
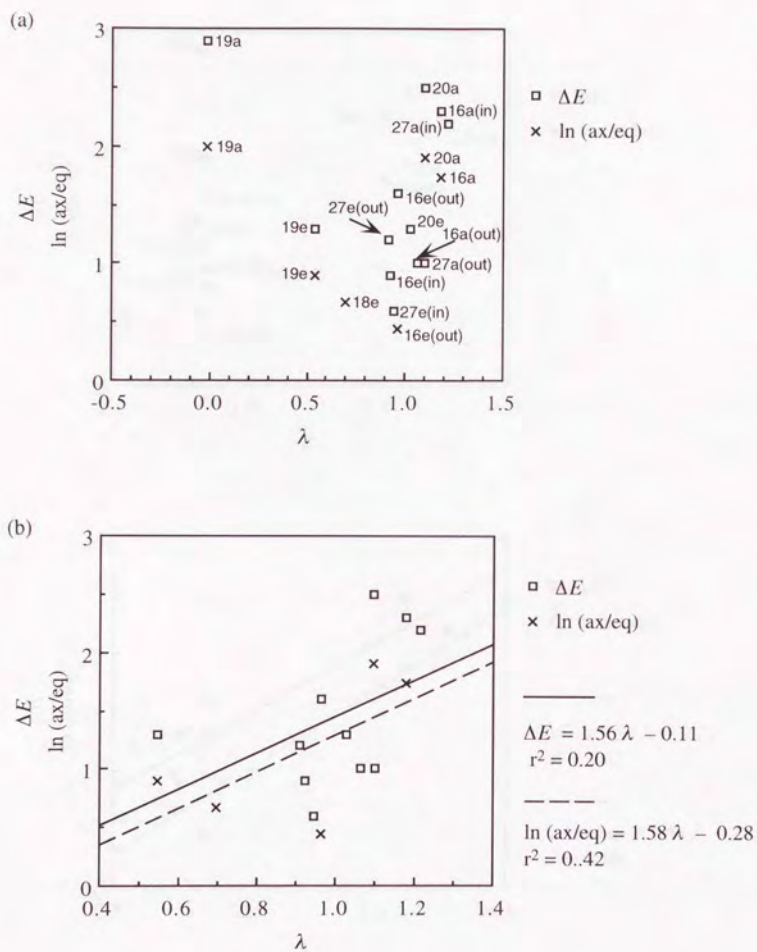
Figure 3-4. Plot of $\ln(ax/eq)$ and ΔE against λ for 4-substituted *trans*-decalones at the HF/3-21G level. (a) with or (b) without *ax*-Cl (**19a**).
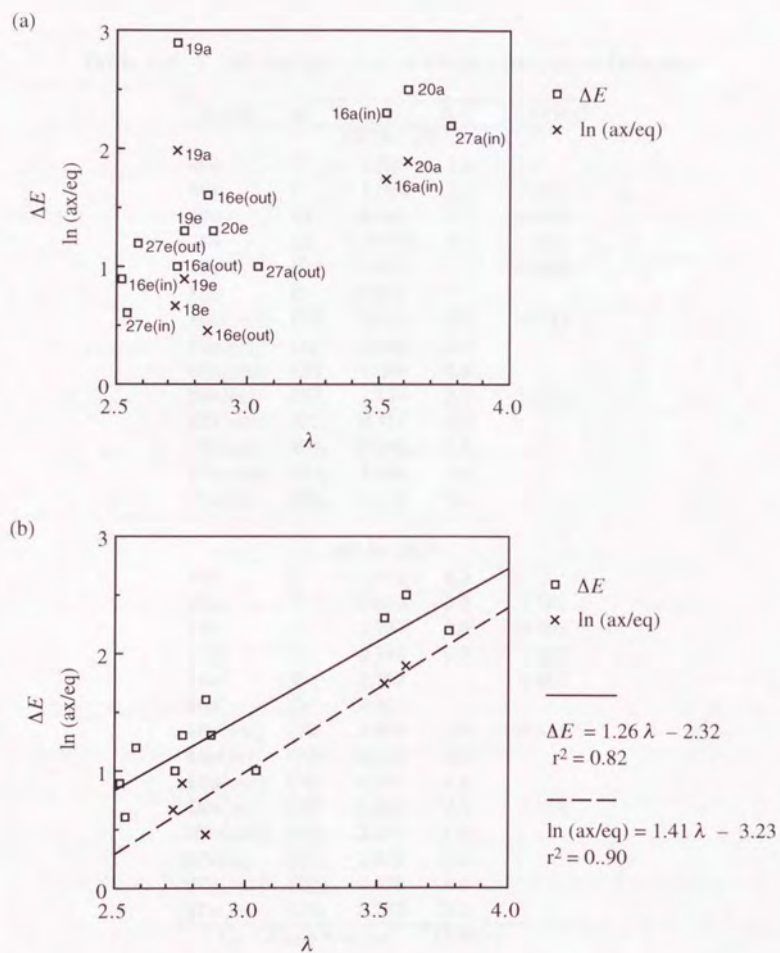
Figure 3-5. Plot of $\ln(ax/eq)$ and ΔE against λ for 4-substituted *trans*-decalones at the HF/6-31G* level. (a) with or (b) without ax-Cl (**19a**).

Table 3-7. λ, ΔE, and $\ln(ax/eq)$ of 4-Substituted *trans*-Decalones

Compd	X	λ	ΔE^a	$\ln(ax/eq)$
		HF/3-21G		
20e	F	1.029	1.3	
20a	F	1.094	2.5	1.901
19e	Cl	0.545	1.3	0.895
19a	Cl	−0.016	2.9	1.992
18e	Br	0.697		0.663
18a	Br	0.697		
16e(out)	OH	0.965	1.6	0.447
16e(in)	OH	0.922	0.9	
16a(out)	OH	1.064	1.0	
16a(in)	OH	1.178	2.3	1.735
27e(out)	NH$_2$	0.911	1.2	
27e(in)	NH$_2$	0.944	0.6	
27a(out)	NH$_2$	1.099	1.0	
27a(in)	NH$_2$	1.214	2.2	
		HF/6-31G*		
20e	F	2.871	1.3	
20a	F	3.612	2.5	1.901
19e	Cl	2.757	1.3	0.895
19a	Cl	2.735	2.9	1.992
18e^b	Br	2.725		0.663
18a^b	Br	3.875		
16e(out)	OH	2.849	1.6	0.447
16e(in)	OH	2.523	0.9	
16a(out)	OH	2.735	1.0	
16a(in)	OH	3.529	2.3	1.735
27e(out)	NH$_2$	2.583	1.2	
27e(in)	NH$_2$	2.538	0.6	
27a(out)	NH$_2$	3.038	1.0	
27a(in)	NH$_2$	3.772	2.2	

^{a} $E_{eq} - E_{ax}$ in kcal mol^{-1}. ^{b} LUMO+1.

Substantial deviation from the linear regression line is again found in 4-ax-chlorodecalone (**19a**). This discrepancy may be attributed to a hyperconjugative interaction involving σ^* orbital of the remote C4 C–Cl substituent . This interaction might be of importance only when the 4-ax-substituent is either chlorine or bromine, as their σ^* levels are substantially lower. A series of transition state calculations seem to support this proposition. Transition state structures of addition of LiH to 4-fluoro-, 4-chloro-, and 4-bromocyclohexanone, with substituents either axial or equatorial, were optimized at various levels of theory. In all theoretical levels, following features are relevant (Table 3-8):

1. When the 4-substituent (X) is equatorial, the C–X bond lengths are virtually the same for both the axial and the equatorial transition state.

2. On the other hand, when the substituent is axial, large elongation of the C–X bond is observed for X = Cl or Br in the axial transition state structures. Even when X = F, marginal elongation is present. Such change in bond length is not observed in the equatorial transition structures.

These changes in bond lengths indicate that some electronic factor is present only in the axial transition state of axially-substituted substrates. The elongation of the C–X bond indicates some amount of electron from the nucleophile delocalizes into the σ^*_{C-X} orbital in the axial transition state. In Figure 3-6, contour diagrams of the LUMO (LUMO+1) at the ground state of 4-fluoro-, 4-chloro-, and 4-bromocyclohexanone calculated at the HF/6-31G* level are depicted. In the case of the LUMO of 4-ax-chloro- and 4-ax-bromocyclohexanone, the σ^*_{C-X} orbital substantially mixes into the π^* orbital at the carbonyl with in-phase relationship (Figure

3-6(b),(c)). On the other hand, no such orbital mixing is observed in the LUMO of 4-*ax*fluorocyclohexanone (Figure 3-6(a)). These orbital mixings are the consequence of the lowering of the energy level of the corresponding σ^* orbitals. σ^*_{C-Cl} and σ^*_{C-Br} are much lower in energy than σ^*_{C-F}, causing large orbital interaction with $\pi^*_{C=O}$.

Table 3-8. The C–X Bond Length (X = F, Cl, Br) of 4-Substituted Cyclohexanones at the Ground State and the Transition States

	ground state[a]	ax-TS			eq-TS		
		C–X[a]	$\Delta^{a,b}$	%[c]	C–X[a]	$\Delta^{a,b}$	%[c]
ax-F							
3-21G	1.4194	1.4224	0.0030	0.21	1.4184	−0.0010	−0.07
6-31G*	1.3827	1.3866	0.0039	0.28	1.3824	−0.0003	−0.02
MP2[d]	1.4128	1.4173	0.0045	0.32	1.4109	−0.0018	−0.13
B3LYP[e]	1.4073	1.4123	0.0050	0.35	1.4051	−0.0022	−0.16
eq-F							
3-21G	1.4099	1.4107	0.0008	0.06	1.4104	0.0005	0.04
6-31G*	1.3741	1.3760	0.0019	0.14	1.3756	0.0014	0.11
MP2[d]	1.4043	1.4045	0.0001	0.01	1.4045	0.0002	0.01
B3LYP[e]	1.3970	1.3945	−0.0025	−0.18	1.3974	0.0004	0.03
ax-Cl							
3-21G	1.9106	1.9201	0.0095	0.50	1.9085	−0.0021	−0.11
6-31G*	1.8164	1.8234	0.0070	0.39	1.8166	0.0002	0.01
MP2[d]	1.8036	1.8095	0.0060	0.33	1.8017	−0.0018	−0.10
B3LYP[e]	1.8443	1.8520	0.0077	0.42	1.8398	−0.0045	−0.24
eq-Cl							
3-21G	1.8960	1.8973	0.0013	0.07	1.8975	0.0015	0.08
6-31G*	1.8045	1.8075	0.0031	0.17	1.8071	0.0027	0.15
MP2[d]	1.7963	1.7969	0.0006	0.03	1.7968	0.0005	0.03
B3LYP[e]	1.8306	—[f]	—[f]	—[f]	1.8289	−0.0017	−0.09
ax-Br							
3-21G*	1.9724	1.9772	0.0048	0.24	1.9716	−0.0008	−0.04
6-31G*	1.9893	1.9983	0.0090	0.45	1.9897	0.0004	0.02
eq-Br							
3-21G*	1.9639	1.9655	0.0015	0.08	1.9637	−0.0002	−0.01
6-31G*	1.9733	1.9769	0.0037	0.19	1.9764	0.0031	0.16

[a] in Å. [b] Difference of the C–X bond length at the transition state and that at the ground state. [c] Percentage of elongation relative to the optimized bond lengths at the ground state. [d] MP2/6-31G*. [e] B3LYP/6-31G*. [f] could not be located.

ax-X   eq-X

(a) X = F

$\pi_{C=O}^*$

F   F

(b) X = Cl

Cl   Cl

(c) X = Br   LUMO

Br   Br

LUMO+1

Br   Br
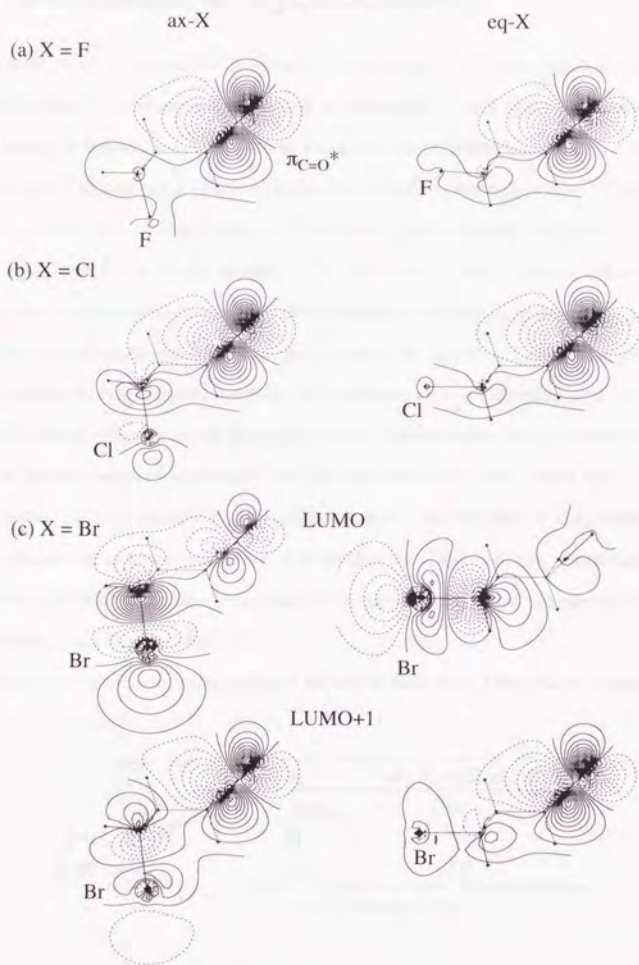
Figure 3-6. Contour diagrams of the LUMO of 4-substituted cyclohexanones calculated at the HF/6-31G* level. (a) X = F, (b) X = Cl, and (c) X = Br. Axially-substituted compounds are shown on the left and equatorially substituted compounds on the right. In (c), both the LUMO and LUMO+1 are shown.

3.2   3-Substituted Cyclohexanones

Cieplak *et al.* reported the reversal of stereoselectivity in nucleophilic additions to 3-substituted cyclohexanones as well as electrophilic additions to 3-substituted methylenecyclohexanones.[107, 108] When the electron-withdrawing ability of the substituent at C3 is increased, relative proportion of axial attack increases (Figure 3-7). He interpreted these results in terms of electron donating ability of the σ_{C2-C3} bond, which is antiperiplanar to the incipient Nu$\cdots$C bond in the equatorial attack. Electronegative substituents decrease electron density of the σ_{C2-C3} bond, so that the delocalization of electrons from the σ_{C2-C3} bond to the σ^* orbital of the incipient bond is reduced. As a result, the ratio of equatorial attack decreases and the net result is the observed increase of the axial attack. On the other hand, Frenking stated that the stereochemical preference can be understood by the FMO theory based on *ab initio* calculations of 3-fluorocyclohexanone.[45] Houk insisted that the electrostatic interaction is more important and neither hyperconjugative σ-assistance nor asymmetric orbital extension is necessary for the explanation of the variation of the stereoselectivity (Figure 3-8).[35, 109]

Calculated results are collected in Tables 3-9 and 3-10. Data for 3-methylcyclo-
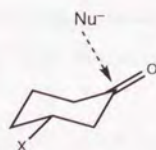
X	ratio of axial attack (%)[a]
SiMe$_3$	15
H	21
CF$_3$	50

[a] CH$_3$Li / Et$_2$O, −78°C

Figure 3-7. Typical experimental results for 3-substituted cyclohexanones.
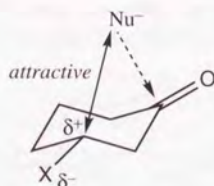
Figure 3-8. Electrostatic attraction proposed by Houk.

hexanones, which are also shown in Tables 2-11 and 2-12, are included again for comparison with other 3-substituted molecules. For X = Me, CF$_3$, F, and Cl, both axial and equatorial substitutions were considered. Additionally, all three possible conformers with respect to C3–O axis are considered for X = OMe.

The EFOE values for the axial side of **29e** (X = CF$_3$), **30e** (X = F), and **31e** (X = Cl), are all larger than those of **5** (X = Me) or **28** (X = Bu^t). For instance, the EFOE density of the axial side of **29e** (X = CF$_3$) (3-21G: 1.322, 6-31G*: 1.998) is larger than that of cyclohexanone (3-21G: 1.275, 6-31G*: 1.940), in agreement with the observed increase of axial selectivity by introducing electronegative substituents at C3. Even larger axial preference is expected for **32** (X = OMe), irrespective of the C–OMe conformation. In the case of 3-axially substituted compounds, the EFOE values for the axial area are uniformly smaller than the corresponding equatorial substituted cases, indicating the EFOE values contain steric information to some extent.

Unfortunately, except for X = Bu^t and Me, experimental results of simple metal hydride reduction of 3-substituted cyclohexanones collected in Tables 3-9 and 3-10 have not been reported in the literature due to their conformational mobility. Therefore, transition state structures of LiH addition of 3-fluorocyclohexanone (**30a**

Table 3-9. EFOE Density, Atomic Accessible Space, Distortion Index, and the LUMO Level of 3-Substituted Cyclohexanones at the HF/3-21G Level

Compd	X	EFOE density (%)		AAS^a (au^3)		δ^b	E_{LUMO}
		ax	eq	ax	eq	(%)	(au)
28	eq Bu^t	1.223	0.609	13.4	55.3	27.9	0.16645
5a	ax Me	0.845	0.558	4.2	57.1	25.6	0.16351
5e	eq Me	1.261	0.592	14.5	55.5	28.2	0.16455
29a	ax CF$_3$	0.440	0.413	3.7	44.6	29.8	0.15358
29e	eq CF$_3$	1.322	0.592	16.8	51.3	28.0	0.14684
30a	ax F	0.899	0.471	11.5	47.7	26.5	0.15854
30e	eq F	1.351	0.579	16.9	53.0	30.6	0.14864
31a	ax Cl	0.990	0.453	10.1	44.9	32.2	0.15064
31e	eq Cl	1.095	0.345	17.0	52.2	14.9	0.12656
32-1^c	eq OMe	1.333	0.624	15.2	44.0	29.1	0.15839
32-2^c	eq OMe	1.322	0.584	16.4	53.6	30.0	0.16080
32-3^c	eq OMe	1.266	0.570	14.6	54.1	31.8	0.15743

^{a} Atomic accessible space. ^{b} Distortion index. ^{c} See the figure below.
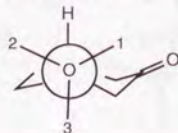
and **30e**) were located at the HF/6-31G* level. Four fully optimized transition state structures along with their relative energies are shown in Figure 3-9. Detailed data are presented in Table 3-11. Energies were estimated by single point calculations at the MP2/6-31G*//HF/6-31G* level, which were corrected with zero-point vibrational energy (ZPVE) computed at the HF/6-31G* level scaled with the recommended scale factor for ZPVE correction (0.9135).[79]

At the ground state, **30a** is energetically the most stable. However, the lowest

(a) TS-1

E_{rel} 3.98
–H   0.00
–Li   11.06
–LiH   0.51

(b) TS-2

E_{rel} 1.75
–H   0.95
–Li   5.97
–LiH   0.43

(c) TS-3

E_{rel} 0.00
–H   4.54
–Li   0.00
–LiH   0.53

(d) TS-4

E_{rel} 2.64
–H   2.36
–Li   5.99
–LiH   0.00
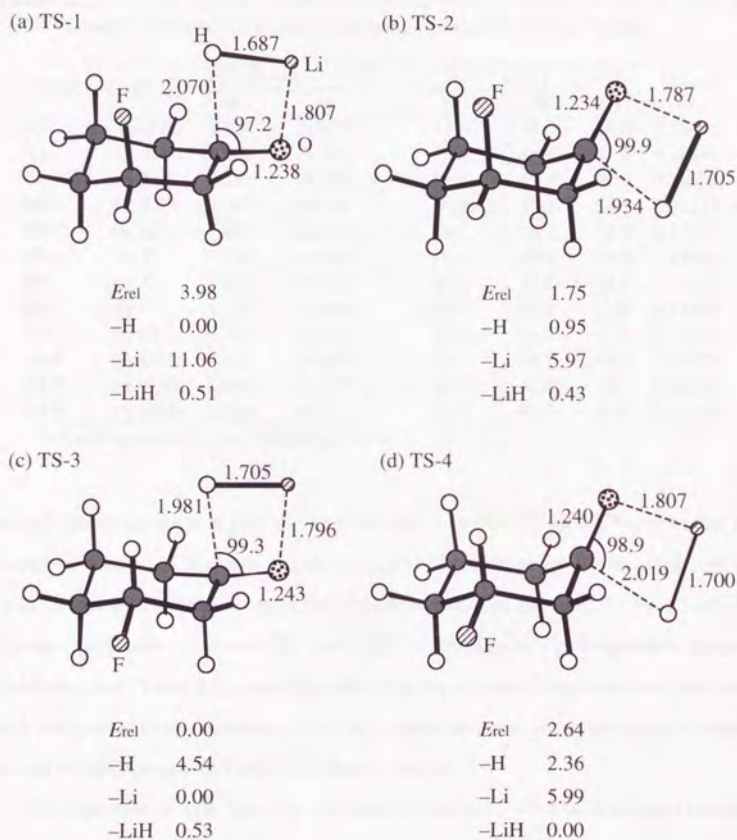
Figure 3-9. Transition state structures of LiH addition to 3-fluorocyclohexanone calculated at the HF/6-31G* level. Selected bond lengths are shown in Å and bond angles in degree. Corrected relative energies (kcal mol^{-1}) are evaluated at the MP2 level using frozen geometries obtained at the HF/6-31G* level.

Table 3-10. EFOE Density, Atomic Accessible Space, Distortion Index, and the LUMO Level of 3-Substituted Cyclohexanones at the HF/6-31G* Level

Compd	X	EFOE density (%)		AAS[a] (au^3)		δ^b	E_{LUMO}
		ax	eq	ax	eq	(%)	(au)
28	eq Bu^t	1.820	0.316	17.3	47.3	49.6	0.16453
5a	ax Me	1.447	0.211	7.9	48.4	52.5	0.16041
5e	eq Me	1.884	0.304	18.4	47.8	47.9	0.16333
29a	ax CF$_3$	0.858	0.112	7.2	37.1	54.1	0.15121
29e	eq CF$_3$	1.998	0.320	19.9	45.7	50.9	0.14933
30a	ax F	1.504	0.163	16.9	40.2	50.9	0.15615
30e	eq F	2.070	0.283	21.6	45.6	54.0	0.14893
31a	ax Cl	1.503	0.148	15.0	38.1	55.8	0.14987
31e	eq Cl	1.865	0.221	20.6	45.5	47.1	0.13697
32-1	eq OMe	2.017	0.341	18.7	39.7	51.4	0.15773
32-2	eq OMe	2.000	0.298	20.3	46.4	52.3	0.15947
32-3	eq OMe	1.920	0.277	18.6	46.5	53.9	0.15694

[a] Atomic accessible space. [b] Distortion index.

energy transition state is that of the axial attack to **30e** (TS-3). TS-1 is higher in energy by about 3.98 kcal mol^{-1} than TS-3. This destabilization can be attributed to an electrostatic repulsion between the hydride and 3-axial fluorine (F···H is 2.89 Å). The energy difference between TS-3 and TS-4 is 2.64 kcal mol^{-1}, larger than that of cyclohexanone (Table 2-9, page 46), indicating higher selectivity would be observed with electronegative substituent, which is in agreement with the experimental results as well as the increase of the EFOE density values.

With removal of LiH from the optimized structures, TS-4 is the most favored, but the differences with the remaining three transition states are very small (ca. 0.5 kcal mol^{-1}). Therefore, steric strain would not be a dominant factor for the stereoselectivity.

Table 3-11. Total Energy, Imaginary Frequency, and ZPVE[a] of the Transition State Structures of LiH Addition to 3-Fluorocyclohexanone

TS		E^b (hartrees)	Freq.[c] (cm^{-1})	ZPVE[c] $(kcal\ mol^{-1})$
TS-1		−415.895 87	−575.79	101.30
	−H	−415.152 85		
	−Li	−408.344 62		
	−LiH	−407.866 10		
TS-2		−415.899 90	−664.80	101.64
	−H	−415.151 35		
	−Li	−408.352 73		
	−LiH	−407.866 24		
TS-3		−415.902 45	−590.18	101.47
	−H	−415.145 62		
	−Li	−408.362 25		
	−LiH	−407.866 08		
TS-4		−415.898 25	−581.10	101.48
	−H	−415.149 09		
	−Li	−408.352 70		
	−LiH	−407.866 92		

[a] Zero-point vibrational energy. [b] MP2/6-31G*//HF/6-31G*. [c] HF/6-31G*//HF/6-31G*.

3.3   Heterocyclic Compounds

3.3.1   1,3-Dioxan-5-one and 1,3-Dithian-5-one

Replacement of the carbon atoms at C3 and C5 in cyclohexanone ring with polar elements has been known to result in intriguing stereochemistries. Jochims *et al.* reported LiAlH$_4$ reduction of 2-phenyl-1,3-dioxan-5-one (**33**).[110] The product ratio of the equatorial and axial alcohol was 96:4, showing **33** has extremely high axial selectivity. Subsequently, they reported results of the reduction of 2-phenyl-1,3-dithian-5-one (**34**).[111] In contrast to **33**, the equatorial attack was predominant in the case of **34** (15:85). This reversal of stereoselectivity was rationalized by torsional strain between the incipient Nu···C bond and adjacent bonds.[110,111]

R = Ph   33   36

H   35   36
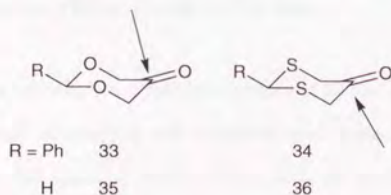
These results have been interpreted in terms of the Cieplak model as well. According to Cieplak's assumption, the electron-donating abilities of the adjacent bonds are in the following order: C–S > C–H > C–C > C–O.[26] Therefore, nucleophile will come from the axial side in the case of **33**, whereas **34** is subject to the predominant equatorial attack since the C–S bond is a better electron donor than the C–H bond.
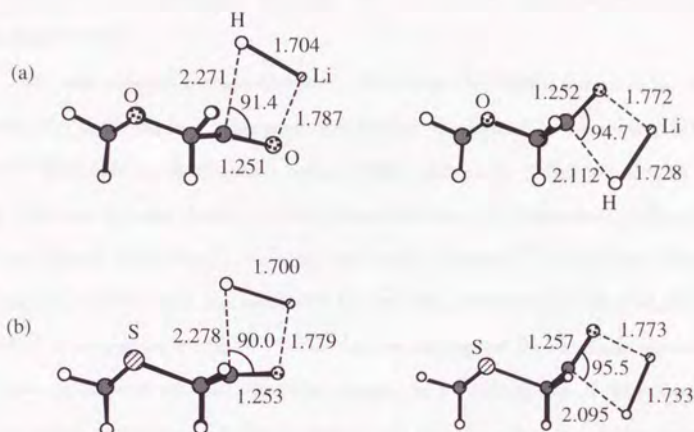
Figure 3-10. Transition structures of LiH addition to (a) 1,3-dioxan-5-one (**35**) and (b) 1,3-dithian-5-one (**36**) at the HF/3-21G level.

Houk *et al.* reported MM2 force field calculations of **33** and **34**.[112] The agreement between experimental selectivities and computational predictions were excellent. They suggested that the torsional strain is responsible for the selectivity. Following this paper, they also performed *ab initio* MO calculations of 1,3-dioxan-5-one (**35**) and 1,3-dithian-5-one (**36**).[109] They successfully located the transition states of LiH addition to these compounds. The calculated structures indicated that the severe torsional strain exists in the equatorial addition of LiH to **35** due to shorter C–O bonds, which make the six-membered ring flatter than cyclohexanone so that the axial attack would be preferred. On the other hand, in the case of **36**, the equatorial attack is less strained due to the longer C–S bonds, which make the dithian ring more

puckered than cyclohexanone. Therefore, the equatorial attack would be favored for **36** (Figure 3-10).

They also pointed out electrostatic interaction play significant roles in determining the preferred face. This point was further emphasized in the subsequent paper.[113] They calculated transition states of SiH_5^- addition to cyclohexanone, **35**, and **36**. This reaction was chosen to mimic previously reported experimental alkoxysiliconate hydride reduction of cyclohexanones in the gas phase.[72] Using these obtained structures, solvent effect was estimated by the self-consistent reaction field (SCRF) method developed by Wong.[114–116] The relative energies of the axial and equatorial addition to **35** were reversed when the solvent effect was included. Houk attributed this reversal of stereoselectivity on going from the gas phase to solution to electrostatic repulsion between a negatively charged nucleophile and the lone pairs on hetero atoms in the ring, which would be tempered by the solvent effects in solution.

Our calculations suggest that there may be no need to invoke electrostatic arguments in explaining the stereochemistries of these compounds (Table 3-12). As seen in the values of the EFOE density and the distortion index, the LUMO of dioxanone (**35**) is strongly distorted to the axial side, indicating the frontier orbital interaction is far greater at the axial side than at the equatorial side. In the case of dithianone (**36**), the LUMO substantially extends to the equatorial side. These trends in orbital distortion agree with the observed stereoselectivities for these compounds in solution. Electrostatic repulsion may be responsible for the selectivity, but the same prediction can be made without it.

Table 3-12. EFOE Density, Atomic Accessible Space, Distortion Index, and the LUMO Level of 1,3-Dioxan-5-one and 1,3-Dithian-5-one

Compd	EFOE density (%)		AAS^a (au^3)		δ^b	E_{LUMO}
	ax	eq	ax	eq	(%)	(au)
HF/3-21G//HF/3-21G						
dioxanone (**35**)	1.355	0.312	72.8	25.5	31.0	0.13426
dithianone (**36**)	0.092	0.874	11.0	66.9	−28.3	0.09869
HF/6-31G*//HF/6-31G*						
dioxanone (**35**)	1.739	0.243	71.2	26.2	40.6	0.13870
dithianone (**36**)	0.277	0.834	18.4	54.6	−20.5	0.10820

^{a} Atomic accessible space. ^{b} Distortion index.

3.3.2   Other Oxygen- or Sulfur-Containing Heterocycles

Similar reversal of stereoselectivities were found in **39**–**42**.[26,117] Hydride reduction of **39** exclusively occurs from the axial side, whereas **40** has a large equatorial preference. **41** has somewhat higher axial preference than decalone itself presumably due to steric hindrance of the axial methyl group. On the other hand, the reversal of stereoselectivity is observed in **42**. These stereochemical results are qualitatively reproduced with the EFOE density (Table 3-13).

Table 3-13. EFOE Density, Atomic Accessible Space, Distortion Index, and the LUMO Level of **37**–**42**
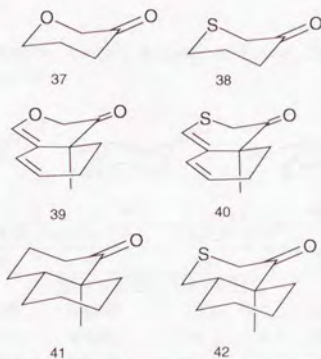
Compd	EFOE density (%)		AAS^a (au^3)		δ^b	E_{LUMO}
	ax	eq	ax	eq	(%)	(au)
	HF/3-21G//HF/3-21G					
37	1.417	0.402	36.0	31.1	34.7	0.14997
38	0.358	0.827	12.3	47.7	−2.2	0.13273
39	0.801	0.542	21.5	11.5	−0.5	0.13389
40	0.320	0.701	14.4	16.0	−22.8	0.12337
41	1.163	0.614	12.0	16.3	19.4	0.16739
42	0.319	0.846	10.5	17.4	−11.4	0.13864
	HF/6-31G*//HF/6-31G*					
37	2.056	0.180	42.1	27.1	53.6	0.15179
38	0.834	0.659	18.9	40.7	18.5	0.14319
39	0.871	0.965	14.0	13.0	−7.8	0.13921
40	0.657	0.829	18.0	14.5	−12.8	0.12674
41	1.705	0.426	14.3	14.3	37.3	0.16588
42	0.649	0.829	13.9	14.6	−3.1	0.14851

^{a} Atomic accessible space. ^{b} Distortion index.

Replacement of C4 with oxygen was examined by Catelani *et al.*[118] The proportion of equatorial attack in LiAlH$_4$ reduction are as follows: **43**: 15%, **44**: 5%, **45**: 5.5%. As is shown in Table 3-14, qualitative agreements are again obtained for these compounds.

Table 3-14. EFOE Density, Atomic Accessible Space, Distortion Index, and the LUMO Level of 4-Pyranones

Compd	EFOE density (%)		AAS^a (au^3)		δ^b	E_{LUMO}
	ax	eq	ax	eq	(%)	(au)
	HF/3-21G//HF/3-21G					
43	1.309	0.605	13.6	52.9	24.0	0.15319
44	1.378	0.605	16.5	54.3	24.2	0.15490
45	1.354	0.619	15.7	53.9	24.1	0.15602
	HF/6-31G*//HF/6-31G*					
43	1.984	0.310	17.4	47.9	51.6	0.15277
44	2.026	0.326	21.7	46.2	49.4	0.15596
45	1.969	0.341	20.7	45.8	48.6	0.15680

^{a} Atomic accessible space. ^{b} Distortion index.
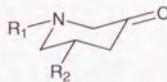
Cieplak pointed out the possibility that the electron donation from the lone pairs of oxygen at the 4-position to the σ^* orbital of the incipient bond facilitates the axial attack. The energy levels of the LUMO seem to have no such symptom of orbital interaction.
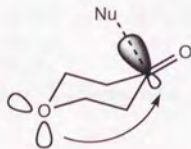
3.3.3 3-Piperidones

The effects of alkyl substitution of 1,5-dialkyl-3-piperidones on the stereoselectivity were reported.[26] As the size of the alkyl group on nitrogen becomes larger, the ratio of the equatorial attack marginally increases. This trend can also be seen qualitatively in the slight decrease in the EFOE densities for the axial side of these compounds.

Table 3-15. EFOE Density, Atomic Accessible Space, Distortion Index, and the LUMO Level of 3-Piperidones

			R_1	R_2
		46	H	H
		47	Me	Me
		48	Et	Me
		49	*i*-Pr	Me
		50	*t*-Bu	Me
		51	*t*-Bu	*t*-Bu
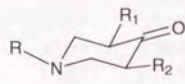
Compd	EFOE density (%)		AAS^a (au^3)		δ^b	E_{LUMO}
	ax	eq	ax	eq	(%)	(au)
		HF/3-21G//HF/3-21G				
46	1.266	0.502	30.2	43.7	30.4	0.16564
47	1.293	0.514	30.5	42.9	29.7	0.16539
48	1.272	0.515	30.0	43.2	30.5	0.16764
49	1.240	0.543	25.2	43.9	29.0	0.16830
50	1.229	0.540	25.6	44.2	29.3	0.16822
51	1.212	0.536	24.6	43.0	30.1	0.16993
		HF/6-31G*//HF/6-31G*				
46	1.851	0.171	42.8	33.4	55.3	0.16153
47	1.816	0.237	40.1	34.4	49.7	0.16478
48	1.786	0.233	39.5	34.4	50.9	0.16704
49	1.755	0.261	34.0	35.1	49.2	0.16790
50	1.754	0.225	36.6	33.8	50.5	0.16719
51	1.710	0.231	36.3	32.9	50.4	0.16782

^{a} Atomic accessible space. ^{b} Distortion index.

3.3.4 4-Piperidones

Effects of 2- and 6-alkyl groups upon the stereoselectivity of 4-piperidones and *N*-methyl-4-piperidones were examined by Geneste *et al.*[119] The experimental selectivities of NaBH$_4$ reduction are summarized in Table 3-16. As the number of methyl group increases, the axial preference decreases. This is presumably due to steric hindrance of the nearby methyl groups which intervene the axial approach of hydride.

Table 3-16. Experimental Selectivity of 4-Piperidones

	R	R$_1$	R$_2$
52	H	H	H
53	H	H	Me
54	H	Me	Me
55	Me	H	H
56	Me	H	Me
57	Me	Me	Me

Compd	% ax	% eq
4-piperidones		
52	90	10
53	86	14
54	56	44
N-methyl-4-piperidones		
55	92	8
56	86	14
57	55	45

Calculated data are shown in Table 3-17. Decrease of the EFOE density for the axial side with increasing the number of methyl group agrees with the experimental trends. To see this relationship more clearly, a plot of a natural logarithm of the ratio of the experimental axial and equatorial selectivity ($\ln(ax/eq)$) against λ (=

Table 3-17. EFOE Density, Atomic Accessible Space, Distortion Index, and the LUMO Level of 4-Piperidones

Compd	EFOE density (%)		AAS^a (au^3)		δ^b	E_{LUMO}
	ax	eq	ax	eq	(%)	(au)
	HF/3-21G//HF/3-21G					
52	1.373	0.607	15.9	54.7	26.6	0.16352
53	1.292	0.618	13.1	52.9	26.1	0.16377
54	1.240	0.629	11.0	48.6	26.2	0.16409
55	1.349	0.596	16.5	54.4	26.9	0.16204
56	1.284	0.599	13.5	52.2	26.4	0.16228
57	1.226	0.577	11.2	48.6	26.5	0.16263
	HF/6-31G*//HF/6-31G*					
52	2.069	0.284	22.4	44.6	53.1	0.16066
53	2.009	0.312	17.3	46.7	52.6	0.16051
54	1.906	0.332	14.1	46.4	52.4	0.16061
55	2.038	0.269	23.0	44.5	53.4	0.15892
56	1.997	0.287	17.6	46.3	52.9	0.15888
57	1.879	0.302	14.3	45.4	52.6	0.15901

^{a} Atomic accessible space. ^{b} Distortion index.

$EFOE(ax)^2 - EFOE(eq)^2$) was considered. Figure 3-11 shows this plot. Although the number of points might not be sufficient, it shows a good correlation between those values. This clearly suggests that the orbital effect is also operative in these heterocyclic systems.
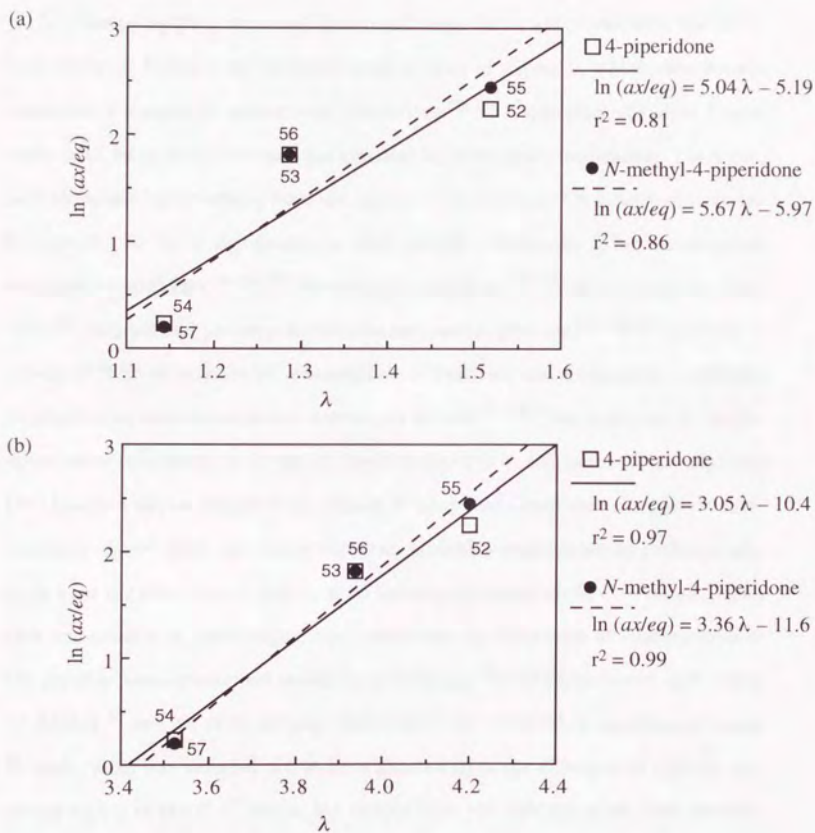
Figure 3-11. Plot of $\ln(ax/eq)$ against λ of 4-piperidones and N-methyl-4-piperidones. (a) HF/3-21G, (b) HF/6-31G*.

3.4   Adamantanones

In order to separate electronic factor and steric factor associated with the stereo-selectivity, le Noble *et al.* have reported a series of papers in which they mainly concerned a number of adamantane derivatives.[120, 121] Using sterically rigid framework, both faces of the carbonyl are assumed to be sterically equivalent. Therefore, only electronic factor arising from the introduction of remote C5 substituents would be expected to be of significance in these model compounds. They investigated nucleophilic additions,[29, 122–127] electrophilic additions,[120, 128] radical capture reactions,[129] thermal and photocycloadditions and rearrangements,[121, 130–134] and rate of solvolysis[135, 136] of substituted adamantane derivatives, and nucleophilic additions to substituted azaadamantanone derivatives as well.[137–139] They interpreted the observed stereoselectivity in terms of hyperconjugative σ assistance of the adjacent C–C bonds, a notion proposed by Cieplak.[26] They postulated that since steric environments of both faces are almost identical, attacking reagents would preferentially come from the side which is *anti* to more electron-donating allylic C–C bonds. However, importance of hyperconjugative interactions in reductions of adamantanones has recently been questioned based on a thorough ^{13}C NMR chemical shift study by Adcock,[40] and an extraordinary high selectivity observed in azaadamantanone *N*-oxide (96:4) was revealed not to be originated from the difference of electron donating ability of the C–C bonds, but simply from the different steric bias between the two faces.[140]

To estimate how much extent orbital factor plays a role in reactions of adamantanones, we have carried out calculations of several adamantanone derivatives. The

results are shown in Table 3-18 and 3-19.

Table 3-18. EFOE Density, Atomic Accessible Space, Distortion Index, and the LUMO Level of Adamantanones at the HF/3-21G Level
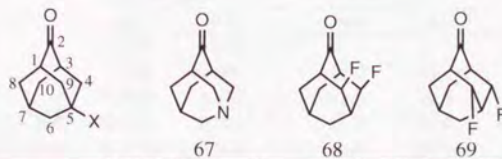
Compd	X	EFOE density (%)		AAS^a (au^3)		δ^b	E_{LUMO}
		syn	anti	syn	anti	(%)	(au)
58	H	0.955	0.954	11.0	11.0	−0.2	0.17095
59	F	0.930	0.907	12.5	10.2	3.5	0.15845
60	Cl	0.498	0.790	12.2	10.5	14.4	0.15055
61	Br(LUMO)	0.141	0.405	11.9	10.8	28.8	0.15060
	(LUMO+1)	0.841	0.458	11.9	10.8	−14.6	0.16266
62	OH(Cs)	0.955	0.917	11.7	10.8	3.0	0.16288
	OH(C$_1$)	0.917	0.894	12.3	10.4	1.7	0.16426
63	NH$_2$(Cs)	0.934	0.892	12.2	10.6	0.3	0.16882
	NH$_2$(C$_1$)	0.951	0.922	11.5	11.0	1.2	0.16829
64	CN	0.987	0.910	11.8	10.8	1.1	0.15357
65	Me	0.969	0.920	11.4	11.2	0.0	0.17010
66	SiH$_3$	0.619	0.344	10.9	11.4	15.1	0.16316
67	5-aza	0.989	0.931	11.5	10.3	1.7	0.16583
68	4,9-di-*ax*-F	0.598	0.890	7.0	8.1	1.4	0.15708
69	4,9-di-*eq*-F	1.199	0.867	13.7	10.4	12.6	0.14073

^{a} Atomic accessible space. ^{b} Distortion index. The *syn* face is positive.

According to the AAS values, steric environment for both faces is virtually the same, but slightly favorable for the *syn* attack. Orbital distortion seems to have nothing to do with the selectivity.

Comparison of the EFOE data with the experimental selectivities is not straightforward. This is due chiefly to rather small selectivities for almost all compounds. In

Table 3-19. EFOE Density, Atomic Accessible Space, Distortion Index, and the LUMO Level of Adamantanones at the HF/6-31G* Level

Compd	X	EFOE density (%)		AAS^a (au^3)		δ^b	E_{LUMO}
		syn	anti	syn	anti	(%)	(au)
58	H	1.097	1.099	11.1	11.1	−0.1	0.17132
59	F	1.066	1.078	12.0	10.4	2.8	0.16053
60	Cl	0.910	1.137	11.9	10.4	4.3	0.15780
61	Br(LUMO)	0.001	0.010	11.8	10.6	50.7	0.13360
	(LUMO+1)	1.231	0.946	11.8	10.6	−0.2	0.15746
62	OH(Cs)	1.108	1.055	11.2	10.9	3.1	0.16415
	OH(C$_1$)	1.045	1.000	11.9	10.4	1.4	0.15859
63	NH$_2$(Cs)	1.072	0.932	11.7	10.3	0.4	0.16776
	NH$_2$(C$_1$)	1.103	1.011	11.1	10.9	1.3	0.16751
64	CN	1.176	1.006	11.7	10.6	1.0	0.15294
65	Me	1.153	0.996	11.2	10.7	0.4	0.16984
67	5-aza	1.156	1.054	11.5	10.2	−1.2	0.16651
68	4,9-di-*ax*-F	0.691	0.960	8.4	7.2	1.4	0.15885
69	4,9-di-*eq*-F	1.381	0.961	11.8	10.2	18.5	0.14322

^{a} Atomic accessible space. ^{b} Distortion index. The *syn* face is positive.

any event, the agreement of the experimental selectivities and the prediction based on the EFOE densities is not very good. Electron withdrawing substituents such as fluorine are known to cause increase of proportion of the *syn* attack, whereas the EFOE density of **59** at the HF/6-31G* level is slightly larger at the *anti* side, not at the expected *syn* side. For X = Cl (**60**), the EFOE density is larger at the *anti* side, which is again opposite to the experimental selectivity. The decrease of the EFOE density at the *syn* side of **60** may be attributed to the fact that the LUMO has a large component of the $\sigma^*_{\text{C−Cl}}$ orbital as in the case of 5-chlorodecalone (**19**) (see section 3.1). Therefore, the EFOE density at the *syn* side somewhat decreases (Figure 3-12). The mixing of the $\sigma^*_{\text{C−X}}$ orbital of a substituent is also observed in

61 (X = Br). In this case, the LUMO is approximately made up of only the σ^*_{C-Br} orbital since the σ^*_{C-Br} orbital is substantially lower in energy than the σ^*_{C-Cl} orbital. The next LUMO (LUMO+1) is built up mainly from the π^* orbital of the carbonyl along with small contribution of the σ^*_{C-Br} orbital. Therefore the EFOE density of the next LUMO should be used in this case (Figure 3-13). Stereoselectivity of 5-azaadamantanone (**67**) was reported to be dependent on the nucleophilic reagent used. Methyllithium preferentially adds to **67** from the *anti* side to yield *Z* alcohol as a major product (*syn:anti* = 45:55), whereas reduction with NaBH$_4$ is *syn* selective (62:38).[137] The EFOE values are larger for the *syn* face, *i.e.*, the correct face in the case of NaBH$_4$ reduction. 5-Cyano- (**64**) and 5-methyladamantan-2-one (**65**) was reported to be slightly *syn* selective, suggesting a methyl group has a weak electron-withdrawing nature.[40] In these cases, the EFOE values are relatively in good agreement with the experimental selectivity. 5-Silyl group causes nucleophiles to attack from the *anti* face, whereas the EFOE density is larger at the *syn* face. This is probably the result of the mixing of the low lying σ^*_{C-Si} orbital into the LUMO. The selectivity of 4,9-dihalo-substituted adamantanones was reported recently.[127] The axial disubstitution gave predominant *anti* attack due to the large steric hindrance around the carbonyl, whereas the equatorial disubstitution resulted in the predominant *syn* attack. These cases were examined with **68** and **69** as model compounds. The results are in qualitative agreement with the experiments.

To gain further insight into the principal effect which differentiates the two faces of adamantanones, transition structures of LiH addition to 5-fluoroadamantan-2-one (**59**) were fully optimized at the HF/3-21G and HF/6-31G* levels of theory, and relative energies between the *syn* and *anti* additions were estimated with the MP2/6-
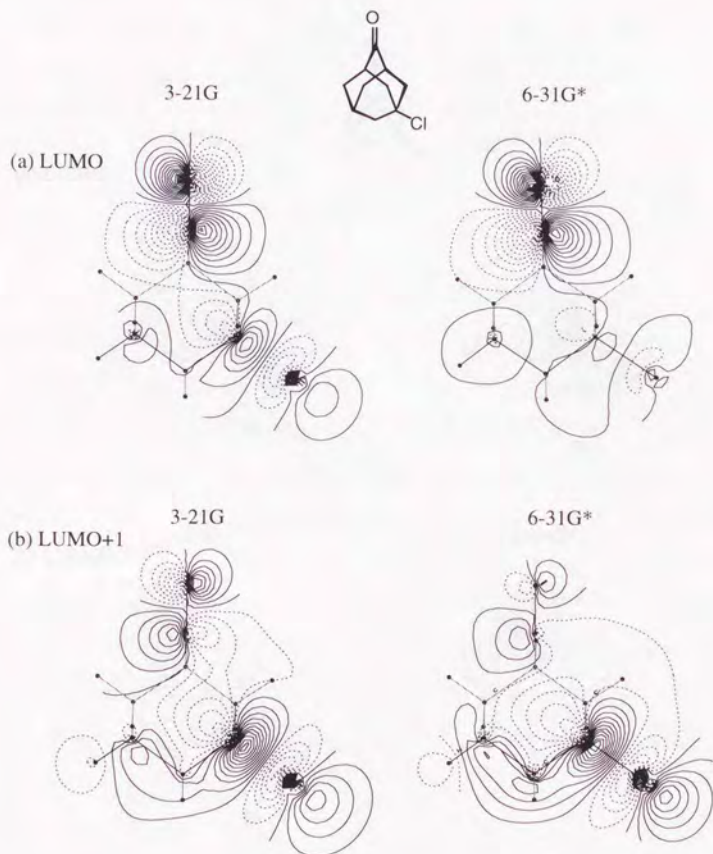
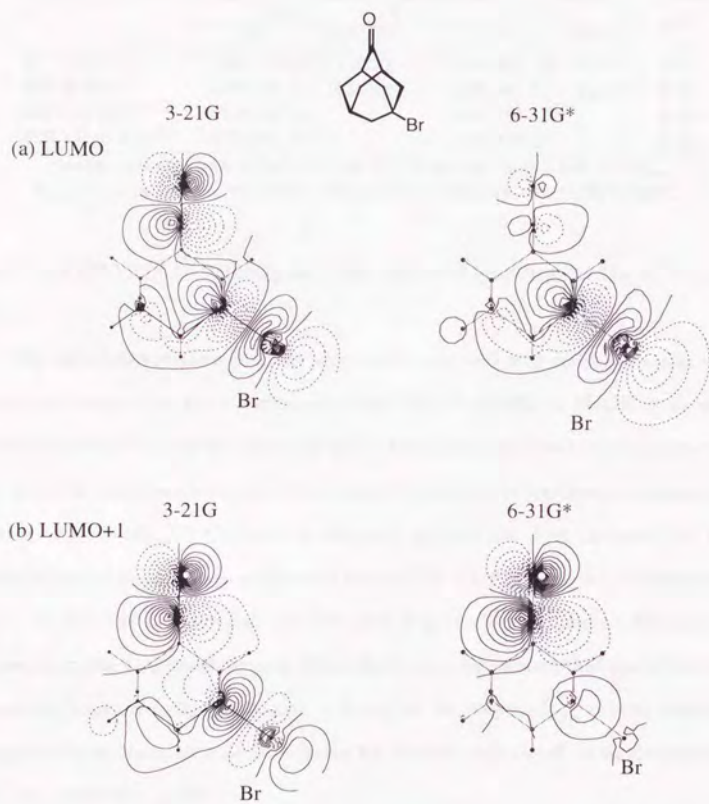**Figure 3-12**. The LUMO and LUMO+1 of 5-Chloroadamantan-2-one.

Figure 3-13. The LUMO and LUMO+1 of 5-Bromoadamantan-2-one.

Table 3-20. Total and ZPVE Corrected Relative Energy^a of Transition State of LiH Addition to 5-Fluoro-2-adamantanone

	syn TS		anti TS		
	E^b	ZPVE^c	E^b	ZPVE^c	ΔE^d
HF/3-21G	−565.463 48	150.22	−565.462 70	150.24	0.50
HF/6-31G*	−568.586 61	150.62	−568.586 22	150.63	0.26
MP2/6-31G*^{e}	−570.249 70		−570.249 41		0.19
B3LYP/6-31G*^{f}	−572.091 11		−572.090 75		0.23

^{a} using recommended scale factors in ref 79. ^{b} in hatrees. ^{c} in kcal mol^{-1}. ^{d} E_{anti} − E_{syn} in kcal mol^{-1}. ^{e} MP2/6-31G*//HF/6-31G*. ^{f} B3LYP/6-31G*//HF/6-31G*.

31G* and B3LYP/6-31G* theory using the optimized geometries at the HF/6-31G* level.

The calculated relative energies between the *syn* and *anti* additions are in very good agreement with the observed selectivity (62:38, NaBH$_4$ in MeOH at 0° or in *i*-PrOH at RT).[29] However, close look at the two optimized structures suggests that no variation in hyperconjugative interaction is present between these two transition states. Specifically, C1–C9 bond is elongated to be 1.550 Å in the anti TS. The same degree of elongation is observed in the syn TS (C1–C8: 1.551 Å). Furthermore, H$^-$···C$_2$ is 2.030 Å in the *anti* TS and 2.032 Å in the *syn* TS, and no difference is observed in the C–F bond lengths. These facts strongly suggest that the σ-electron donation from the antiperiplanar σ_{C-C} bonds to the vacant $\sigma^{*\ddagger}_{H\cdots C_2}$ orbital, which is proposed by le Noble as a decisive factor for the selectivity, is of no significance for the face selectivity of **59**.

The origin of the transition state energy difference is uncertain. It may be that electrostatic interaction is responsible in this case. However, it is clear that the Cieplak model is not valid in this case.
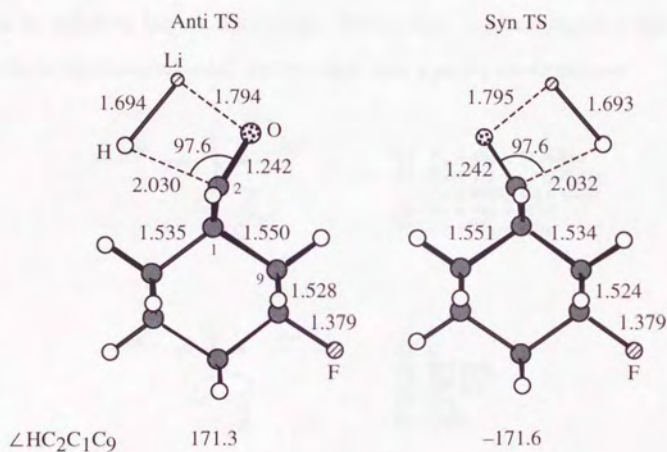
Figure 3-14. Transition State Structures of LiH Addition to 5-Fluoro-2-adamantanone calculated at the HF/6-31G* level. Bond lengths are shown in Å, and bond angles and torsion angles in degree.

3.5   7-Norbornanones

Another study of π-facial stereoselectivity of sterically unbiased rigid cyclic com-
pounds has been reported by Mehta *et al.* They investigated face selectivity of *endo*-
substituted 7-norbornanone[30] and 7-alkylidenenorbornane derivatives.[141] Both faces
of these compounds are assumed to be sterically equivalent due to a constraint im-
posed by inflexible bicyclic frameworks. Hence, they may be suitable model com-
pounds to eliminate unwanted factors other than a purely electronic one.

70   R₁ = R₂ = COOMe
71   R₁ = R₂ = CH₂OCH₃
     R₁ = vinyl, R₂ = ethyl
72   R₁ = R₂ = vinyl
73   R₁ = R₂ = ethyl

         R
84   O
85   NH (out)
86   NH (in)
87   CH₂
88   CMe₂
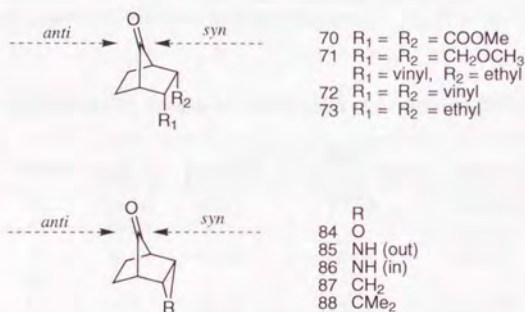
Mehta ascribed the observed stereoselectivity to the hyperconjugative stabiliza-
tion by the antiperiplanar σ bonds (*i.e.*, the Cieplak model). Namely, electron-
withdrawing substituents decrease electron densities of the σ_{C-C} bonds, causing
the attacking reagent to come from the *syn* face. If the substituents are electron-
donating, the reverse is true.

On the other hand, Paddon-Row *et al.* rationalized the stereoselectivity in terms
of electrostatic interaction.[36] They performed *ab initio* calculations of several tran-
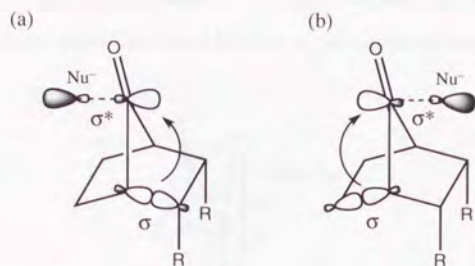
Figure 3-15. Schematic representations of hyperconjugative σ-assistance in 7-norbornanones. (a) R = electron-withdrawing group, (b) R = electron-donating group.

Table 3-21. Experimental Results of Nucleophilic Additions to 7-Norbornanones[a]

Compd	*syn:anti* ratio			
	NaBH$_4$[b]	LiAlH$_4$[c]	(*t*-BuO)$_3$LiAlH[c]	CH$_3$Li[c]
70	84:16	87:13	77:23	>90:<10
71	40:60			34:66
72	36:64	35:65	34:66	27:73
73	25:75			
74	20:80	21:79	29:71	17:83

[a] Ref 30. [b] in MeOH. [c] in dry Et$_2$O.

sition state structures of LiH addition to 7-norbornanones. The calculated relative energies of the *syn* and *anti* addition were in agreement with the observed selectivity. Since there is no geometrical difference around the carbonyl, they stated that the torsional effect, which is important in cyclohexanones, is of no significance in these systems. The calculated relative energies were heavily dependent on the orientation of the polar substituents, which cannot be accounted for in terms of the Cieplak model, as the orientation of the substituents would have no correlation with the

electron-donating ability of the allylic C–C bonds. Instead, they insisted that the predominant attack occurs from the side where a preferable electrostatic interaction exists.
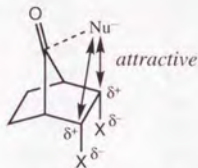
We have been interested in these systems and studied several norbornanones computationally. Tables 3-22 and 3-23 show the calculated data. C_s symmetry was imposed on the molecular geometries of **72**, **74–76**, **78**, **80–83** to shorten the time required for the geometry optimization. Therefore, the calculated properties of molecules having flexible substituents (such as vinyl (**72**), ethyl (**74**), etc.) would not reflect the values at the global minimum. However, they could be used for, at least, qualitative arguments.

As intuitively relevant, steric environments of the two faces are almost equal as can be seen in the AAS values, though the *syn* face is generally slightly more congested than the *anti* face.

Examination of the EFOE values suggests following points: (i) in the case of **71** (R = CH$_2$OMe), **72** (R = vinyl), and **74** (R = Et), the *anti* preference is qualitatively reproduced (see Table 3-21). The ratio of the experimental *anti* attack increases in this order, so does the EFOE value for these compounds calculated at the HF/3-21G level. However, those computed at the HF/6-31G* level lack this systematic trend, which can easily be seen in corresponding λ values ($= EFOE(syn)^2 - EFOE(anti)^2$

Table 3-22. EFOE Density, Atomic Accessible Space, Distortion Index, and the LUMO Level of Bicyclo[2.2.1]heptanones at the HF/3-21G level

Compd	R	EFOE density (%)[a]		AAS[b] (au³)		δ^c	E_{LUMO}
		syn	*anti*	*syn*	*anti*	(%)	(au)
70	COOMe	0.457	0.777	17.7	15.3	−23.7	0.15130
71	CH₂OMe	0.908	1.060	16.3	16.5	3.7	0.16482
72	vinyl	0.334	0.663	14.7	16.6	−34.3	0.14733
74	Et	0.904	1.076	14.4	17.8	4.3	0.16828
81	Me	0.962	1.038	14.5	17.0	−2.5	0.16825
75	F	1.257	0.929	21.4	17.0	11.8	0.13539
76	Cl	0.644	0.328	18.0	16.1	−27.5	0.09398
77	OH	1.196	0.959	18.7	18.2	6.3	0.15244
78	CH₂F	0.886	1.942	16.1	15.8	2.7	0.14900
79	CH₂OH	0.899	1.072	13.4	16.2	2.0	0.15644
80	COOH	0.453	0.776	17.7	15.3	−23.9	0.14613
82	OMe	1.188	0.976	18.3	17.9	8.5	0.15963
83	SiH₃	0.540	0.374	12.8	18.9	−27.5	0.13542
84	O	1.092	0.950	28.3	16.0	3.0	0.15555
85	NH(out)	1.053	1.014	26.1	16.4	−2.3	0.17075
85	NH(in)	0.923	1.038	21.9	17.6	−8.0	0.15991
86	CH₂	0.930	1.076	21.7	16.8	−3.8	0.17399
87	CMe₂	1.095	1.923	18.6	16.1	−1.6	0.17627

[a] Lattice unit is 0.1 Å. [b] Atomic accessible space. [c] Distortion index. The *syn* face is positive.

) (Table 3-24). The λ for **72** (R = vinyl) obtained at the HF/6-31G* is unexpectedly small. This may be the result of mixing of the π^* orbital at the vinyl moieties into the LUMO at the carbonyl, which is indicated by the decrease of the EFOE values for both sides of the molecule.

The EFOE values for other molecules are generally in agreement with the experimental results or the computed relative energies reported by Paddon-Row *et al.*[36] The effect of the electronic nature of *endo* substituents is qualitatively reproduced, *i.e.*, electron-withdrawing substituents increase the *syn* attack, whereas electron-

Table 3-23. EFOE Density, Atomic Accessible Space, Distortion Index, and the LUMO level of Bicyclo[2.2.1]heptanones at the HF/6-31G* Level

Compd	R	EFOE density (%)[a]		AAS[b] (au³)		δ^c	E_{LUMO}
		syn	anti	syn	anti	(%)	(au)
70	COOMe	0.385	1.127	14.3	15.4	−26.4	0.15609
71	CH₂OMe	0.806	1.316	14.3	15.6	1.8	0.16540
72	vinyl	0.239	0.821	13.0	16.5	−40.5	0.14757
74	Et	0.795	1.371	12.8	17.0	5.8	0.16949
81	Me	0.753	1.287	12.7	16.5	3.3	0.16851
75	F	1.583	1.102	18.6	15.7	22.3	0.13916
76	Cl	1.154	0.523	14.6	15.6	−2.6	0.11775
77	OH	0.402	1.517	14.3	15.5	−26.0	0.15062
78	CH₂F	1.225	1.003	15.7	16.9	4.9	0.15358
79	CH₂OH	0.758	1.326	14.1	15.6	−0.6	0.15209
80	COOH	0.784	1.359	13.4	16.2	−0.8	0.15918
82	OMe	1.337	1.081	15.6	16.6	11.8	0.16073
83	SiH₃	0.408	0.222	11.9	17.5	−39.0	0.13346
84	O	1.202	1.227	22.7	16.7	−8.7	0.16313
85	NH(out)	1.181	1.269	21.9	16.3	−3.0	0.17436
85	NH(in)	0.880	1.394	18.2	18.1	−15.3	0.16338
86	CH₂	0.905	1.433	14.3	15.6	−7.9	0.17612
87	CMe₂	0.647	1.462	15.8	15.8	−4.3	0.17928

[a] Lattice unit is 0.1 Å. [b] Atomic accessible space. [c] Distortion index. The syn face is positive.

Table 3-24. Experimental Selectivity and Calculated λ

Compd	R	Exp.[a]	λ	
		syn:anti	3-21G	6-31G*
71	CH₂OMe	40:60	−0.299	−1.082
72	vinyl	36:64	−0.328	−0.617
74	Et	20:80	−0.342	−1.240

[a] NaBH₄ reduction in MeOH (see Table 3-21.)

donating groups force the reagent to attack from the *anti* side. For instance, **81**(R = Me) has marginal *anti* selectivity,[142] which is correctly predicted with the larger EFOE density value at the *anti* side of **81**. It should be noted here in this case methyl group has electron-donating character in contrast to 5-methyladamantan-2-one (**65**) (see section 3.4). In the case of **75** (R = F), where the *syn* attack would be expected from the electron-withdrawing nature of fluorine, the EFOE value predicts the predominance of the *syn* attack. Transition state calculations of addition of LiH to **75** support this prediction ($\Delta E = E_{anti} - E_{syn} = 4.3$ kcal mol^{-1} at the HF/6-31G* level.)

Discrepancies between the qualitative prediction based on the EFOE density and experimental selectivity or transition state calculation are found in three cases. Experimentally, **70** (R = COOMe) has high *syn* selectivity independent of the reaction conditions (Table 3-21). On the other hand, the EFOE density at the *syn* side of **70** turned out to be unexpectedly too small. This may be due to the effect of two ester groups which possess low lying orbitals. The predominance of the *syn* attack for **70** can also be attributed to the electrostatic effect pointed out by Paddon-Row[36] or Mehta.[142] It is worthwhile to comment on the distortion index of **70**. The δ value of **70** is large negative value, indicating the LUMO at the carbonyl carbon strongly distorts to the anti direction. In contrast to this, Dannenberg reported using the PPFMO method that the polarization of the p orbital of the carbonyl carbon slightly directs to the *syn* side which agrees to the experimental selectivity.[59] However, he also admitted that the value of polarization is quite small and even reversed with other rotamers. This correct polarization may be an artifact due to the use of the STO-3G basis set. In the case of **83** (R = SiH₃), the *anti* attack was predicted

based on the transition state calculations,[36] whereas the EFOE density predicts the
syn attack. This may also be due to the substantial mixing of the low lying orbitals
of silicon to the LUMO at the carbonyl. The selectivity of **85** (NH(out)) is com-
plicated. Exclusive *syn* attack was reported for N–Ph derivative,[143] and transition
state calculation of **85** also predicted *syn* attack, though the energy difference was
too small (ca. 0.2 kcal mol^{-1}).[36] The EFOE density at the 3-21G level predicts *syn*
attack, whereas that at 6-31G* level predicts the reverse preference.

Table 3-25. Predicted Selectivity with the EFOE Values, Experimental Selectivity,
and Predicted Selectivity with Calculated ΔE

Compd	R	EFOE^a	Exp^b	ΔE^c
70	COOMe	anti	syn	syn
71	CH$_2$OMe	anti	anti	
72	vinyl	anti	anti	anti
74	Et	anti	anti	
81	Me	anti	anti	anti
75	F	syn		syn^d
76	Cl	syn		
77	OH	anti		
78	CH$_2$F	syn		syn
79	CH$_2$OH	anti		anti
80	COOH	anti		anti
82	OMe	anti		
83	SiH$_3$	syn		anti
85	NH(out)	anti	syn^e	syn
85	NH(in)	anti		anti
86	CH$_2$	anti	anti	anti
87	CMe$_2$	anti	anti	

^{a} HF/6-31G*. ^{b} Data for **70**–**74** are taken from ref
30, **81** from ref 142, **85**–**87** from refs 144 and 143. ^{c}
Ref 36. ^{d} This work. ^{e} NPh in the experiment.

3.6   4,4-Disubstituted Dienones

During the course of total synthesis of antitumor antibiotic aranorosin, Wipf *et al.* found some interesting selectivity in 4,4-disubstituted dienones. They investigated this curious stereoselectivity using following model compounds and performed molecular orbital calculations as well.[41] They suggested electrostatic interaction is responsible for the selectivity based on the linear relationship found between calculated dipole moments and the natural logarithm of the ratio of the observed selectivities.
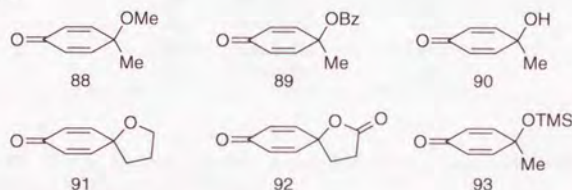
Face selectivities of the above compounds using various metal reagents reported by them vary substantially with the reagents used (Table 3-26), but the reduction of **88** by NaBH$_4$ and LiAlH$_4$ showed virtually no selectivity. The calculated EFOE values for **88** at the HF/3-21G level quite nicely reproduce this result (Table 3-27).

The EFOE method does not incorporate effects of reagent, since it relies on the early transition state assumption and reactant-like transition state. This assumption may be valid for simple metal hydride reductions with sterically nondemanding nucleophiles such as NaBH$_4$ or LiAlH$_4$.

This method would not be intended to be applied to reactions whose transition states appear late or to the cases where interactions between substrate and reagent would be fairly large. The failure of the EFOE model in reproducing high α selectivity observed in Grignard reactions may be attributed to the result of the neglect

Table 3-26. Experimental Results of Face Selectivity of Dienones.

dienone	nucleophile	α/β
88	MeMgBr	4.8:1
88	NaBH$_4$ or LAH	1:1
88	HC≡CMgBr	1:1
88	H$_9$C$_4$C≡CLi	1.1:1
88	PhMgBr	3.6:1
88	MeLi/THF	2.1:1
88	MeLi/Et$_2$O	3.3:1
88	BnOCH$_2$Li	3:1
89	MeMgBr	8.6:1
90	MeMgBr	10.1:1
91	MeMgBr	32:1
92	MeMgBr	7.9:1
93	MeMgBr	17.7:1

Table 3-27. EFOE Density, Atomic Accessible Space, Distortion Index, and the LUMO Level of Dienones (HF/3-21G).

Compd	EFOE density (%)		AAS^a (au^3)		δ^b	LUMO level
	α	β	α	β	(%)	(au)
88	0.545	0.522	66.4	56.3	−12.9	0.08105
89	0.536	0.513	65.6	61.9	−13.4	0.08136
91	0.517	0.483	65.7	62.3	−1.3	0.06278
92	0.540	0.516	65.9	55.8	−3.5	0.07880
93	1.038	0.521	44.1	58.7	−0.9	0.07584

^{a} Atomic accessible space. ^{b} Distortion index. The α face is positive.

of reagent's characters or the deformed transition states of these reactions from the ground state geometries. However, it should be commented that the selectivities are well-replicated by the EFOE values in the case of NaBH$_4$ and LiAlH$_4$ reductions as well as C–C bond formations using alkynyllithium reagents.

3.7 Benzoheptenones

In contrast to the geometrical similarity to cyclohexanone, benzocycloheptenone derivatives show an intriguing stereoselectivity. Houk *et al.* reported a combined work of force field model calculations of **94–96** and experimental results of reductions of **95–96**.[145] Since local environments about the carbonyl group of these compounds seem to be roughly identical to that of cyclohexanone, it is expected that the axial attack is predominant. On the other hand, the equatorial preference was observed in all cases except for **94**. These selectivities were also successfully predicted by MM2 calculations. Houk insisted that the torsional strain suggested by Felkin is responsible for the selectivity and neither transition state hyperconjugation nor orbital effect is necessary for the explanation of the selectivity. However, this view was severely criticized by Cieplak, who stated that the axial face of benzocycloheptenones are very dissimilar to that of cyclohexanone and the results can also be explicable with his model.[108] le Noble pointed out possible involvement of π orbitals on benzene ring which coordinate to the lithium cation at the initial complex formation.[123]
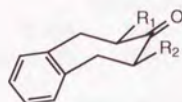
	R_1	R_2
94	H	H
95	Me	H
96	Me	Me

Calculated data for **94** and **96** are summarized in Table 3-28. The large orbital distortion to the axial side in each case suggests that the orbital distortion model fails to account for the experimental selectivity. The AAS values at the axial side are less than half to those of cyclohexanone (19.4 au³ at 6-31G* level), indicating

steric hindrance should play a substantial role for the determination of the stereose-
lectivity. This decrease of the AAS values is the results of the ring puckering which
is seen in X-ray structure reported by Houk.[145] The larger EFOE density values
for the equatorial side correctly predict the equatorial preference of **96**. Though
Houk's MM2 calculation predicted the equatorial preference for **94**, the EFOE val-
ues suggest the axial attack would be favored. Unfortunately, the selectivity of **94** is
not verifiable with experiment, and furthermore no high level transition state com-
putational results have not been reported for these compounds. Further detailed
information in any form should be needed to extend a meaningful discussion on this
subject.

Table 3-28. EFOE Density[a], Atomic Accessible Space, Distortion Index[a], and the
LUMO+2 Level of Benzocycloheptenones

Compd	EFOE density (%)		AAS[b] (au³)		δ^c	$E_{\text{LUMO}+2}$
	ax	eq	ax	eq	(%)	(au)
	HF/3-21G//HF/3-21G					
H (**94**)	0.952	0.802	7.7	63.8	15.8	0.16432
di-*eq*-Me (**96**)	0.664	0.887	5.0	36.6	13.2	0.16618
	HF/4-31G//HF/3-21G					
H (**94**)	0.884	0.580	7.7	63.8	–	–
di-*eq*-Me (**96**)	0.579	0.741	5.0	36.6	8.0	–
	HF/6-31G*//HF/6-31G*					
H (**94**)	1.586	0.603	10.3	56.9	42.6	0.16398
di-*eq*-Me (**96**)	0.863	0.930	5.5	36.4	28.6	0.16117

[a] LUMO+2. [b] Atomic accessible space. [c] Distortion index.

3.8   Miscellaneous Cyclic Ketones

Yano *et al.* reported that sodium borohydride reduction of tricyclo [5.2.0.0]non-3-en-6-one (**97**) gave 95% of *endo* alcohol.[146] In this case, hydride preferentially comes from the more hindered side (**A**) (see Table 3-29). They did not comment on the reason of the selectivity. Cieplak later provided an interpretation that electron donation from the π orbital of the double bond stabilizes the transition state of the *endo* attack. Our calculation suggests that the LUMO at the carbonyl is distorted to the preferential side (**A**). Therefore, the frontier orbital theory correctly predicts the stereoselectivity of **97**. Note here the EFOE values at the 3-21G level give an incorrect assignment.
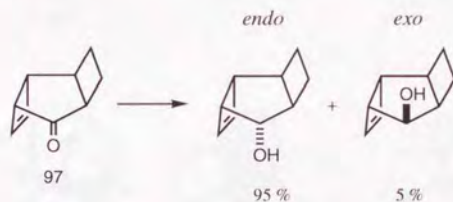
Varech *et al.* reported the reduction of 2-methylbicyclo [2.2.2]octanone (**98**).[147-149] In this case, nucleophile preferentially approaches from the more hindered side of the carbonyl (*syn* to the methyl group). This stereoselectivity can be understood in terms of both the distortion index and the EFOE density, which are both larger at the *syn* side. This orbital distortion is presumably caused by the proximate methyl group, which forces the 2s orbital of the carbonyl carbon to mix into the LUMO at the carbonyl with in-phase fashion.

Nucleophilic additions of bicyclo[3.2.1]octan-8-one (**99**) and bicyclo[4.2.1]nonan-9-one (**100**) are known to proceed preferentially from the sterically less hindered side (**A**). These preferences may be attributed to the large steric hindrance at the less preferred side (**B**) which is indicated by the significantly small AAS values at the less preferred face. This can also be pictorially indicated by the space-filling models of these compounds (Figure 3-16).
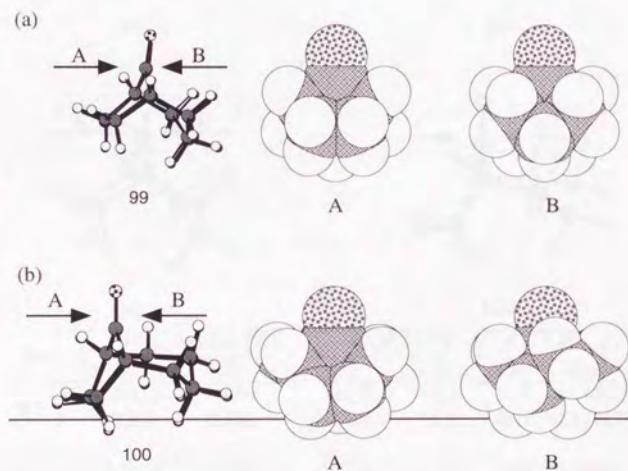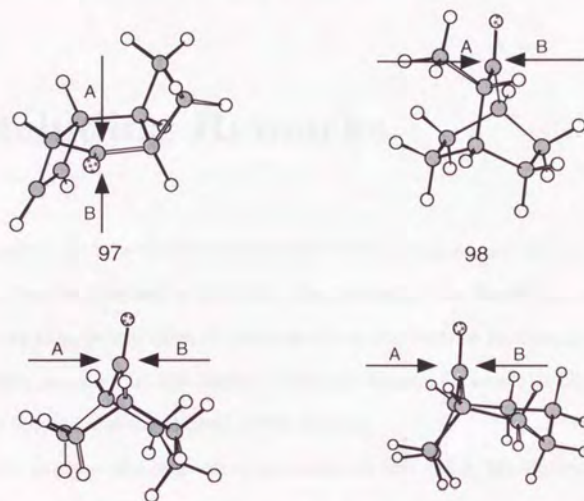

Figure 3-16. Space-filling models of the two faces of **99** and **100**.

Table 3-29. Data for Miscellaneous Cyclic Ketones[a]

| Compd | EFOE density (%) | | AAS[b] (au³) | | δ^c | E_{LUMO} |
	A	B	A	B	(%)	(au)
97	0.514	0.605	11.7	20.6	31.7	0.14355
	0.801	0.695	15.3	19.8	31.1	0.14422
98	0.955^d	0.598^d	7.6	21.0	9.0	0.16752
	1.354^d	0.439^d	8.2	17.2	26.7	0.16427
99	1.110^d	0.541^d	34.5	5.6	9.1	0.16796
	1.318^d	0.596^d	29.5	6.2	12.9	0.16748
100	0.988^d	0.088^d	49.8	1.2	12.1	0.16196
	1.097^d	0.138^d	42.8	2.1	14.3	0.15989

[a] In each compound, the upper row corresponds to data at the HF/3-21G level and the lower row at the HF/6-31G* level. [b] Atomic accessible space. [c] Distortion index. [d] Lattice unit is 0.1 au.

Concluding Remarks

The origin of the π-facial diastereoselectivity of hydride reduction of cyclic ketones has been scrutinized in this work. In contrast to the recent disputes on this subject, the stereoselectivities of many six-membered ketones have been revealed to be generally governed by the frontier orbital interaction between the LUMO of the substrate ketones and the HOMO of the hydride.

For the purpose of quantitative evaluation of this effect, the Exterior Frontier Orbital Extension (EFOE) model has been introduced. The variation of the EFOE values for both faces of the carbonyl has been shown to be a good indicator as to the predominance of the LUMO effect upon the determination of the preferential course of hydride reduction using sterically undemanding reagents in general. The linear relationship between the EFOE values and the experimentally determined activation enthalpy differences gives its physical meaning, which allows one to gain insight into the contribution of the orbital effect at the initial stage of the reaction to the activation enthalpy difference which is directly related to the observed product ratio.

Even in the case of sterically unbiased rigid ketones or those with polar substituents, the LUMO seems to play some roles for the selectivity. Other factors such

as steric or electrostatic factor seem to be of importance in several cases where the variation of the orbital extension is marginal.

Hyperconjugative stabilization, which constitutes the central part of both the Felkin-Anh and the Cieplak model has been revealed to be of secondary importance compared to the fontier orbital effects. We are currently investigating the generality of this finding using not only cyclic ketones but a number of acyclic carbonyl compounds as model systems. Tentative results clearly show that the hyperconjugative interaction is indeed not important in general. Detailed results will hopefully be published in due course.

References and Notes

(1) For instance, comprehensive collections of the results of LiAlH$_4$ and metal alkoxyaluminum hydride reductions are found in: *Organic Reactions*, Vol. 6, pp.469-509 (1951), Vol. 34, pp.1-317 (1985), and Vol. 36, pp.249-590 (1988): John Wiley & Son's inc., New York.

(2) Kamernitzky, A. V.; Akhrem, A. A. *Tetrahedron* **1962**, *18*, 705. Reprinted from *Uspekhi Khimii XXX*, **1961**, *2*, 145.

(3) Menger, F. M. *Tetrahedron* **1983**, *39*, 1013.

(4) Wigfield, D. C. *Tetrahedron* **1979**, *35*, 449.

(5) Ashby, E. C.; Laemmle, J. T. *Chem. Rev.* **1975**, *75*, 521.

(6) Cram, D. J.; Abd Elhafez, F. A. *J. Am. Chem. Soc.* **1952**, *74*, 5828.

(7) Cornforth, J. W.; Cornforth, R. H.; Mathew, K. K. *J. Chem. Soc.* **1959**, 112.

(8) Karabatsos, G. J. *J. Am. Chem. Soc.* **1967**, *89*, 1367.

(9) Barton, D. H. R. *J. Chem. Soc.* **1953**, 1027.

(10) Richer, J.-C. *J. Org. Chem.* **1965**, *30*, 324.

(11) Dauben, W. G.; Fonken, G. J.; Noyce, D. S. *J. Am. Chem. Soc.* **1956**, *78*, 2579.

(12) Brown, H. C.; Wheeler, O. H.; Ichikawa, K. *Tetrahedron* **1957**, *1*, 214.

(13) Chérest, M.; Felkin, H.; Prudent, N. *Tetrahedron Lett.* **1968**, 2199.

(14) Chérest, M.; Felkin, H. *Tetrahedron Lett.* **1968**, 2205.

(15) Anh, N. T.; Eisenstein, O. *Tetrahedron Lett.* **1976**, 155.

(16) Anh, N. T.; Eisenstein, O. *Nouv. J. Chim.* **1977**, *1*, 61.

(17) Anh, N. T. *Topics in Current. Chem.* **1980**, *88*, 145.

(18) Bürgi, H. B.; Dunitz, J. D.; Shefter, E. *J. Am. Chem. Soc.* **1973**, *95*, 5065.

(19) Bürgi, H. B.; Lehn, J. M.; Wipff, G. *J. Am. Chem. Soc.* **1974**, *96*, 1956.

(20) Bürgi, H. B.; Dunitz, J. D.; Lehn, J. M.; Wipff, G. *Tetrahedron* **1974**, *30*, 1563.

(21) Bürgi, H. B.; Dunitz, J. D.; Shefter, E. *Acta Crystallogr. B* **1974**, *30*, 1517.

(22) Bürgi, H.-B. *Angew. Chem. Int. Ed. Engl.* **1975**, *14*, 460.

(23) The authors only mentioned that they performed Hartree-Fock-SCF-LCGO-MO calculation. Other computational details are not clear.

(24) Caramella, P.; Rondan, N. G.; Paddon-Row, M. N.; Houk, K. N. *J. Am. Chem. Soc.* **1981**, *103*, 2438.

(25) Paddon-Row, M. N.; Houk, N. G. R. N. *J. Am. Chem. Soc.* **1982**, *104*, 7162.

(26) Cieplak, A. S. *J. Am. Chem. Soc.* **1981**, *103*, 4540.

(27) Gung, B. W. *Tetrahedron* **1996**, *52*, 5263.

(28) Mazzocchi, P. H.; Stahly, B.; Dodd, J.; Rondan, N. G.; Domelsmith, L. N.; Rozeboom, M. D.; Caramella, P.; Houk, K. N. *J. Am. Chem. Soc.* **1980**, *102*, 6482.

(29) Cheung, C. K.; Tseng, L. T.; Lin, M.-H.; Srivastava, S.; le Noble, W. J. *J. Am. Chem. Soc.* **1986**, *108*, 1598.

(30) Mehta, G.; Khan, F. A. *J. Am. Chem. Soc.* **1990**, *112*, 6140.

(31) Halterman, R. L.; McEvoy, M. A. *J. Am. Chem. Soc.* **1990**, *112*, 6690.

(32) Halterman, R. L.; McCarthy, B. A.; McEvoy, M. A. *J. Org. Chem.* **1992**, *57*, 5585.

(33) Senda, Y.; Nakano, S.; Kunii, H.; Itoh, H. *J. Chem. Soc., Perkin Trans. 2* **1993**, 1009.

(34) Senda, Y.; Sakurai, H.; Nakano, S.; Hiroaki, I. *Bull. Chem. Soc. Jpn.* **1996**, *69*, 3297.

(35) Wu, Y.-D.; Tucker, J. A.; Houk, K. N. *J. Am. Chem. Soc.* **1991**, *113*, 5018.

(36) Paddon-Row, M. N.; Wu, Y.-D.; Houk, K. N. *J. Am. Chem. Soc.* **1992**, *114*, 10638.

(37) Coxon, J. M.; Houk, K. N.; Luibrand, R. T. *J. Org. Chem.* **1995**, *60*, 418.

(38) Wu, Y.-D.; Houk, K. N. *J. Org. Chem.* **1993**, *58*, 4625.

(39) Kaufmann, E.; Schleyer, P. v. R.; Houk, K. N.; Wu, Y.-D. *J. Am. Chem. Soc.* **1985**, *107*, 5560.

(40) Adcock, W.; Cotton, J.; Trout, N. A. *J. Org. Chem.* **1994**, *59*, 1867.

(41) Wipf, P.; Kim, Y. *J. Am. Chem. Soc.* **1994**, *116*, 11678.

(42) Klein, J. *Tetrahedron Lett.* **1973**, 4307.

(43) Klein, J.; Dunkelblum, E.; Eliel, E. L.; Senda, Y. *Tetrahedron Lett.* **1968**, 6127.

(44) Klein, J.; Lichtenberg, D. *J. Org. Chem.* **1970**, *35*, 2654.

(45) Frenking, G.; Köhler, K. F.; Reetz, M. T. *Angew. Chem. Int. Ed. Engl.* **1991**, *30*, 1146. German version: *Angew. Chem.*, **1991**, *103*, 1167.

(46) Liotta, C. L. *Tetrahedron Lett.* **1975**, 519.

(47) Liotta, C. L. *Tetrahedron Lett.* **1975**, 523.

(48) Burgess, E. M.; Liotta, C. L. *J. Org. Chem.* **1981**, *46*, 1703.

(49) Liotta, C. L.; Burgess, E. M.; Eberhardt, W. H. *J. Am. Chem. Soc.* **1984**, *106*, 4849.

(50) Giddings, M. R.; Hudec, J. *Can. J. Chem.* **1981**, *59*, 459.

(51) Inagaki, S.; Fukui, K. *Chem. Lett.* **1974**, 509.

(52) Inagaki, S.; Fujimoto, H.; Fukui, K. *J. Am. Chem. Soc.* **1976**, *98*, 4054.

(53) Fukui, K.; Nagata, C.; Yonezawa, T.; Kato, H.; Morokuma, K. *J. Chem. Phys.* **1957**, *31*, 287.

(54) Fukui, K.; Morokuma, K.; Yonezawa, T.; Nagata, C. *Bull. Chem. Soc. Jpn.* **1960**, *33*, 963.

(55) Strozier, R. W.; Caramella, P.; Houk, K. N. *J. Am. Chem. Soc.* **1979**, *101*, 1340.

(56) Möller, C.; Plesset, M. S. *Phys. Rev.* **1934**, *46*, 618.

(57) Reed, A. E.; Weinhold, F. *J. Chem. Phys.* **1983**, *78*, 4066.

(58) Huang, X. L.; Dannenberg, J. J.; Duran, M.; Bertrán, J. *J. Am. Chem. Soc.* **1993**, *115*, 4024.

(59) Huang, X. L.; Dannenberg, J. J. *J. Am. Chem. Soc.* **1993**, *115*, 6017.

(60) Franck, R. W.; Kaila, N.; Blumenstein, M.; Geer, A.; Huang, X. L.; Dannenberg, J. J. *J. Org. Chem.* **1993**, *58*, 5335.

(61) Dewar, M. J.; Zoebisch, E. G.; Healy, E. F.; Stewart, J. J. P. *J. Am. Chem. Soc.* **1985**, *107*, 3902.

(62) Shi, Z.; Boyd, R. J. *J. Am. Chem. Soc.* **1993**, *115*, 9614.

(63) Bader, R. F. W. *Atoms in Molecules: A Quantum Theory*; Oxford University Press: Oxford, 1990.

(64) Bader, R. F. W. *Chem. Rev.* **1991**, *91*, 893.

(65) Eliel, E. L.; Ro, R. S. *J. Am. Chem. Soc.* **1957**, *79*, 5992.

(66) Boone, J. R.; Ashby, E. C. In *Topics in Stereoselectivity*, Eliel, E. L.; Allinger, N. L., Eds.; Interscience: New York, 1979; p 53.

(67) Davis, R. E.; Kenson, R. E.; Kibby, C. L.; Lloyd, H. H. *Chem. Commun.* **1965**, 593.

(68) Stockmayer, W. H.; Miller, R. R.; Zeto, R. J. *J. Phys. Chem.* **1961**, *65*, 1076.

(69) Wigfield, D. C.; Phelps, D. J. *J. Org. Chem.* **1976**, *41*, 2396.

(70) Wigfiled, D. C.; Gowland, F. W. *Can. J. Chem.* **1977**, *55*, 3616.

(71) Refs 16, 22, 31 in ref. 25.

(72) Ho, Y.; Squires, R. R. *J. Am. Chem. Soc.* **1992**, *114*, 10961.

(73) Hammond, G. S. *J. Am. Chem. Soc.* **1955**, *77*, 334.

(74) Becke, A. D. *J. Chem. Phys.* **1993**, *98*, 5648.

(75) Becke, A. D. *Phys. Rev.* **1988**, *A 38*, 3098.

(76) Lee, C.; Yang, W.; Parr, R. G. *Phys. Rev.* **1988**, *B 37*, 785.

(77) Frisch, M. J.; Trucks, G. W.; Schlegel, H. B.; Gill, P. M. W.; Johnson, B. G.; Robb, M. A.; Cheeseman, J. R.; Keith, T.; Petersson, G. A.; Montgomery, J. A.; Raghavachari, K.; Al-Laham, M. A.; Zakrzewski, V. G.; Ortiz, J. V.; Foresman, J. B.; Cioslowski, J.; Stefanov, B. B.; Nanayakkara, A.; Challacombe, M.; Peng, C. Y.; Ayala, P. Y.; Chen, W.; Wong, M. W.; Andres, J. L.; Replogle, E. S.; Gomperts, R.; Martin, R. L.; Fox, D. J.; Binkley, J. S.; Defrees, D. J.; Baker, J.; Stewart, J. P.; Head-Gordon, M.; Gonzalez, C.; Pople, J. A. *Gaussian 94, Revision D1*; Gaussian, Inc.: Pittsburgh PA, 1995.

(78) This method implemented on Gaussian 94 is a slightly modified version of the original Becke's functional[74] and it uses the correlation functional of both LYP[76] and VWN[150] functional as local and non-local correlation functional. This was briefly described in: Stephens, P. J.; Devlin, F. J.; Frisch, M. J.; Chabalowski, C. F. *J. Phys. Chem.* **1994**, *98*, 11623.

(79) Scott, A. P.; Radom, L. *J. Phys. Chem.* **1996**, *100*, 16502.

(80) Reed, A. E.; Curtiss, L. A.; Weinhold, F. *Chem. Rev.* **1988**, *88*, 889.

(81) Houk, K. N. *React. Intermed.* **1978**, 326.

(82) Imamura, A. *Mol. Phys.* **1968**, *15*, 225.

(83) Hoffmann, R. *J. Chem. Phys.* **1963**, *39*, 1397.

(84) Mullikken, R. S.; Reike, C. A.; Orloff, D.; Orloff, H. *J. Chem. Phys.* **1949**, *17*, 1248.

(85) Kurita, Y.; Takayama, C. *Tetrahedron* **1990**, *46*, 3789.

(86) Bondi, A. *J. Phys. Chem.* **1964**, *68*, 441.

(87) Probability density ($|\Psi(r)|^2$) corresponds to electron density when occupied orbitals are considered. When vacant orbitals are in concern, it may be appropriate to term it as "hole" density.

(88) Huzinaga, S. *Gaussian Basis Sets for Molecular Orbital Calculations*; Elsevier Science Publishers B.V.: Amsterdam, 1984.

(89) When integrated within the entire space, *EFOE* equals to unity.

(90) Ohno, K.; Mutoh, H.; Harada, Y. *J. Am. Chem. Soc.* **1983**, *105*, 4555.

(91) Ohno, K.; Matsumoto, S.; Harada, Y. *J. Chem. Phys.* **1984**, *81*, 2183.

(92) Ohno, K.; Matsumoto, S.; Harada, Y. *J. Chem. Phys.* **1984**, *81*, 4447.

(93) Ohno, K.; Ishida, T. *Int. J. Quant. Chem.* **1986**, *29*, 677.

(94) Ohno, K. *Theor. Chim. Acta* **1988**, *74*, 239.

(95) Ishida, T.; Ohno, K. *Int. J. Quant. Chem.* **1989**, *35*, 257.

(96) Harada, Y.; Ohno, K. *Nippon Kagaku Kaishi (J. Chem. Soc. Jpn, Chemistry and Industrial Chemistry)* **1988**, 1.

(97) Ohno, K.; Harada, Y. In *Theoretical Models of Chemical Bonding*, Springer-Verlak: Berlin, 1991; p 199.

(98) Ohno, K.; Imai, K.; Harada, Y. *J. Am. Chem. Soc.* **1985**, *107*, 8078.

(99) Ohno, K.; Ishida, T.; Naitoh, Y.; Izumi, Y. *J. Am. Chem. Soc.* **1985**, *107*, 8082.

(100) Ohno, K.; Takano, S.; Mase, K. *J. Phys. Chem.* **1986**, *90*, 2015.

(101) Aoyama, M.; Masuda, S.; Ohno, K.; Harada, Y.; Yew, M. C.; Hua, H. H.; Yong, L. S. *J. Phys. Chem.* **1989**, *93*, 1800.

(102) Takami, T.; Mitsuke, K.; Ohno, K. *J. Chem. Phys.* **1991**, *95*, 918.

(103) Fujisawa, S.; Oonichi, I.; Masuda, S.; Ohno, K.; Harada, Y. *J. Phys. Chem.* **1991**, *95*, 5742.

(104) Ohno, K.; Sunada, S. *Proc. Indian. Acad. Sci. (Chem. Sci.)* **1994**, *106*, 327.

(105) Hehre, W. J.; Radom, L.; Schleyer, P. v. R.; Pople, J. A. *Ab Initio Molecular Orbital Theory*; Wiley: New York, 1986.

(106) Wigfield, D. C.; Feiner, S.; Phelps, D. J. *J. Org. Chem.* **1975**, *40*, 2533.

(107) Johnson, C. R.; Tait, B. D.; Cieplak, A. S. *J. Am. Chem. Soc.* **1987**, *109*, 5875.

(108) Cieplak, A. S.; Tait, B. D.; Johnson, C. R. *J. Am. Chem. Soc.* **1989**, *111*, 8447.

(109) Wu, Y.-D.; Houk, K. N.; Paddon-Row, M. N. *Angew. Chem. Int. Ed. Engl.* **1992**, *31*, 1019. German version: *Angew. Chem.* **1992**, *104*, 1087.

(110) Jochims, J. C.; Kobayashi, Y.; Skrzelewski, E. *Tetrahedron Lett.* **1974**, 571.

(111) Kobayashi, Y. M.; Lambrecht, J.; Jochims, J. C.; Burkert, U. *Chem. Ber.* **1978**, *111*, 3442.

(112) Wu, Y.-D.; Houk, K. N. *J. Am. Chem. Soc.* **1987**, *109*, 908.

(113) Wu, Y.-D.; Houk, K. N. *J. Am. Chem. Soc.* **1993**, *115*, 10992.

(114) Wong, M. W.; Wiberg, K. B. *J. Chem. Phys.* **1991**, *1991*, 8991.

(115) Wong, M. W.; Frisch, M. J.; Wiberg, K. B. *J. Am. Chem. Soc.* **1991**, *113*, 4776.

(116) Wong, M. W.; Wiberg, K. B.; Frisch, M. J. *J. Am. Chem. Soc.* **1992**, *114*, 523.

(117) Terasawa, T.; Okada, T. *J. Chem. Soc., Perkin Trans. 1* **1978**, 1252.

(118) Catelani, G.; Monti, L.; Ugazio, M. *J. Org. Chem.* **1980**, *45*, 919.

(119) Geneste, P.; Durand, R.; Hugon, I.; Reminiac, C. *J. Org. Chem.* **1979**, *44*, 1971.

(120) Srivastava, S.; le Noble, W. J. *J. Am. Chem. Soc.* **1987**, *109*, 5874.

(121) Chung, W.-S.; Turro, N. J.; Srivastava, S.; Li, H.; le Noble, W. J. *J. Am. Chem. Soc.* **1988**, *110*, 7882.

(122) Lin, M.-H.; Cheung, C. K.; le Noble, W. J. *J. Am. Chem. Soc.* **1988**, *110*, 6562.

(123) Lin, M.-H.; Silver, J. E.; le Noble, W. J. *J. Org. Chem.* **1988**, *53*, 5155.

(124) Xie, M.; le Noble, W. J. *J. Org. Chem.* **1989**, *54*, 3836.

(125) Li, H.; le Noble, W. J. *Tetrahedron Lett.* **1990**, *31*, 4391.

(126) Kaselj, M.; Adcock, J. L.; Luo, H.; Zhang, H.; Li, H.; le Noble, W. J. *J. Am. Chem. Soc.* **1995**, *117*, 7088.

(127) Kaselj, M.; le Noble, W. J. *J. Org. Chem.* **1996**, *61*, 4157.

(128) Bodepudi, V. R.; le Noble, W. J. *J. Org. Chem.* **1994**, *59*, 3265.

(129) Bodepudi, V. R.; le Noble, W. J. *J. Org. Chem.* **1991**, *56*, 2001.

(130) Lin, M.-h.; Watson, W. H.; Kashyap, R. P.; le Noble, W. J. *J. Org. Chem.* **1990**, *55*, 3597.

(131) Chung, W.-S.; Turro, N. J.; Srivastava, S.; le Noble, W. J. *J. Org. Chem.* **1991**, *56*, 5020.

(132) Li, H.; Silver, J. E.; Watson, W. H.; Kashyap, R. P.; le Noble, W. J. *J. Org. Chem.* **1991**, *56*, 5932.

(133) Mukherjee, A.; Schulman, E. M.; le Noble, W. J. *J. Org. Chem.* **1992**, *57*, 3120.

(134) Mukherjee, A.; Wu, Q.; le Noble, W. J. *J. Org. Chem.* **1994**, *59*, 3270.

(135) Xie, M.; le Noble, W. J. *J. Org. Chem.* **1989**, *54*, 3839.

(136) Song, I. H.; le Noble, W. J. *J. Org. Chem.* **1994**, *59*, 58.

(137) Hahn, J. M.; le Noble, W. J. *J. Am. Chem. Soc.* **1992**, *114*, 1916.

(138) Gonikberg, E. M.; le Noble, W. J. *J. Org. Chem.* **1995**, *60*, 7751.

(139) Lau, J.; Gonikberg, E. M.; Hung, J.-T.; le Noble, W. J. *J. Am. Chem. Soc.* **1995**, *117*, 11421.

(140) Gung, B. W.; Wolf, M. A. *J. Org. Chem.* **1996**, *61*, 232.

(141) Mehta, G.; Khan, F. A. *J. Chem. Soc., Chem. Commun.* **1991**, 18.

(142) Ganguly, B.; Chandrasekhar, J.; Khan, F. A.; Mehta, G. *J. Org. Chem.* **1993**, *58*, 1734.

(143) Gassman, P. G.; Shaffhausen, J. H.; Starkey, F. D.; Raynolds, P. W. *J. Am. Chem. Soc.* **1982**, *104*, 6411.

(144) Gassman, P. G.; Schaffhausen, J. H.; Raynolds, P. W. *J. Am. Chem. Soc.* **1982**, *104*, 6408.

(145) Mukherjee, D.; Wu, Y.-D.; Fronczek, F. R.; Houk, K. N. *J. Am. Chem. Soc.* **1988**, *110*, 3328.

(146) Yano, K.; Isobe, M.; Yoshida, K. *J. Am. Chem. Soc.* **1978**, *100*, 6166.

(147) Varech, D.; Jacques, J. *Tetrahedron Lett.* **1973**, 4443.

(148) Brienne, M. J.; Varech, D.; Jacques, J. *Tetrahedron Lett.* **1974**, 1233.

(149) Chérest, M.; Felkin, H.; Tacheau, P.; Jacques, J.; Varech, D. *J. Chem. Soc., Chem. Commun.* **1977**, 372.

(150) Vosko, S. H.; Wilk, L.; Nusair, M. *Can. J. Phys.* **1980**, *58*, 1200.

(151) Wavefunction, Inc.

(152) Frisch, M. J.; Trucks, G. W.; Head-Gordon, M.; Gill, P. M. W.; Wong, M. W.; Foresman, J. B.; Johnson, B. G.; Schlegel, H. B.; Robb, M. A.; Replogle, E. S.; Gomperts, R.; Andres, J. L.; Raghavachari, K.; Binkley, J. S.; Gonzalez, C.; Martin, R. L.; Fox, D. J.; Defrees, D. J.; Baker, J.; Stewart, J. J. P.; Pople, J. A. *Gaussian 92, Revision D2*; Gaussian, Inc.: Pittsburgh PA, 1992.

(153) Hehre, W. J.; Stewart, R. F.; Pople, J. A. *J. Chem. Phys.* **1969**, *51*, 2657.

(154) Collins, J. B.; Schleyer, P. v. R.; Binkley, J. S.; Pople, J. A. *J. Chem. Phys.* **1976**, *64*, 5142.

(155) Binkley, J. S.; Pople, J. A.; J., H. W. *J. Am. Chem. Soc.* **1980**, *102*, 939.

(156) Gordon, M. S.; Binkley, J. S.; Pople, J. A.; Pietro, W. J.; Hehre, W. J. *J. Am. Chem. Soc.* **1982**, *104*, 2797.

(157) Pietro, W. J.; Francl, M. M.; Hehre, W. J.; Defrees, D. J.; Pople, J. A.; Binkley, J. S. *J. Am. Chem. Soc.* **1982**, *104*, 5039.

(158) Ditchfield, R.; Hehre, W. J.; Pople, J. A. *J. Chem. Phys.* **1971**, *54*, 724.

(159) Hehre, W. J.; Ditchfield, R.; Pople, J. A. *J. Chem. Phys.* **1972**, *56*, 2257.

(160) Hariharan, P. C.; Pople, J. A. *Mol. Phys.* **1974**, *27*, 209.

(161) Gordon, M. S. *Chem. Phys. Lett.* **1980**, *76*, 163.

(162) Frisch, M. J.; Pople, J. A.; Binkley, J. S. *J. Chem. Phys.* **1984**, *80*, 3265.

(163) Minnesota Supercomputer Center, Inc.

(164) Schaftenaar, G. *QCPE Bulletin* **1992**, *12*, 3. QCPE Program No. 619.

Appendix A

Computational Details

Molecular coordinate data were produced with either of the following two methods.

- Z-matrix written by hand

- Using BUILDER module of Spartan[151]

All the geometry optimizations were performed using standard gradient optimization techniques with Gaussian 92,[152] or 94[77] suite of programs, or Spartan version 2.0, 3.0, or 4.1.1.[151] Standard built-in basis sets (STO-3G,[153,154] 3-21G,[155-157] 4-31G,[158-161] 6-31G*, 6-31G**[158-162]) were used except for bromine, for which basis set of Huzinaga *et al.*[88] (43321/4321/311*) was employed for calculations at the HF/6-31G* level.

Molecular orbital coefficients needed for the EFOE calculations were obtained through single point *ab initio* calculations using Gaussian.

Calculations of the EFOE density, AAS values, distortion indices were performed with our original program. This program was originally written by Prof. S. Tomoda, and subsequently amended for use on workstations by Dr. M. Iwaoka. It was improved for efficiency and several additional routines were created by the author.
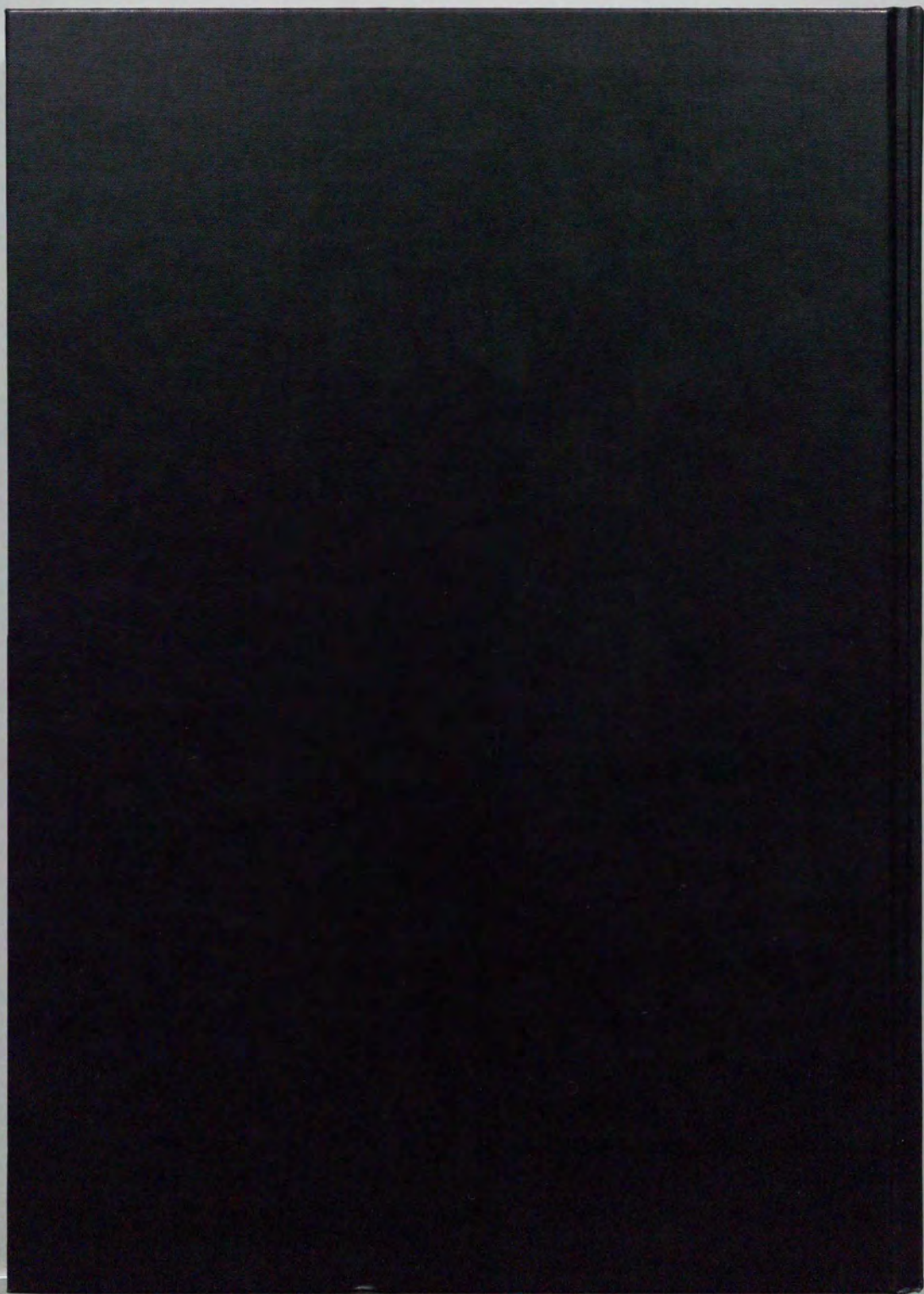
Ab initio calculations were carried out on the following workstations:

- Sun Microsystems SPARCstation 2

- Hewlett-Packard HP/9000 model 715

- SiliconGraphics Indigo (R4000)

- SiliconGraphics Power Indigo^2 (R8000)

For large and time-consuming calculations, especially transition state geometry optimizations and their vibrational frequency analyses were performed on the IBM SP2 workstations at the Computer Center of the Institute for Molecular Science in Okazaki, Japan.

Graphical visualization of molecular structures was mainly done using XMol (version 1.3.1),[163] Spartan and Molden 3.1[164] on Unix workstations.

Contour diagrams of molecular orbitals were produced with Molden 3.1.